CARE–20006-009-BENE
CERN–2006–005
ECFA/06/242
22 May 2006

ORGANISATION EUROPÉENNE POUR LA RECHERCHE NUCLÉAIRE
CERN EUROPEAN ORGANIZATION FOR NUCLEAR RESEARCH

Beams for European Neutrino Experiments (BENE)
Midterm scientific report

BENE

Edited by the (extended) BENE Steering Group

A. Baldini (Pisa), R. Bennett (RAL), A. Blondel (Geneva), J. E. Campagne (LAL), C. Cavata (Saclay), A. Donini (Madrid), M. Dracos (Strasbourg), J. Dumarchez (Paris VI), R. Edgecock (RAL), I. Efthymiopoulos (CERN), R. Garoby (CERN), P. Huber (Madison), K. Long (IC London), M. Lindroos (CERN), F. Méot (Saclay & Grenoble), M. Mezzetto (Padua), V. Palladino (Naples), G. Rees (RAL), P. Sievers (CERN), P. Strolin (Naples), C. Volpe (IPNO)

Geneva
2006

CERN–350 copies printed–May 2006

Abstract

The activities of BENE during 2004 and 2005 are reviewed. Neutrino oscillation experiments at accelerators offer the richest possibilities of precision studies of neutrino mixing and mass differences, with the potential of important discoveries including leptonic CP or T violation. Two main options for a major initiative have been studied: 1) a high-energy Neutrino Factory coupled to a large dense magnetized detector; 2) a lower energy betabeam and conventional superbeam, coupled to a very large low-density, non-magnetic, detector. Both offer significant scientific breakthroughs over other planned facilities. Much remains to be done to optimize and establish the cost, performance, and feasibility of either solution so as to allow comparison and decision. The proposal of a FP7 Design Study of a Neutrino Facility to be completed by the end of the decade is being prepared. Its success will require strong support and engagement at CERN and other European laboratories and funding agencies. International contributors are already engaged in the framework of an international scoping study. The recommendations and milestones proposed by BENE towards a complete conceptual design are summarized.

BENE

BENE (Beams for European Neutrino Experiments) is a FP6 Networking Activity (NA) approved by the European Commission for the years 2004–2008 within the CARE Integrating Infrastructure Initiative. It is rooted in the ECFA study groups, chaired by Alain Blondel (Geneva), and has been active since 1998. Co-ordinated by Vittorio Palladino (Naples), BENE brings together 220 members in Europe from 13 nodes, CERN, INFN, CEA, RAL, IN2P3, GSI, FZJ, PSI, three consortia of laboratories and universities co-ordinated by Imperial College London in the UK, the University of Geneva in Switzerland, TU Munich in Germany, CSIC in Spain, UC Louvain in Belgium. Groups from Poland, Greece, Finland and Bulgaria are in contact.

BENE integrates and co-ordinates the activities of the accelerator and particle physics communities working together, in a worldwide context, dedicated to the study of a forefront neutrino beam facility for Europe. The final objectives are

- to establish a road map for upgrade of our present facility and the design and construction of a new one;
- to assemble a community capable of sustaining the technical realization and scientific exploitation of these facilities;
- to establish and propose the necessary R&D efforts to achieve these goals.

This document summarizes progress made up to the end of the second of its five years of existence. A final report is due in December 2008.

The Networking Activity is organized in a physics work package:

- the ECFA/BENE Neutrino Oscillations group co-ordinated by Mauro Mezzetto (Padua) and Pilar Hernandez (Valencia), recently joined also by Andrea Donini (Madrid)

and the four accelerator packages of the European Neutrino Group co-ordinated by R. Edgecock (RAL) and H. Haseroth (CERN):

- the proton driver work package, co-ordinated by Christian Cavata (CEA Saclay),
- the high-power target work package co-ordinated by Roger Bennett (RAL),
- the collector work package co-ordinated by Marcos Dracos (IRES Strasbourg),
- a work package on novel neutrino beams, itself divided into three activities:
  muon front-end studies co-ordinated by Ken Long (Imperial College),
  muon acceleration and storage ring co-ordinated by Franois Mot (CEA Grenoble),
  betabeam co-ordinated by Mats Lindroos (CERN).

At the start of the International Scoping Study (ISS) a working group on detector design and R&D was also introduced.

BENE maintains close contact with the ongoing long-baseline neutrino experiments in Europe (OPERA, ICARUS) and abroad (MINOS, T2K), with the proposed European projects (Double CHOOZ) and abroad (NOA), and with the internationally conducted R&D experiments (HARP, MUSCAT, HIPPI, MUCOOL, PRISM, MICE and MERIT in particular).

BENE holds plenary meetings two or three times a year and participates actively in the preparation of the international workshops of the NUFACT series.

In preparation for the FP7 design study proposal, an International Scoping Study (ISS) was launched on the occasion of NUFACT05 in Frascati, in collaboration with the international partners of BENE. The ISS will seek to identify the R&D and design efforts that will be necessary in order to be ready to propose a major new neutrino initiative, which could be located in Europe, by about 2010.

Executive summary

The aim of BENE is to investigate the feasibility and performance of an ambitious accelerator neutrino-oscillation facility that could be located in Europe. Precision measurements of neutrino mixing angles and mass hierarchy, with the ultimate aim of discovery and study of leptonic CP violation, provide a very strong physics case, independent of the explorations at high-energy colliders. This document summarizes the state of advancement of BENE after nearly two years.

The facilities that have been considered more specifically are

1. A Neutrino Factory, based on a high-brilliance muon beam, would provide high-energy electron neutrinos (up to 2050 GeV), aimed at magnetic detectors situated 700 to 7000 km away. This is by far the best tool to perform very precise and unambiguous measurements of oscillation parameters, neutrino mass hierarchy, CP violation, and tests of universality in the neutrino sector.

2. A neutrino betabeam facility, that would provide from beta decay of specific ions a very clean beam of electron (anti)neutrinos of energies up to 2 GeV. The very large detectors that are required may be the same as those needed to extend the search for proton decay and astrophysical neutrinos. In combination with a conventional muon-neutrino beam ('superbeam') of the same energy, betabeams could provide interesting sensitivity in the search for leptonic CP and T violation.

Both facilities would extend considerably our knowledge of neutrino masses and mixings over other proposals. Both offer appreciable synergies with other fields within or outside particle physics, and both options have proponents and experts in the international community. New, promising ideas building on these primary concepts arise continuously. A number of open questions have been outlined concerning their feasibility, cost and performance, both in absolute terms and relative to each other. Answers to these questions require theoretical and conceptual work, a co-ordinated design study, and R&D experiments.

Considerable progress has been made over the last two years towards achieving these goals. BENE organized the *MultiMegawatt Workshop* in 2004 and two workshops in 2005, *NNN05* and *NuFact05*. The HARP experiment to measure particle production on various targets and proton beam energies has now produced its first results. The target experiment MERIT, to lay the foundations of a multimegawatt neutrino target station, is now under construction at CERN; the MICE experiment, to test the practical feasibility of muon cooling, is progressing at RAL; all are being carried out by international collaborations. The betabeam design study is taking place in the context of EURISOL, and a preliminary feasibility study of a megaton detector in the Frjus laboratory is under way.

The priority is now the preparation of the Design Study of a high-performance Neutrino Facility, to be completed by the end of the decade. BENE is now engaged in the preparatory phase of this FP7 Proposal. To this effect, an International Scoping Study (ISS) was launched at the NuFact05 workshop, with the aim of establishing a strong international collaboration of experts. Physics studies, detector development, and accelerator aspects are being considered, and should deliver the programme for the design study. The aim of the design study is to be able to propose a choice and a full conceptual design. The increased and co-ordinated contributions that will be required by European laboratories and funding agencies are outlined.

Contents

Introduction: towards a precision neutrino facility

There is a great paradox of particle physics at the turn of the twenty-first century: the Standard Model (SM) triumphed with the precision measurements at LEP and SLD, the last missing quark was discovered at Fermilab, the quark mixing scheme was confirmed in a splendid manner at the B factories. At the same time, the observation of neutrino oscillations, demonstrating that neutrinos have mass and mix, gave the first direct signal of physics beyond the SM.

Neutrino masses could, in principle, be incorporated in a trivial extension of the SM, but this would require i) the addition of a new conservation law that is not now present in the SM, fermion number conservation, and ii) the introduction of an extraordinarily small Yukawa coupling for neutrinos, of the order of $m_\nu/m_{top} \cong 10^{-12}$. More natural theoretical interpretations, such as the see-saw mechanism, lead to the consequence that neutrinos are their own antiparticles, and that the smallness of the neutrino masses comes from their mixing with very heavy partners at the mass scale of Grand Unification (GUT). For the first time, solid experimental facts open a possible window of observation on physics at the GUT scale.

There are many experimental and fundamental implications of this discovery. Perhaps the most spectacular one is the possibility that the combination of fermion number violation and CP violations in the neutrino system could, via leptogenesis, provide an explanation for the baryon asymmetry of the Universe.

The experimental implications are no less exciting. Fermion number violation, and the absolute mass scale of light neutrinos, should be testable in neutrinoless double-beta decay. The direct measurement of the average mass of electron-neutrinos in beta decay could lead to an observable result. The precise values of mass differences, the ordering of masses and the determination of mixing angles must be accessed by neutrino oscillation experiments. Last but not least, the discovery of CP or T violation in neutrino oscillations appears to be feasible, but it requires a new type of experimentation: precision appearance neutrino oscillation measurements involving electron-neutrinos. Precision neutrino oscillation experiments, and the CP asymmetry search in particular, require accelerator-based neutrino beams, on which we concentrate in the following.

There is currently a vast experimental programme around the world that has begun this investigation, as described in the physics section of this report. The Fermilab-based NUMI beam turned on in 2005 with first results from the MINOS experiment expected in the course of 2006. The CERN-based CNGS will start in 2006 with the goal of observing the tau neutrino appearance. The reactor experiment Double CHOOZ is expected to start in 2007/8. The first experiment dedicated to the search for the so far unobserved $\nu_e \leftrightarrow \nu$ oscillation, T2K, will begin in 2009, followed possibly by an off-axis upgrade of the NUMI experimentation, called NovA. The $\nu_e \leftrightarrow \nu$ (or $\nu_e \leftrightarrow \nu_\tau$) transition is remarkable in that it is driven both by the solar oscillation and by the atmospheric oscillation. The latter term is proportional to the yet unknown mixing angle θ_{13}. These experiments may have a chance to establish the neutrino mass hierarchy and should reach a sensitivity to θ_{13} of about 0.01 by 2010–2012. This information will be crucial in the final design of the wave of experimentation that will follow, and that will set its aim on the discovery of CP violation.

It is not too early to develop the techniques that will allow Europe to play a major role in the next generation of experiments, and be able to propose hosting a major neutrino facility. The combined requirements on flux intensity, purity and quality, combined with the requirements on detector mass and capabilities, are very challenging and require novel ideas.

There is growing confidence that novel neutrino beams can be produced from proton accelerators, overcoming the intrinsic limitations of conventional neutrino beams. Neutrino parents can be fully selected, collimated, accelerated, and stored in a decay ring. This can be done with muons in a Neutrino Factory and with radioactive ions in a betabeam. These promise greatly superior performance with respect to conventional neutrino beams, based on a pion decay tunnel, even if the significant intensity upgrades currently envisaged turn some of them into first-generation ‘superbeams’.

Studies towards novel beams have been taking place in Europe now for seven years and R&D projects (HARP, MUSCAT, HIPPI, MERIT, MICE and more) are being carried out by worldwide collaborations. BENE was approved in 2004 and a first betabeam design started in 2005 within the Eurisol Design Study. The fact that these studies are being pursued despite the scarcity of resources available during construction of the LHC tells us a great deal about the motivation and determination of the people involved.

The comparison, as of today, of the CP discovery potential of superbeams, betabeams and Neutrino Factories, in combination with appropriate far neutrino detectors (Fig. 17 of the next section), somewhat favours the Neutrino Factory for small values of θ_{13}, and points to the sensitivity to systematic errors for large values of θ_{13}. This conclusion cannot be considered final. Cost, timescale, performance and practicality of different accelerator systems, performance and optimization of detectors, choice of optimal baselines, systematic errors, and more must again be addressed systematically and coherently by a complete Design Study, leading to a choice by the beginning of the next decade.

The challenge of very large neutrino detectors is being posed on a yet larger scale and the Design Study will have to be made in close contact with existing R&D efforts and promote other efforts if necessary. Water Cherenkov, liquid argon, and possibly liquid scintillator tanks would suit a betabeam/superbeam. Magnetized segmented calorimeters and emulsion cloud chambers could be used for a Neutrino Factory, where magnetized liquid argon could also be employed to great benefit.

The Design Study should also cover the opportunities offered by a new neutrino facility in other sectors of particle physics like a search for forbidden transitions of slow muons, or physics of neutrino interactions with near detector stations.

Turning to accelerator aspects, a driver with several megawatts of proton beam power is the backbone of any future high-intensity facility, both for neutrino and other applications. Preliminary studies indicate that the best choice of the proton kinetic energy ranges from 3 to 5 GeV for a CERN–Fréjus superbeam, and 5 to 30 GeV for a Neutrino Factory. HARP data on pion production are now becoming available and will finally settle these values.

R&D for the first stage (180 MeV or so) of a future high-power driver is being carried out in the HIPPI project. For the higher energy sections, there is a second conceptual study of a 4 MW Superconducting Proton Linac in progress at CERN, extending the proton energy to 3.5 GeV from the 2.2 GeV of the first study. A 8 GeV linac is being designed at Fermilab. Design work on multimegawatt rapid-cycling synchrotron rings of 5, 15 GeV and more has been done at RAL. Upgrade of the power of the JPARC 50 GeV synchrotron is being vigorously pursued. Finally, FFAGs are now also being considered for high-power proton beams.

Flexibility and multiple options will prove very important as the choice of the optimal power, energy, and technology of the proton driver will be made in a larger context, with special emphasis on LHC performance and attention to other applications.

The design of a pion production target and collector, operating in a multimegawatt environment with a long enough lifetime, and of the safety and radiation containment station around it, is probably the most difficult challenge in this sector. No established solution exists for the large energy density involved, 300–1000 J cm^{-3}. In 2007 the MERIT experiment will run at CERN a proof-of-principle test of a liquid metal (mercury) jet at full design flow, 15 T magnetic field and pulse power commensurate with that of a neutrino factory or superbeam. Fundamental studies of a variety of problems for neutrino and EURISOL targets at CERN, solid target studies at BNL on low thermal expansion materials, and tantalum target studies at 2000 K at RAL all deserve strong support. More work is necessary on the design of a solenoid collector beyond that of US study II and on horn collectors beyond the CNGS design.

In the US and CERN schemes for a neutrino factory, a ‘front-end’ prepares the muon beam for acceleration. Energy spread is reduced by phase rotation and emittance by ionization cooling, that results from the combination of energy loss in low-*Z* material and re-acceleration by RF. The MICE experiment at RAL is being built to prove the feasibility of ionization cooling and study its properties extensively. The main priorities for the Design Study in this sector are to complete the MICE experimental programme in its second phase and to revive design work at CERN.

Muon acceleration studies have led to the cost-effective FFAG option, rediscovered in Japan in the last few years. Mastering this technique in Europe seems essential. An alternative type of FFAG, the so-called non-scaling FFAG, has recently been invented and shown to have a number of advantages. A proof-of-principle machine should show that non-scaling optics work and plans are being made to build an electron model (EMMA) at the Daresbury Laboratory in the UK to do this. Optimization studies of a muon storage ring are also necessary.

A design study has started with the objective of establishing feasibility of a $\gamma = 100$ betabeam at CERN, with a frozen parameter list, re-using a maximum of the existing CERN accelerator infrastructure. The technical challenges being addressed are sufficient production of ^{18}Ne and ^{6}He, ionization and bunching of the produced ions at unprecedented intensities, collimation and magnet protection, space charge and physical aperture limitations, the small duty cycle required for rejection of atmospheric background. A low-energy accumulator ring has been added to the design so as to increase design flexibility and boost ion intensities. The study of much higher intensity and γ betabeams, promising enhanced physics reach, is not included. It requires additional resources and should be done before the next neutrino facility is chosen.

In summary, although the contents of the Design Study will be defined by the ongoing scoping study, it appears likely to include, in the accelerator sector, the conceptual feasibility study of the following components:

– a high-power proton driver with energy up to about 4–5 GeV or more,
– the engineering of the handling, containment and safety aspects of a high-power target and collection station,
– a well-performing and cost-effective muon phase rotation and cooling channel,
– non-scaling FFAGs for acceleration of muons (and possibly protons),
– an optimized storage ring for muons,
– higher gamma and higher intensity beta beams,

and a number of technical preparatory (R&D) projects, aimed at demonstrating:

– the existence of at least one adequate choice of target,
– an extended lifetime of the horn prototypes at high rate and radiation,
– muon ionization cooling, by completion of the MICE experimental programme,
– operation of a non-scaling FFAG,
– RF cavities and kicker magnets for fast manipulation of muon beams.

At the same time it will require specific detector R&D and design efforts on a number of topics:

– photodetector development for very large far detectors,

- developments of the liquid argon technique including the presence of magnetic field,
- study and tests of a magnetic calorimeter with a mass of up to 100 kt,
- detectors dedicated for tau detection such as the emulsion cloud chamber,
- and last but not least, the necessary near-detector concepts and beam instrumentation that are crucial for the precise monitoring of neutrino and antineutrino event rates needed for CP violation measurements.

The above structure reproduces that of existing working groups that are enthusiastic to realize this programme. A strong support from CERN and other funding agencies will be crucial for the success of this enterprise.

Physics of massive neutrinos and the role of accelerator experiments

1 Neutrino mass limits from laboratories

Direct laboratory limits on neutrino masses are obtained from kinematical studies. The most stringent current upper limit is that on the $\bar{\nu}_e$ mass, coming from the Mainz experiment measuring the end-point of the electron energy spectrum in tritium beta decay [1]

$$m_{\overline{\nu}_{\rm e}} \leq 2.2 \text{ eV (95\% CL)} .$$

The Troitsk group has also published a similar limit [2]:

$$m_{\overline{\nu}_{\rm e}} \leq 2.1 \text{ eV (95\% CL)} ,$$

however, they must include an *ad hoc* step function near the end-point to avoid the problem of negative mass squared.

The proposed KATRIN experiment aims to improve the sensitivity to $m_{\bar{\nu}_e} \sim 0.3$ eV [3]. Similar sensitivities are the goal of the longer term MARE experiment [4] based on an array of several thousand microbolometers. These measurements are sensitive to

$$m_{\bar{\nu}_e} = \left(\sum_i |U^2_{ei}|\, m^2_i \right)^{1/2} = \left(\cos^2\theta_{13}(m^2_1 \cos^2\theta_{12} + m^2_2 sin^2\theta_{12}) + m^2_3 sin^2\theta_{13} \right)^{1/2} . \qquad (1)$$

An important constraint on Majorana neutrino masses arises from neutrinoless double-β decay, in which an (A, Z) nucleus decays to $(A, Z + 2) + 2\, e^-$, without any neutrino emission. This process can be used to constrain the combination

$$|m_{\beta\beta}| = \left| \sum_i U^{*2}_{ei}\, m_i \right| = \left| \cos^2\theta_{13}(m_1 \cos^2\theta_{12} + m_2 e^{2i\alpha} sin^2\theta_{12}) + m_3 e^{2i\beta} sin^2\theta_{13} \right| , \qquad (2)$$

which involves a coherent sum over all the different Majorana neutrino masses m_i, weighted by their mixings with the electron flavour eigenstate, which may include CP-violating phases, as discussed below. This observable is therefore distinct from the quantity observed in tritium β decay.

The interpretation of neutrinoless double-β decay data depends on calculations of the nuclear matrix elements entering in this process.

A claim for a neutrinoless double-β signal has been made [5] analysing the Heidelberg–Moscow data on ^{76}Ge:

$$T^{0\nu}_{1/2} = 1.19 \cdot 10^{25} \text{ years}$$

corresponding to

$$< m_{\beta\beta} >= 0.05 - 0.85 \text{ eV (95\% CL)}$$

the uncertainty coming from the choice of the nuclear matrix element calculation.

This result is in contrast with the limit computed with a combined analysis of a subset of the Heidelberg-Moscow data and IGEX experiments [6] and to that reported by a separate group of the original collaboration [7], reporting no evidence for a signal.

Recent results on ^{130}Te from the Cuoricino Collaboration [8]: $T^{0\nu}_{1/2} > 1.8 \times 10^{24}$ years corresponding to $m_{\beta\beta} < 0.2$–1.1 eV and on ^{100}Mo from the NEMO3 Collaboration [9]: $T^{0\nu}_{1/2} > 4.6 \times 10^{23}$ years corresponding to $m_{\beta\beta} < 0.7$–2.8 eV do not confirm the germanium claim, but are not sensitive enough to rule it out.

The approved future experiments at LNGS, CUORE [10] and GERDA [11], will have the required sensitivity to unambiguously clarify this experimental situation: having a sensitivity of $m_{\beta\beta} = 0.024$–0.14 eV and $m_{\beta\beta} = 0.09$–0.29 eV, respectively.

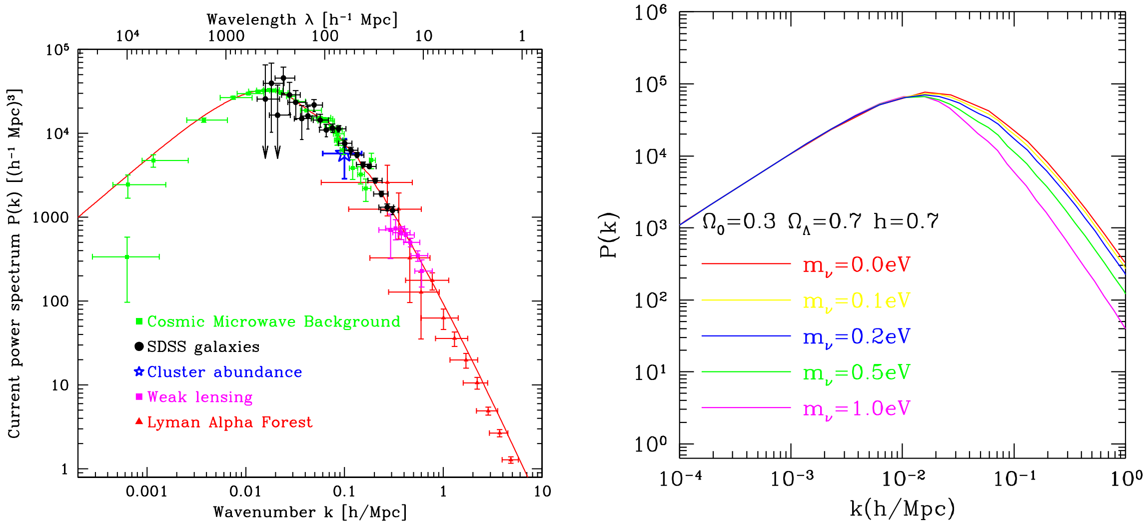

Fig. 1: Left: observational power spectrum from CMB fluctuations, galaxy clustering, gravitational-lensing shear, cluster abundances and Lyman α clouds, compared with the prediction of ΛCDM model. The figure is taken from the SDSS paper, Tegmark *et al.* [22]. Right: Power spectrum predicted in the ΛCDM model including massive neutrinos with a degenerate mass specified in the legend. The top curve represents the case of massless neutrinos.

2 Massive neutrinos in cosmology[1]

There are two places in cosmology where the mass of neutrinos would play a significant role. One is leptogenesis in the early Universe, and the other is the evolution of mass density fluctuations that are explored with cosmic-microwave-background (CMB) fluctuations and the formation of cosmic structure. There is one more place where the presence of neutrinos is generally important—primordial nucleosynthesis, but the effect of neutrino mass is negligible unless it is unrealistically heavy.

One of the promising ideas for baryogenesis is the generation of baryon asymmetry via leptogenesis from the Majorana mass term in the presence of the action of sphalerons of electroweak interactions [13]. According to the latest analyses with Boltzmann equation yield [14–16], these models work provided that

$$m_{\nu_i} < 0.1 \text{ eV} , \tag{3}$$

for all species of neutrinos.

In the last ten years, all observations converged to pointing towards a Universe where dark matter (i.e., dark matter that was non-relativistic when it was decoupled from the thermal bath) dominates the matter component of the Universe, and where the cosmological constant dominates the energy of the Universe. The recent results from WMAP [17] and SDSS [18] strongly support this standard view based on the ΛCDM Universe, as demonstrated by the convergence of the cosmological parameters [19–21] to $H_0 = 71 \pm 5$ km s^{-1}Mpc^{-1}, $\Omega_m = 0.28 \pm 0.03$, $\Omega_\Lambda = 0.72 \pm 0.03$, $\Omega_m + \Omega_\Lambda = 1.01 \pm 0.01$. We also know that baryons amount to only 1/6 of Ω_m, and only 6% of them are comprised in stars and stellar remnants. Another important measure is the power spectrum that characterizes matter fluctuations,

$$P(k) = \int d^3x e^{ik\cdot x} \langle \delta(x)\delta(0) \rangle , \tag{4}$$

where $\delta(x)$ is the density contrast at position x. A variety of observations at vastly different cosmological epochs (CMB at $z = 1090$, galaxy clustering at $z \sim 0.1$–0.4, gravitational lensing at $z \sim 0.5$–1, cluster abundances at $z \sim 0.1$–0.2), when scaled to $z = 0$, yield $P(k)$ that is described by $|k|^n T(k)$ with

[1] Material for this section is taken mainly from Ref. [12].

$n = 1 \pm 0.02$ and the transfer function $T(k)$ predicted by the ΛCDM model with the cosmological parameters specified above [22, 23] (see Fig. 1, left).

The massive neutrinos contribute to the mass density of the Universe by the amount

$$\Omega_\nu = \frac{\sum m_\nu}{94.1 \text{ eV}} h^{-2} , \tag{5}$$

where $h = 0.71$ is the conventional notation for the Hubble constant.

A successful model is obtained for cosmic structure formation without massive neutrinos. This means that massive neutrinos only disturb the agreement between theory and observations, hence leading to a limit on the neutrino mass.

The well-known effect of massive neutrinos is relativistic free streaming that damps fluctuations within the horizon scale. One-electron-volt neutrinos are still relativistic at matter–radiation equality, which takes place at $T \approx 1$ eV, and then tend to smear fluctuations up to $\sim$100 Mpc comoving scale, thus diminishing the power of $P(k)$ for these scales. This effect becomes stronger as the cosmological mass density of neutrinos, hence the neutrino mass, increases (see Fig. 1, right) and Refs. [24, 25]. Therefore the empirical knowledge of $P(k)$ across large to small scales gives a constraint on the summed mass of neutrinos:

(1) Limits derived from galaxy clustering vary from $\sum m_\nu < 0.6$ eV [19] to 2.1 eV [26] at a 95% confidence level, both authors using 2dFGRS data (see also Ref. [27]). The limit using the SDSS data is $\sum m_\nu < 1.7$ eV [20]. (See also Ref. [28], where $\sum m_\nu < 0.75$ eV is concluded using SDSS and 2dFGRS.)

(2) With the Lyman α cloud absorption power derived from fluctuating optical depths, one can explore $P(k)$ at the smallest scale [29, 30], giving the strongest limit $\sum m_\nu < 0.42$ eV (95%) [31] (see Ref. [32] for earlier work). This result, however, is more model-dependent in the sense that one must invoke simulations to extract $P(k)$ from observed flux power spectrum, which suffer from significant uncertainties associated with modelling and simulations.

(3) With gravitational lensing one can directly explore mass fluctuations. For the moment the statistical error is not sufficiently small, but this provides us with a promising method. This may also be used to set the normalization of the power spectrum derived from galaxy clustering.

Elgarøy and Lahav [33] give a summary of limits obtained in the literature.

3 Neutrino oscillations

The observation of neutrino oscillations has now established beyond doubt that neutrinos have mass and mix. This existence of neutrino masses is in fact the first solid experimental fact requiring physics beyond the Standard Model.

The present status of the field is as follows. Since 1989, we know from LEP [34] that there are only three families of active light neutrinos coupling to the weak interaction.

Since the early 1970s we have hints from solar neutrino experiments that electron neutrinos produced in the Sun undergo disappearance on their way to Earth, and, from the different disappearance rates for experiments sensitive to different neutrino energy ranges (chlorine [35], gallium [36, 37], water Cherenkov [38]) we have indications that matter effects in the Sun play an important role. This 'solar neutrino puzzle' was closed in 2002 with the results from the SNO experiment [39], which allowed simultaneously a direct measurement of the total flux of active neutrinos by the neutral current reaction in agreement with solar neutrino flux calculations, and a measurement of the electron neutrino component, by the charged current reaction, determining that they represent less than half of the total flux, in agreement with previous observations. The KamLAND experiment [40] provided at the same time a

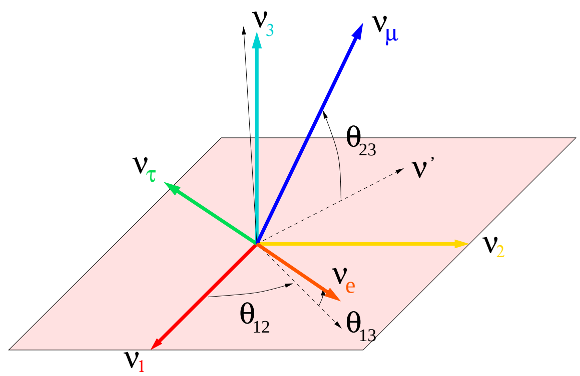

Fig. 2: Representation of the three-dimensional rotation between the flavour and mass neutrino eigenstates

measurement of disappearance of electron antineutrinos from nuclear fission reactors in Japan and Korea, providing, in combination with the solar neutrino results, a precise determination of the relevant neutrino mixing angle and of the corresponding mass difference, see Table 1.

Since the late 1980s there has been indication from atmospheric neutrino experiments that the muon neutrinos undergo disappearance when going through the Earth; this was finally unambiguously demonstrated by the Super-Kamiokande experiment in 1998 [41], a result well supported by the Soudan2 [42] and Macro [43] experiments. This disappearance takes place at a much shorter wavelength than for solar neutrinos ($L/E \sim 500$ km/GeV) [44]; it is not seen for electron neutrinos, a fact that has been best established by the CHOOZ reactor experiment [45]. This disappearance has been confirmed by the K2K experiment in Japan [46], the first accelerator, neutrino, long-baseline experiment designed since neutrino masses were established, and a prototype for future ones.

The above experimental observations are consistently described by three families ν_1, ν_2, ν_3 with mass values m_1, m_2 and m_3 that are connected to the flavour eigenstates ν_e, ν_μ and ν_τ by a mixing matrix U, usually parametrized as

$$U(\theta_{12},\theta_{23},\theta_{13},\delta_\mathrm{CP}) = \begin{pmatrix} c_{13}c_{12} & c_{13}s_{12} & s_{13}e^{-i\delta_\mathrm{CP}} \\ -c_{23}s_{12} - s_{13}s_{23}c_{12}e^{i\delta_\mathrm{CP}} & c_{23}c_{12} - s_{13}s_{23}s_{12}e^{i\delta_\mathrm{CP}} & c_{13}s_{23} \\ s_{23}s_{12} - s_{13}c_{23}c_{12}e^{i\delta_\mathrm{CP}} & -s_{23}c_{12} - s_{13}c_{23}s_{12}e^{i\delta_\mathrm{CP}} & c_{13}c_{13} \end{pmatrix} \quad (6)$$

where the short-form notation $s_{ij} \equiv \sin\theta_{ij}, c_{ij} \equiv \cos\theta_{ij}$ is used. As a result, the neutrino oscillation probability depends on three mixing angles, $\theta_{12}, \theta_{23}, \theta_{13}$, see Fig. 2, two mass differences, $\Delta m^2_{12} = m^2_2 - m^2_1$, $\Delta m^2_{23} = m^2_3 - m^2_2$, and a CP phase δ_CP. Additional phases are present in case neutrinos are Majorana particles, but they do not influence at all neutrino flavour oscillations. Furthermore, the neutrino mass hierarchy, the ordering with which mass eigenstates are coupled to flavour eigenstates, can be fixed by measuring the sign of Δm^2_{23}. In vacuum the oscillation probability between two neutrino flavours α, β is

$$P(\nu_\alpha \to \nu_\beta) = -4\sum_{k>j}\mathrm{Re}[W^{jk}_{\alpha\beta}]\sin^2\frac{\Delta m^2_{jk}L}{4E_\nu} \pm 2\sum_{k>j}\mathrm{Im}[W^{jk}_{\alpha\beta}]\sin^2\frac{\Delta m^2_{jk}L}{2E_\nu}\ , \quad (7)$$

where $\alpha = e, \mu, \tau$, $j = 1, 2, 3$, $W^{jk}_{\alpha\beta} = U_{\alpha j}U^*_{\beta j}U^*_{\alpha k}U_{\beta k}$. In the case of only two neutrino flavour oscillation can it be written as:

$$P(\nu_\alpha \to \nu_\beta) = \sin^2 2\theta\cdot \sin^2\frac{1.27\ \Delta m^2(\mathrm{eV}^2)\cdot L(\mathrm{km})}{E_\nu(\mathrm{GeV})}\ . \quad (8)$$

Table 1: Neutrino oscillation parameters as of NUFACT05 [48]

'solar parameters'	$\delta m^2 = (7.92 \pm 0.72) \cdot 10^{-5}$ eV^2	$\sin^2\theta_{12} = 0.314^{+0.030}_{-0.025}$
'atmospheric parameters'	$\Delta m^2 = \pm(2.4^{+0.5}_{-0.6}) \cdot 10^{-3}$ eV^2	$\sin^2\theta_{23} = 0.44^{+0.18}_{-0.10}$
'absolute mass'	$m_\nu \leq 2.2$ eV (tritium decay)	
	$\sum m_\nu \leq \mathcal{O}(1$ eV$)$ (cosmology)	

Conventionally, $\Delta m^2_{12} \equiv m^2_2 - m^2_1 > 0$ and $\theta_{12} > 0$ [47]. Since atmospheric neutrino disappearance has only been observed for muon neutrinos, which couple weakly to electron neutrinos at the relevant wavelength, we cannot (yet) tell the sign of the mass difference Δm^2_{13}, or Δm^2_{23}.

The present values of oscillation parameters are summarized in Table 1.

Before leaving this section on the status of the field, it is worth remembering a further indication of $\overline{\nu}_\mu \to \overline{\nu}_{\rm e}$ oscillations with a Δm^2 of 0.3–20 eV^2 which comes from the beam-dump LSND experiment detecting a 4σ excess of $\overline{\nu}_{\rm e}$ interactions in a neutrino beam produced by π^+ decays at rest where the $\overline{\nu}_{\rm e}$ component is highly suppressed ($\sim 7.8 \times 10^{-4}$) [49]. The KARMEN experiment [50], with a very similar technique but with a lower sensitivity (a factor 10 less for the lower Δm^2), and the NOMAD experiment at the WANF of the CERN SPS [51] (for $\Delta m^2 > 10$ eV^2) do not confirm the result, excluding a large part of the allowed region of the oscillation parameters. The LSND result does not fit the overall picture of neutrino oscillations and several non-standard explanations, for instance sterile neutrinos, have been put forward to solve this experimental conflict. The MiniBooNE experiment at FNAL, currently taking data, is designed to settle this puzzle with a 5σ sensitivity [52]. If this were true, this will lead to even more exciting phenomenology.

3.1 Present generation of long-baseline experiments[2]

Over the next five years the present generation of oscillation experiments at accelerators with long-baseline ν_μ beams (Table 2), K2K at KEK [46], MINOS [54] at the NuMI beam from FNAL [55] and ICARUS [56] and OPERA [57] at the CNGS beam from CERN [58] are expected to confirm the atmospheric evidence of oscillations and measure $\sin^2 2\theta_{23}$ and $|\Delta m^2_{23}|$ within 10–15% accuracy if $|\Delta m^2_{23}| > 10^{-3}$ eV^2. K2K and MINOS are looking for neutrino disappearance by measuring the ν_μ survival probability as a function of neutrino energy, while ICARUS and OPERA will search for evidence of ν_τ interactions in a ν_μ beam, the final proof of $\nu_\mu \to \nu_\tau$ oscillations. K2K completed its data taking at the end of 2004, while MINOS started data taking at the beginning of 2005. CNGS is expected to start operations in the second half of 2006.

Table 2: Main parameters for present long-baseline neutrino beams

Neutrino facility	Proton momentum (GeV/c)	L (km)	E_ν (GeV)	pot/yr (10^{19})
KEK PS	12	250	1.5	2
FNAL NuMI	120	735	3	20–34
CERN CNGS	400	732	17.4	4.5–7.6

In all these facilities, conventional muon neutrino beams are produced through the decay of π and K mesons generated by a high-energy proton beam hitting needle-shaped light targets. Positive (negative) mesons are sign-selected and focused (defocused) by large-acceptance magnetic lenses into a long evacuated decay tunnel where ν_μ's ($\overline{\nu}_\mu$'s) are generated. In case of positive charge selection, the ν_μ beam has typically a contamination of $\overline{\nu}_\mu$ at the few-per-cent level (from the decay of the residual

[2]Material for this section is taken mainly from Ref. [53].

π^-, K$^-$ and K^0) and $\sim 1\%$ of ν_e and $\overline{\nu}_e$ coming from three-body K$^\pm$, K$_0$ decays and μ decays. The precision on the evaluation of the intrinsic ν_e to ν_μ contamination is limited by the knowledge of π and K production in the primary proton beam target. Hadroproduction measurements at 400 and 450 GeV/c performed with the NA20 [59] and SPY [60] experiments at the CERN SPS provided results with 5–7% intrinsic systematic uncertainties.

The CNGS ν_μ beam has been optimized for the $\nu_\mu \to \nu_\tau$ appearance search. The beam-line design was achieved on the basis of previous experience with the WANF beam at the CERN SPS [61]. The expected muon neutrino flux at the Gran Sasso site will have an average energy of 17.4 GeV and $\sim 0.6\%$ ν_e contamination for $E_\nu < 40$ GeV. Owing to the long-baseline (L = 732 km) the contribution to neutrino beam from the K^0 and mesons produced in the reinteraction processes will be strongly reduced with respect to the WANF [62]: the ν_e/ν_μ ratio is expected to be known within $\sim 3\%$ systematic uncertainty [63].

Current long-baseline experiments with conventional neutrino beams can look for $\nu_\mu \to \nu_e$ oscillations even if they are not optimized for θ_{13} studies. MINOS at NuMI is expected to reach a sensitivity of $\sin^2 2\theta_{13} = 0.08$ [54] integrating 14×10^{20} protons on target (pot) in five years according to the FNAL proton plan evolution [64]. The main MINOS limitation is the poor electron identification efficiency of the detector. OPERA [57] can reach a 90% CL sensitivity $\sin^2 2\theta_{13} = 0.06$ ($\Delta m^2_{23} = 2.5 \times 10^{-3}$ eV^2, convoluted to CP and matter effects) [65, 66], a factor ~ 2 better than CHOOZ for five years' exposure to the CNGS beam at nominal intensity for shared operation 4.5×10^{19} pot/yr. A plot of θ_{13} sensitivities is reported in Fig. 3. According to the CERN PS and SPS upgrade studies [67], the CNGS beam intensity could be improved by a factor 1.5, allowing for more sensitive neutrino oscillation searches for the OPERA experiment.

It is worth mentioning that the sensitivity on θ_{13} measurement of the current long-baseline experiments with conventional neutrino beams, like NuMI and CNGS, will be limited by the power of the proton source which determines the neutrino flux and the event statistics, by the not optimized L/E_ν, and by the presence of the ν_e intrinsic beam contamination and its related systematics. This is particularly true for CNGS where the neutrino energy, optimized to overcome the kinematic threshold for τ production and to detect the τ decay products, is about ten times higher than the optimal value for θ_{13} searches at that baseline.

Another approach to searching for non-vanishing θ_{13} is to look at $\overline{\nu}_\mathrm{e}$ disappearance using nuclear reactors as neutrino source. A follow-up of CHOOZ, Double CHOOZ [68], has been proposed to start in 2008 with a two-detector set-up, aiming to push systematic errors down to 0.6% and to reach a sensitivity on $\sin^2 2\theta_{13} \simeq 0.024$ (90% CL, $\Delta m^2_{23} = 2.5 \times 10^{-3}$) in a three-year run.

A sketch of θ_{13} sensitivities as a function of time, following the schedule reported in the experimental proposals, computed for the approved experiments, is reported in Fig. 4.

3.2 Three-family oscillations and CP or T violation

It was soon realized that with three families and for a favourable set of parameters, it would be possible to observe violation of CP or T symmetries in neutrino oscillations [69]. This observation reinforced the considerable interest for precision measurements of neutrino oscillation parameters. We know since 2002 with the results from SNO [39] and KamLAND [40] that the neutrino parameters belong to the so-called LMA solution which suggests that leptonic CP violation could be large enough to be observed in high-energy neutrino-oscillation appearance experiments.

This has led to extensive studies, such as those published recently in a CERN Report [70], or in a recent BENE [71] workshop on physics at a high-intensity proton driver [72]. The phenomenon of CP (or T) violation in neutrino oscillations manifests itself by a difference in the oscillation probabilities of say, $P(\nu_\mu \to \nu_\mathrm{e})$ vs. $P(\overline{\nu}_\mu \to \overline{\nu}_\mathrm{e})$ (CP violation), or $P(\nu_\mu \to \nu_\mathrm{e})$ vs. $P(\nu_\mathrm{e} \to \nu_\mu)$ (T violation).

It can be observed right away that observation of this important phenomenon requires appearance

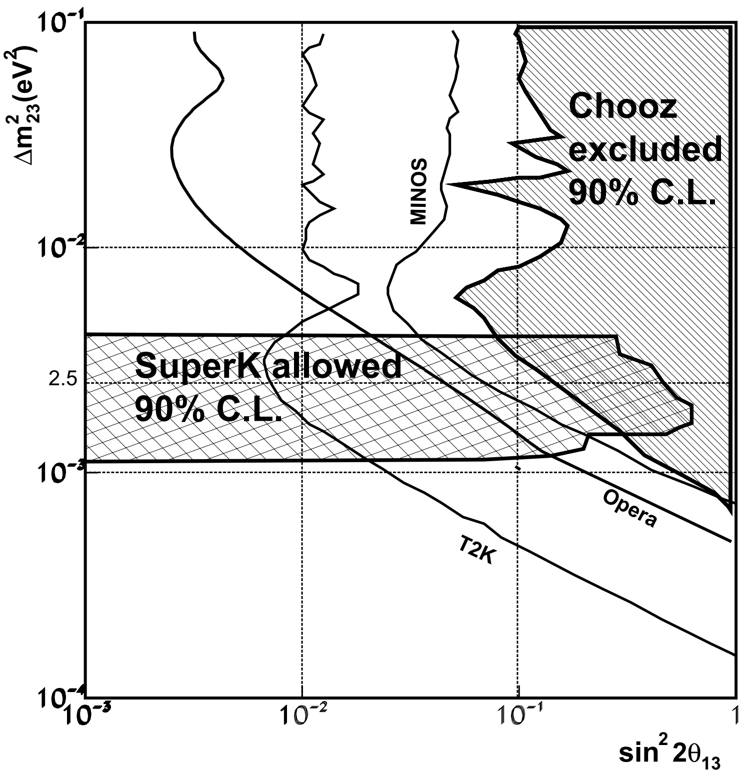

Fig. 3: Expected sensitivity on the θ_{13} mixing angle (matter effects and CP violation effects not included) for MINOS, OPERA, and for the next T2K experiment, compared to the CHOOZ exclusion plot

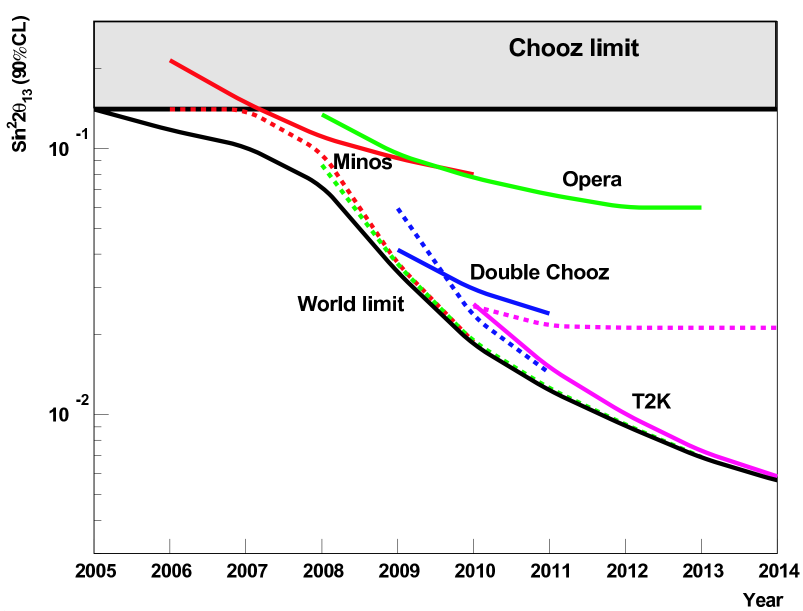

Fig. 4: Evolution of sensitivities on $\sin^2 2\theta_{13}$ as a function of time. For each experiment are displayed the sensitivity as a function of time (solid line) and the world sensitivity computed without the experiment (dashed line). The comparison of the two curves shows the discovery potential of the experiment during its data taking. The overall world sensitivity over time is also displayed. The comparison of the overall world sensitivity with the world sensitivity computed without a single experiment shows the impact of the results of the single experiment. Experiments are assumed to provide results after the first year of data taking.

experiments; indeed a reactor or solar neutrino experiment, sensitive to the disappearance $P(\nu_{\rm e} \to \nu_{\rm e})$ which is clearly time-reversal invariant, would be completely insensitive to it. This can be seen as an advantage in view of a precise and unambiguous measurement of the mixing angles; for the long-term goal of observing and studying CP violation, we are confined to appearance experiments.

The $\nu_\mu \to \nu_{\rm e}$ transition probability in case of small matter effects can be parametrized as [73]:

$$\begin{aligned} P(\nu_\mu \to \nu_e) &= 4c_{13}^2 s_{13}^2 s_{23}^2 \sin^2 \frac{\Delta m_{13}^2 L}{4E_\nu} \times \left[1 \pm \frac{2a}{\Delta m_{13}^2}(1-2s_{13}^2)\right] \\ &+ 8c_{13}^2 s_{12}s_{13}s_{23}(c_{12}c_{23}\cos\delta_{\rm CP} - s_{12}s_{13}s_{23})\cos\frac{\Delta m_{23}^2 L}{4E_\nu}\sin\frac{\Delta m_{13}^2 L}{4E_\nu}\sin\frac{\Delta m_{12}^2 L}{4E_\nu} \\ &\mp 8c_{13}^2 c_{12}c_{23}s_{12}s_{13}s_{23}\sin\delta_{\rm CP}\sin\frac{\Delta m_{23}^2 L}{4E_\nu}\sin\frac{\Delta m_{13}^2 L}{4E_\nu}\sin\frac{\Delta m_{12}^2 L}{4E_\nu} \\ &+ 4s_{12}^2 c_{13}^2\{c_{13}^2 c_{23}^2 + s_{12}^2 s_{23}^2 s_{13}^2 - 2c_{12}c_{23}s_{12}s_{23}s_{13}\cos\delta_{\rm CP}\}\sin\frac{\Delta m_{12}^2 L}{4E_\nu} \\ &\mp 8c_{12}^2 s_{13}^2 s_{23}^2 \cos\frac{\Delta m_{23}^2 L}{4E_\nu}\sin\frac{\Delta m_{13}^2 L}{4E_\nu}\frac{aL}{4E_\nu}(1-2s_{13}^2)\ . \end{aligned} \tag{9}$$

The first line of this parametrization contains the term driven by θ_{13}, the second and third contain CP even and odd terms, respectively, and the fourth is driven by the solar parameters. The last line parametrizes matter effects developed at the first order where a [eV^2] $= \pm 2\sqrt{2}G_F n_e E_\nu$ = 7.6 $\times$ $10^{-5}\rho$ [g/cm^3]E_ν [GeV]. The $\pm$ and $\mp$ terms refer to neutrinos and antineutrinos. A sketch of $P(\nu_\mu \to \nu_{\rm e})$ as a function of *L* for 1 GeV neutrinos is shown in Fig. 5.

When matter effects are not negligible, following Eq. (1) of Ref. [74], the transition probability $\nu_e \to \nu_\mu$ ($\bar\nu_e \to \bar\nu_\mu$) at second order in perturbation theory in θ_{13}, $\Delta m_{12}^2/\Delta m_{23}^2$, $|\Delta m_{12}^2/a|$ and $\Delta m_{12}^2 L/E_\nu$ (see also Ref. [75]) is

$$P^\pm(\nu_e \to \nu_\mu) = X_\pm \sin^2(2\theta_{13}) + Y_\pm \cos(\theta_{13})\sin(2\theta_{13})\cos\left(\pm\delta - \frac{\Delta m_{23}^2 L}{4E_\nu}\right) + Z\ , \tag{10}$$

where $\pm$ refers to neutrinos and antineutrinos, respectively. The coefficients of the two equations are

$$\left\{ \begin{array}{lcl} X_\pm &=& \sin^2(\theta_{23})\left(\frac{\Delta m_{23}^2}{|a-\Delta m_{23}^2|}\right)^2 \sin^2\left(\frac{|a-\Delta m_{23}^2|L}{4E_\nu}\right)\ , \\ Y_\pm &=& \sin(2\theta_{12})\sin(2\theta_{23})\left(\frac{\Delta m_{12}^2}{a}\right)\left(\frac{\Delta m_{23}^2}{|a-\Delta m_{23}^2|}\right)\sin\left(\frac{aL}{4E_\nu}\right)\sin\left(\frac{|a-\Delta m_{23}^2|L}{4E_\nu}\right)\ , \\ Z &=& \cos^2(\theta_{23})\sin^2(2\theta_{12})\left(\frac{\Delta m_{12}^2}{a}\right)^2 \sin^2\left(\frac{aL}{4E_\nu}\right) \end{array} \right. \tag{11}$$

[remember that a changes sign by changing neutrinos with antineutrinos and that $P(\nu_e \to \mu_\mu, \delta_{\rm CP}) = P(\nu_\mu \to \nu_e, -\delta_{\rm CP})$].

The θ_{13} searches look for experimental evidence of $\nu_{\rm e}$ appearance in excess of what is expected from the solar terms. These measurements will be experimentally hard because the CHOOZ limit on the $\overline{\nu}_e$ disappearance, $\theta_{13} < 11^\circ$ for $\Delta m_{23}^2 \simeq 2.5 \times 10^{-3}$ eV^2, translates into a $\nu_\mu \to \nu_e$ appearance probability less than 10% at the appearance maximum in a high-energy muon neutrino beam.

One of the interesting aspects of this formula is the occurrence of matter effects which, unlike the straightforward θ_{13} term, depend on the sign of the mass difference sign(Δm_{23}^2). These terms should allow extraction of the mass hierarchy, but could also be seen as a background to the CP-violating effect, from which they can be distinguished by the very different neutrino energy dependence, matter effects being larger for higher energies, with a 'matter resonance' at about 12 GeV. The CP violation can be seen

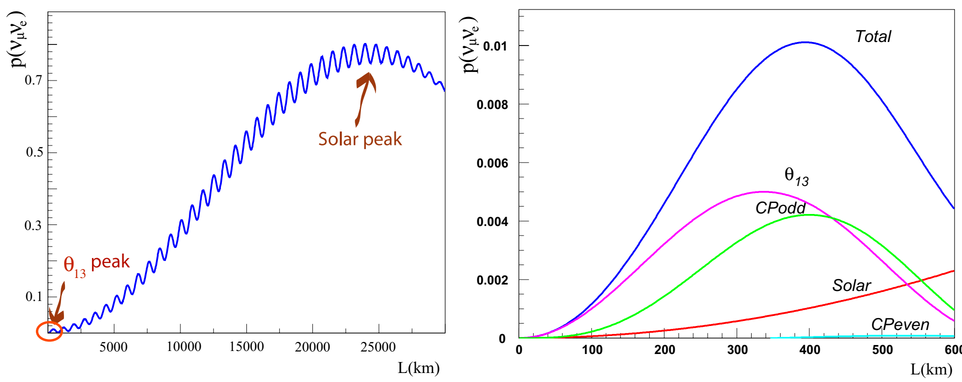

Fig. 5: Sketch of $P(\nu_\mu \to \nu_e)$ as a function of the baseline computed for monochromatic neutrinos of 1 GeV in the solar baseline regime for δ_{CP} = 0 (left) and in the atmospheric baseline regime for $\delta_{CP} = -\pi/2$ (right), where the different terms of Eq. (9) are displayed. The following oscillation parameters were used in both cases: $\sin^2 2\theta_{13} = 0.01$, $\sin^2 2\theta_{12} = 0.8$, $\Delta m^2_{23} = 2.5 \times 10^{-3}$ eV^2, $\Delta m^2_{12} = 7 \times 10^{-5}$ eV^2. From Ref. [53].

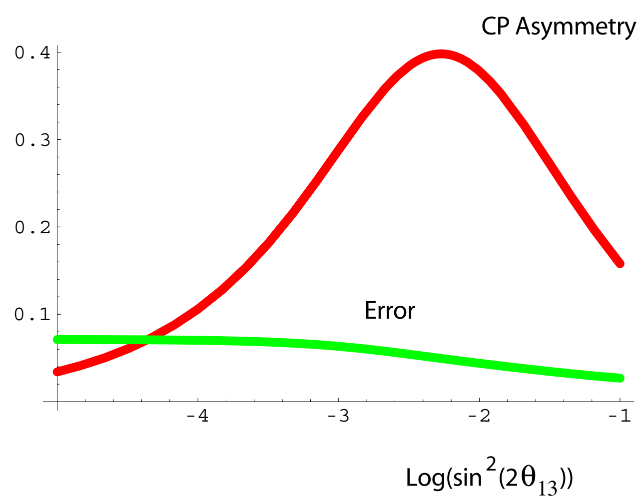

Fig. 6: Magnitude of the CP asymmetry at the first oscillation maximum, for $\delta = 1$ as a function of the mixing angle $\sin^2 2\theta_{13}$. The curve marked 'error' indicates the dependence of the statistical+systematic error on such a measurement. The curves have been computed for the baseline betabeam option at the fixed energy $E_\nu = 0.4$ GeV, L = 130 km, statistical + 2% systematic errors.

as interference between the solar and atmospheric oscillation for the same transition. Of experimental interest is the CP-violating asymmetry A_{CP}:

$$A_{CP} = \frac{P(\nu_\mu \to \nu_e) - P(\overline{\nu}_\mu \to \overline{\nu}_e)}{P(\nu_\mu \to \nu_e) + P(\overline{\nu}_\mu \to \overline{\nu}_e)} \tag{12}$$

displayed in Fig. 6, or the equivalent time-reversal asymmetry A_T.

The asymmetry can be large and its value increases for decreasing values of θ_{13} up to the value when the two oscillations (solar and atmospheric) are of the same magnitude. The following remarks can be made:

1. The ratio of the asymmetry to the statistical error is fairly independent of θ_{13} for large values of this parameter, which explains the relative flatness of the sensitivity curves.

2. This asymmetry is valid for the first maximum. At the second oscillation maximum the curve is shifted to higher values of θ_{13} so that it could be then an interesting possibility for measuring the CP asymmetry, although the reduction in flux is considerable (roughly a factor of 9).
3. The asymmetry has opposite sign for $\nu_{\rm e} \to \nu_\mu$ and $\nu_{\rm e} \to \nu_\tau$, and changes sign when going from one oscillation maximum to the next.
4. The asymmetry is small for large values of θ_{13}, placing a challenging emphasis on systematics.

The richness of the $\nu_\mu \to \nu_{\rm e}$ transition is also its weakness: it will be very difficult for pioneering experiments to extract all the genuine parameters unambiguously. Correlations are present between θ_{13} and $\delta_{\rm CP}$ [74]. Moreover, in the absence of information about the sign of Δm^2_{23} [76, 77] and the approximate $[\theta_{23}, \pi/2 - \theta_{23}]$ symmetry for the atmospheric angle [78], additional clone solutions arise. In general, the measurement of $P(\nu_\mu \to \nu_e)$ and $P(\bar{\nu}_\mu \to \bar{\nu}_e)$ will result in eight allowed regions of the parameter space, the so-called eightfold degeneracy [77].

As already pointed out, the $\nu_\mu \to \nu_e$ experimental sensitivity with conventional ν_μ beams is limited by an unavoidable $\nu_{\rm e}$ beam contamination of about 1%. The ν_μ to ν_τ oscillations, with E_ν above the τ mass production threshold, generate background due to a significant number of ν_τ charged-current interactions where a large fraction of τ's decay into electrons. Finally, neutral pions in both neutral-current or charged-current interactions can fake an electron providing also a possible background for the ν_e's.

Therefore the measurement of the θ_{13} mixing angle and the investigation of the leptonic CP violation will require

– neutrino beams with high performance in terms of intensity, purity, and low associated systematics. Event statistics, background rates and systematic errors will play a decisive role in detecting $\nu_{\rm e}$ appearance;
– the use of detectors of unprecedented mass, granularity and resolution. Again event statistics is the main concern, while high detector performance is necessary to keep the event backgrounds (such as π^0's from ν_μ neutral-current interactions, mis-identified as $\nu_{\rm e}$ events) at rates as low as possible;
– ancillary experiments to measure meson production (for knowledge of the neutrino beam), neutrino cross-sections, particle identification capability. The optimization of proton driver characteristics and the best possible estimation of the systematic errors will require these kinds of dedicated experiments. The HARP hadroproduction experiment at the CERN PS [79] took data for primary protons between 3 and 14.5 GeV in 2001 and 2002 with different target materials. These data contribute to the proton driver optimization, the determination of the K2K [80] and MiniBooNE neutrino beam fluxes, and to the study of atmospheric-neutrino interaction rates.

4 Description of accelerator neutrino facilities

According to the present experimental situation, conventional neutrino beams can be improved and optimized for $\nu_\mu \to \nu_e$ searches. The design of such a new superbeam facility for a very-high-intensity and low-energy ν_μ flux will demand:

– a new, higher power proton driver, exceeding one megawatt, to deliver more intense proton beams on target;
– a tunable L/E_ν in order to explore the Δm^2_{23} parameter region as indicated by the previous experiments with neutrino beams and atmospheric neutrinos;
– narrow-band beams with $E_\nu \sim$ 1–2 GeV;
– a lower intrinsic ν_e beam contamination which can be obtained by suppressing K^+ and K^0 production by the primary proton beam in the target.

An interesting option for the superbeams is the possibility to tilt the beam axis a few degrees with respect to the position of the far detector (off-axis beams) [81, 82]. According to two-body π-decay kinematics, all the pions above a given momentum produce neutrinos of similar energy at a given angle $\theta \neq 0$ with respect to the direction of the parent pion (contrary to the $\theta = 0$ case where the neutrino energy is proportional to the pion momentum).

These neutrino beams have several advantages with respect to the corresponding on-axis ones: they are narrower, have lower energy and smaller ν_{e} contamination (since ν_e's come mainly from three-body decays) although the neutrino flux can be significantly smaller.

The intrinsic limitations of conventional neutrino beams are overcome if the neutrino parents can be fully selected, collimated, and accelerated to a given energy. This can be attempted within the muon or a beta-decaying ion lifetime. The neutrino beams from their decays would then be pure and perfectly predictable. The first approach brings us to Neutrino Factories [83], the second to betabeams [84]. However, the technical difficulties associated with developing and building these novel-conception neutrino beams suggest, for the medium-term option, to improve the conventional beams by new high-intensity proton machines, optimizing the beams for the $\nu_\mu \to \nu_e$ oscillation searches (superbeams).

4.1 Off-axis superbeams: T2K, T2HK and NOνA

The T2K (Tokai to Kamioka) experiment [81] will aim neutrinos from the Tokai site to the Super-Kamiokande detector 295 km away. The neutrino beam is produced by pion decay from a horn-focused beam, with a system of three horns and reflectors. The decay tunnel length (130 m) is optimized for the decay of 2–8 GeV pions and is short enough to minimize the occurrence of muon decays. The neutrino beam is situated at an angle of 2–3 degrees from the direction of the Super-Kamiokande detector, assuring a pion-decay peak energy of 0.6 GeV. The beam line is equipped with a set of dedicated on-axis and off-axis detectors at a distance of 280 m.

The main goals of the experiment are as follows:

1. The highest priority is the search for ν_e appearance to detect sub-leading $\nu_\mu \to \nu_{\mathrm{e}}$ oscillations. It is expected that the sensitivity of the experiment in a five-year ν_μ run, will be of the order of $\sin^2 2\theta_{13} \leq 0.006$ [81].
2. Disappearance measurements of ν_μ's. This will improve the measurement of Δm^2_{23} down to a precision of a 0.0001 eV^2 or so. The exact measurement of the maximum disappearance is a precise measurement of $\sin^2 2\theta_{23}$. These precision measurements of already known quantities require a good knowledge of flux shape, absolute energy scale, experimental energy resolution, and of the cross-section as a function of energy. They will be crucial for measuring the tiny $\nu_\mu \to \nu_{\mathrm{e}}$ oscillations [85, 86].
3. Neutral-current disappearance (in events tagged by π^0 production) will allow for a sensitive search of sterile neutrino production.

The T2K experiment is planned to start in 2009 with a beam intensity reaching 1 MW beam power on target after a couple of years, see Fig. 7. It has an upgrade path which involves a 2 km near-detector station featuring a water Cherenkov detector, a muon monitor, and a fine-grain detector (possibly liquid argon). Phase II of the experiment, often called T2HK, foresees an increase of beam power up to the maximum feasible with the accelerator and target (4 MW beam power), antineutrino runs, and a very large water Cherenkov (HyperKamiokande) with a rich physics programme in proton decay, atmospheric and supernova neutrinos,and, perhaps, leptonic CP violation, which could be built in about 15 to 20 years from now.

The NOνA experiment with an upgraded NuMI off-axis neutrino beam [87] ($E_\nu \sim 2$ GeV and a ν_e contamination lower than 0.5%) and with a baseline of 810 km (12 km off-axis), has been recently proposed at FNAL with the aim of exploring the $\nu_\mu \to \nu_e$ oscillations with a sensitivity 10 times better

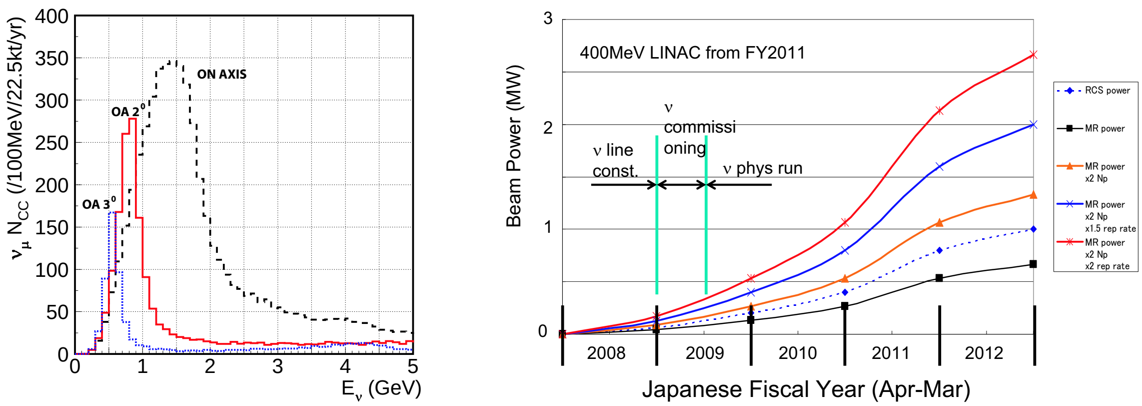

Fig. 7: Left: T2K neutrino-beam energy spectrum for different off-axis angle θ. Right: expected evolution of T2K beam power as a function of time. The baseline option is the second-lowest solid curve.

than MINOS. If approved in 2006, the experiment could start data taking in 2011. The NuMI target will receive a 120 GeV/c proton flux with an expected intensity of 6.5×10^{20} pot/year (2×10^7 s/year are considered available to NuMI operations while the other beams are normalized to 10^7 s/year). The experiment will use a near and a far detector, both using liquid scintillator (TASD detector). In a five-year ν_μ run, with 30 kt active-mass far detector, a sensitivity on $\sin^2 2\theta_{13}$ slightly better than T2K, as well as a precise measurement of $|\Delta m^2_{23}|$ and $\sin^2 2\theta_{23}$, can be achieved. NOνA can also allow one to solve the mass hierarchy problem for a limited range of the $\delta_{\rm CP}$ and ${\rm sign}(\Delta m^2_{23})$ parameters [87].

As a second phase, the new proton driver of 8 GeV/c and 2 MW, could increase the NuMI beam intensity to 17.24–25.2×10^{20} pot/year, allowing one to improve the experimental sensitivity by a factor two and to initiate the experimental search for CP violation.

4.2 SPL superbeam

In the CERN-SPL superbeam project [88–90] the planned 4 MW Superconducting Proton Linac (SPL) would deliver a 2.2 GeV/c proton beam, on a Hg target to generate an intense π^+ (π^-) beam focused by a suitable magnetic horn in a short decay tunnel. As a result, an intense ν_μ beam will be produced mainly via the π decay, $\pi^+ \to \nu_\mu\ \mu^+$, providing a flux $\phi \sim 3.6 \times 10^{11} \nu_\mu$/year/m^2 at 130 km distance, and an average energy of 0.27 GeV. The ν_e contamination from K will be suppressed by threshold effects and the resulting ν_e/ν_μ ratio ($\sim 0.4\%$) will be known within 2% error. The use of a near and a far detector (the latter at $L = 130$ km in the Fréjus area [91], see Section 4.2.1) will allow for both ν_μ disappearance and $\nu_\mu \to \nu_e$ appearance studies. The physics potential of the 2.2 GeV SPL superbeam (SPL-SB) with a water Cherenkov far detector with a fiducial mass of 440 kt has been extensively studied [89].

New developments show that the potential of the SPL-SB could be improved by raising the SPL energy to 3.5 GeV [92], to produce more copious secondary mesons and to focus them more efficiently. This seems feasible if state-of-the-art RF cavities were used in place of the previously foreseen LEP cavities [93].

The focusing system (magnetic horns), originally optimized in the context of a Neutrino Factory [94, 95], has been redesigned considering the specific requirements of a superbeam. The most important points are that the phase spaces that are covered by the two types of horns be different, and that for a superbeam the pions to be focused should have an energy of the order of $p_\pi\ ({\rm MeV})/3 \approx E_\nu \geq 2L\ ({\rm km})$ to obtain a maximum oscillation probability. In practice, this means that one should collect 800 MeV/c pions to get a mean neutrino energy of 300 MeV, see Fig. 8. At higher beam energy, the kaon rates grow rapidly compared to the pion rates, an experimental confirmation [79] of such numbers is highly desirable.

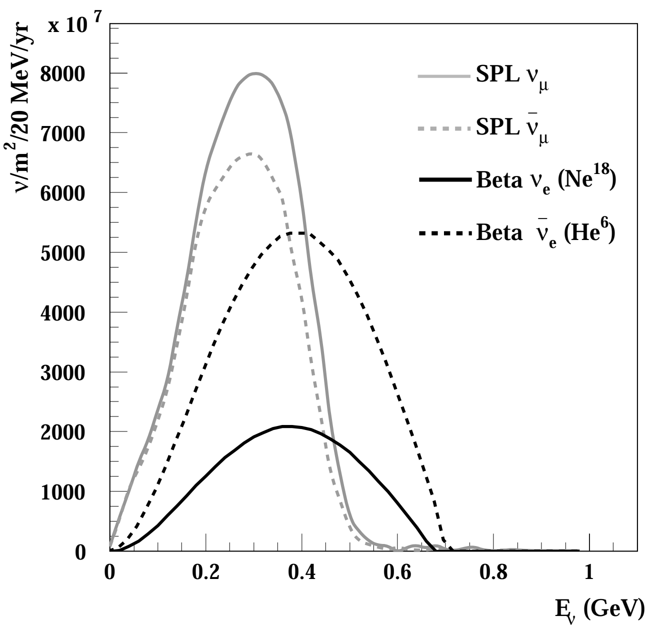

Fig. 8: Neutrino flux of β beam ($\gamma = 100$) and CERN-SPL superbeam, 3.5 GeV, at 130 km distance

In this upgraded configuration, neutrino flux could be increased by a factor ~ 3 with respect to the 2.2 GeV configuration, the number of expected charged-current ν_μ's is about 95 per kt $\cdot$ yr.

A sensitivity $\sin^2 2\theta_{13} < 0.8 \times 10^{-3}$ can be obtained in a five-year ν_μ plus five-year $\overline{\nu}_\mu$ run ($\delta = 0$ intrinsic degeneracy accounted for, sign and octant degeneracies not accounted for), allowing one to discover CP violation (at the 3σ level) if $\delta_{\rm CP} \geq 25^\circ$ and $\theta_{13} \geq 1.4^\circ$ [96,97]. The expected performances are shown in Figs. 10 and 17 along with those of other set-ups.

4.2.1 The MEMPHYS detector

The MEMPHYS (MEgaton Mass Physics) detector is a megaton-class water Cherenkov in the straight extrapolation of the well-known and robust technique used for the Super-Kamiokande detector. It is designed to be located at Fréjus, 130 km from CERN and it is an alternative design of the UNO [98] and Hyper-Kamiokande [81] detectors and shares the same physics case from both the non-accelerator domain (nucleon decay, SuperNovae neutrino from burst event or from relic explosion, solar and atmospheric neutrinos) and from the accelerator (superbeam, betabeam) domain. For the physics part not covered by this document, this kind of megaton water detector can push the nucleon decay search up to 10^{35} yr in the $e^+\pi^0$ channel and up to few 10^{34} yr in the $K^+\overline{\nu}$ channel, just to cite these benchmark channels. MEMPHYS can register as many as 150 000 events from a SN at 10 kpc from our galaxy and 50 events or so from Andromeda. To detect relic neutrinos from past SuperNovae explosions one can use pure water and get a flux of 250 events/10 yr/500 kt or increase this number by a factor 10 by adding gadolinium salt.

A recent civil engineering pre-study to envisage the possibility of large cavity excavation located under the Fréjus mountain (4800 m.e.w.) near the present Modane Underground Laboratory has been undertaken. The main result of this pre-study is that MEMPHYS may be built with current techniques as a three- or four-shaft modular detector, $250\ 000\ \mathrm{m}^3$ each 65 m in diameter, 65 m in height for the total water containment. Each of these shafts corresponds to about five times the present Super-Kamiokande cavity. For the present physical study, the fiducial volume of 440 kt which means three shafts and an Inner Detector (ID) of 57 m in diameter and 57 m in height is assumed. Each ID may be equipped with

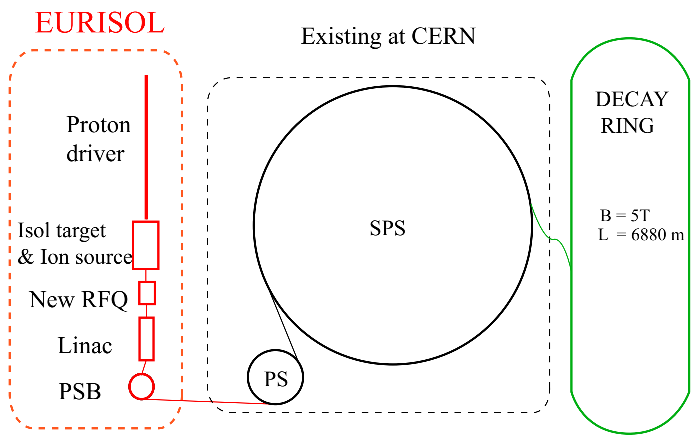

Fig. 9: A schematic layout of the betabeam complex. At left, the low-energy part is largely similar to the EURISOL project [99]. The central part (PS and SPS) uses existing facilities. At right, the decay ring has to be built.

photodetectors (PMT, HPD, etc.) with a surface coverage at least 30%. The Fréjus site offers natural protection against cosmic rays by a factor 10^6.

The decision on whether to dig the cavities is fixed for 2010 after an intense Detector Design Study (e.g., cavity excavation, photodetector R&D) performed in parallel with the digging of at least a safety gallery in the Fréjus road tunnel. One may note that this key date may also be decisive for SPL construction as well as for the choice of the EURISOL site. After that, the excavation and photomultiplier tube production are envisaged to take seven years or so, and the non-accelerator programme can start before the beginning of the accelerator programme (superbeam and betabeam) which may start before 2020.

A first estimate of the costs of such a detector is reported in Table 3.

Table 3: Preliminary cost estimate of the MEMPHYS detector (millions of euros)

Three shafts	240
Total cost of 250 k 12-inch PMTs	250
Infrastructure	100
Total	590

4.3 Betabeams

Betabeams were introduced by P. Zucchelli in 2001 [84]. The idea is to generate pure, well-collimated and intense ν_e ($\overline{\nu}_e$) beams by producing, collecting, and accelerating radioactive ions and storing them in a decay ring in 10 ns long bunches, to suppress the atmospheric neutrino backgrounds. The resulting betabeam fluxes could be easily computed by the properties of the beta decay of the parent ion and by its Lorentz boost factor γ and would be virtually background-free. The best ion candidates so far are ^{18}Ne and ^{6}He for ν_e and $\overline{\nu}_e$, respectively. The schematic layout of a betabeam is the following (see also Fig. 9).

Ion production Protons are delivered by a high-power linac. Betabeam targets need 100 μA proton beam, at energies between 1 and 2 GeV.

In case the Superconducting Proton Linac (SPL) [88] were used, betabeams could be fired to the same detector together with a neutrino superbeam [89]. The SPL is designed to deliver 2 mA of 2.2 GeV (kinetic energy) protons; in such a configuration betabeams would use 10% of the total proton intensity, leaving room for a very intense conventional neutrino beam.

The ^{6}He target consists either of a water-cooled tungsten core or of a liquid-lead core which works as a proton-to-neutron converter surrounded by beryllium oxide [100], aiming for 10^{15} fissions per second. The ^{18}Ne can be produced by spallation reactions, in this case protons will directly hit a magnesium oxide target. The collection and ionization of the ions is performed using the ECR technique [101].

This stage could be shared with nuclear physicists aiming for a source of radioactive ions of the same intensity as needed by a betabeam. A design study has recently been approved by the E.U., EURISOL [99], where both nuclear and neutrino physics issues will be studied.

Ion acceleration The CERN PS and SPS can be used to accelerate the ions. There is well-established experience at CERN with ion accelerators. Ions are first accelerated to MeV/u by a linac and to 300 MeV/u, in a single batch of 150 ns, by a rapid cycling synchrotron. Sixteen bunches (consisting of 2.5×10^{12} ions each in the case of ^{6}He) are then accumulated in the PS, and reduced to eight bunches during their acceleration to intermediate energies. The SPS will finally accelerate the eight bunches to the desired energy using a new 40 MHz RF system and the existing 200 MHz RF system, before ejecting them in batches of eight 10 ns bunches into the decay ring. The SPS could accelerate ^{6}He ions at a maximum γ value of $\gamma_{^6\mathrm{He}} = 150$.

Decay ring The decay ring has a total length of 6880 m and straight sections of 2500 m each (36% useful length for ion decays). These dimensions are fixed by the need to bend ^{6}He ions up to $\gamma = 150$ using 5 T superconducting magnets. Because of the relativistic time dilatation, the ion lifetimes reach several minutes, so that stacking the ions in the decay ring is mandatory to get enough decays and hence high neutrino fluxes. The challenge is then to inject ions in the decay ring and merge them with existing high-density bunches. As conventional techniques with fast elements are excluded, a new scheme (asymmetric merging) was specifically conceived [102].

In summary, the main features of a neutrino beam based on the betabeam concept are

- the beam energy depends on the γ factor. The ion accelerator can be tuned to optimize the sensitivity of the experiment;
- the neutrino beam contains a single flavour with an energy spectrum and intensity known *a priori*. Therefore, unlike conventional neutrino beams, close detectors are not necessary to normalize the fluxes;
- neutrino and antineutrino beams can be produced with a comparable flux;
- as opposed to superbeams, betabeam experiments search for $\nu_e \to \nu_\mu$ transitions, requiring a detector capable of distinguishing muons from electrons. Moreover, since the beam does not contain ν_μ's or $\bar{\nu}_\mu$'s in the initial state, magnetized detectors are not needed. This is in contrast with the neutrino factories (see Section 4.4) where the determination of the muon sign is mandatory.

A baseline study for a betabeam complex (Fig. 9) has been carried out at CERN [103]. The reference betabeam fluxes are $5.8{\times}10^{18}$ ^{6}He useful decays/year and $2.2{\times}10^{18}$ ^{18}Ne decays/year if a single ion species circulates in the decay ring.

The water Cherenkov could be a suitable technology for a large detector. The physics potential has been initially computed in Refs. [104, 105] for $\gamma_{^6\mathrm{He}} = 60$, $\gamma_{^{18}\mathrm{Ne}} = 100$ and with a 440 kt detector at 130 km.

The most updated sensitivities for the baseline betabeam are computed in a scheme where both ions are accelerated at $\gamma = 100$, the optimal set-up for the CERN–Fréjus baseline of 130 km, [106]. The θ_{13} sensitivity curve, computed with a six-parameter fit minimized over the solar and the atmospheric parameters and projected over θ_{13}, is shown in Fig. 10 [106]. Degeneracies induced by the unknown values of $\mathrm{sign}(\Delta m^2_{23})$ and θ_{23} are not accounted for in these first plots. They are properly included in Fig. 11.

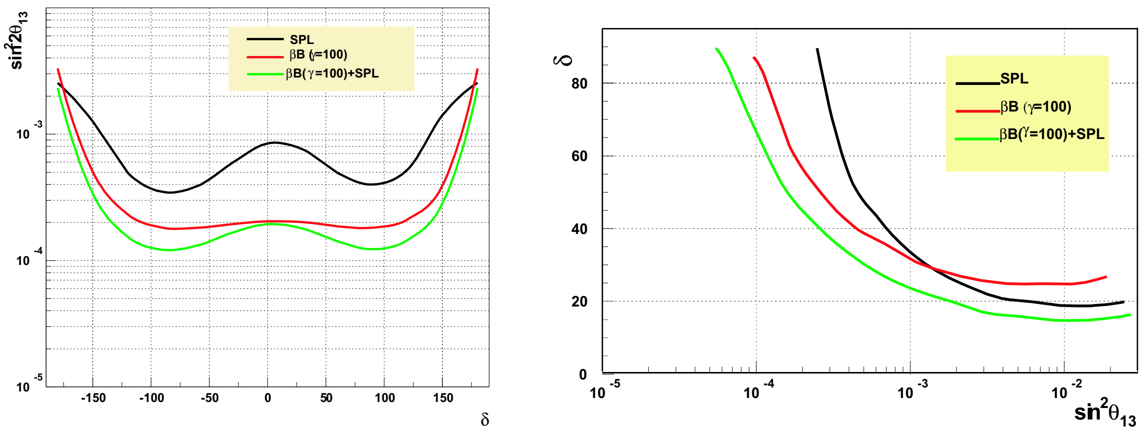

Fig. 10: Left: θ_{13} 90% CL sensitivity as a function of $\delta_{\rm CP}$ for $\Delta m^2_{23} = 2.5 \times 10^{-3}$ eV^2, sign$(\Delta m^2_{23}) = 1$, 2% systematic errors. SPL-SB sensitivities have been computed for a 10-year ν_μ run, βB and βB$_{100,100}$ for a 10-year $\nu_{\rm e}$+ $\overline{\nu}_{\rm e}$ run. Right: $\delta_{\rm CP}$ discovery potential at 3σ (see text) computed for 10 years running time (5 years ν + 5 years $\overline{\nu}$ for both the facilities). The SPL-SB 3.5 GeV, betabeam with $\gamma = 100, 100$ and their combination are shown.

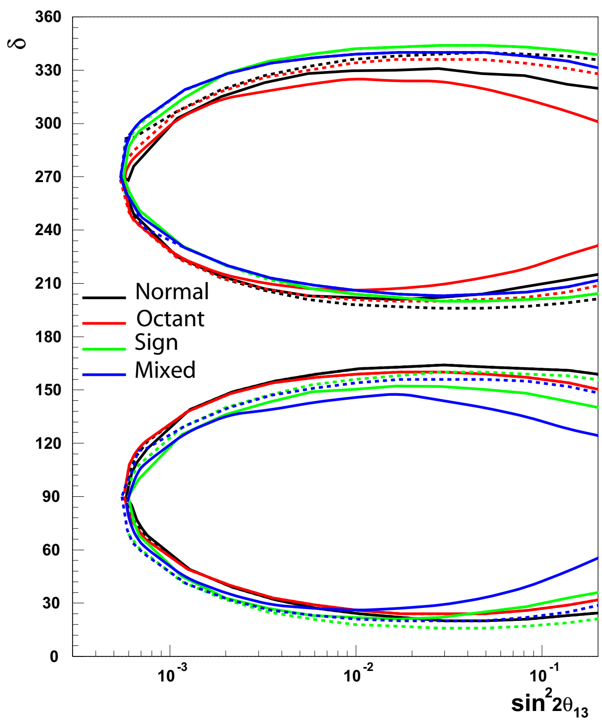

Fig. 11: Leptonic CP violation discovery potential at $3\sigma(\Delta\chi^2 > 9.0)$ of the betabeam with $\gamma = 100$ computed for the four different options about the true values of sign(Δm^2_{23}) and θ_{23} and including all the possible degeneracies (see text). Dotted curves are computed neglecting the effects of the clone solutions. Taken from Ref. [106].

The leptonic CP violation discovery potential (LCPV) has been computed with the following procedure. For any choice of a true value of θ_{13}, $\bar{\theta}_{13}$, a loop on test values of $\delta_{\rm CP}$, $\bar{\delta}_{CP}$, is initiated, until the fit around ($\bar{\theta}_{13}, \bar{\delta}_{CP}$) is 3σ away from any solution at $\delta_{\rm CP} = 0$ and $\delta_{\rm CP} = \pi$. While in Ref. [107] this procedure is performed in the full (θ_{13},$\delta_{\rm CP}$) space (3σ corresponding to $\Delta\chi^2 = 11.8$), here the solution is searched for having marginalized out θ_{13} (GLoBES function `GblChiDelta` [108]). The LCPV at 3σ ($\Delta\chi^2 = 9.0$) is shown in Fig. 11. It takes into account all the parameter errors and all the possible degeneracies [106]. As is common practice in the literature, $\theta_{23} = 40°$ has been used, to leave room for the octant ($\pi/2 - \theta_{23}$) degeneracy. Each of the four true values of $\mathrm{sign}(\Delta m^2_{23})$ and θ_{23}: normal: $\mathrm{sign}(\Delta m^2_{23})$ = 1, $\theta_{23} < \pi/4$; sign: $\mathrm{sign}(\Delta m^2_{23})$ = –1, $\theta_{23} < \pi/4$; octant: $\mathrm{sign}(\Delta m^2_{23})$ = 1, $\theta_{23} > \pi/4$; mixed: $\mathrm{sign}(\Delta m^2_{23})$ = –1, $\theta_{23} > \pi/4$ has been fitted with the four possible fit combinations, the worst case is then taken. Also shown are the leptonic CP violation discovery potentials neglecting the degenerate solutions (that is choosing the right combination of $\mathrm{sign}(\Delta m^2_{23})$ and θ_{23} for the fit). The effects of degeneracies are sometimes visible for high values of θ_{13}, precisely the region where they can be reduced by a combined analysis with atmospheric neutrinos [109].

Betabeams require a proton driver in the energy range of 1–2 GeV, 0.5 MW power. The SPL can be used as injector, at most 10% of its protons would be consumed. This allows a simultaneous βB and SPL-SB run, the two neutrino beams having similar neutrino energies (cf. Fig. 8). The same detector could then be exposed to 2×2 beams (ν_μ and $\overline{\nu}_\mu \times \nu_{\rm e}$ and $\overline{\nu}_{\rm e}$) having access to CP, T and CPT violation searches in the same run. This is particularly important because CP and T channels would have different systematics and different backgrounds, allowing for independent checks of the same signal. Furthermore, the SPL ν_μ and $\overline{\nu}_\mu$ beams would be the ideal tool to measure signal cross-sections in the close detector.

With this combination of neutrino beams a sensitivity to $\sin^2 2\theta_{13} \geq 2{\times}10^{-4}$ (90% CL) exploiting a CP violation discovery potential at 3σ if $\delta_{\rm CP} \geq 18°$ and $\theta_{13} \geq 0.55°$ [96] (Fig. 10).

Betabeam capabilities for the maximum values of γ available with the SPS, $\gamma^6{\rm He} = 150$ have been computed in Ref. [110].

Betabeam capabilities for ions accelerated at higher energies than those allowed by the SPS were first computed in Ref. [111] and subsequently in Refs. [110, 112, 113]. These studies assume that the same ion fluxes of the baseline scenario can be maintained. However, this is not the case if the number of stored bunches is kept constant in the storage ring. On the other hand, by increasing γ (i.e. the neutrino energy) the atmospheric neutrinos' background constraint on the total bunch length [84] tends to vanish. Studies are in progress at CERN in order to define realistic neutrino fluxes as a function of γ [114].

The outcome of these studies shows, anyway, that higher energy betabeams have a CP discovery potential competitive with a neutrino factory, as shown in the plots of Fig. 12 [113].

It is worth noting that if a high-intensity betabeam with $\gamma \sim$ 300–500 (requiring a higher energy accelerator than SPS, like the Super-SPS [115]) can be built, a 40 kt iron calorimeter located at the Gran Sasso Laboratory will have the possibility to discover a non-vanishing $\delta_{\rm CP}$ if $\delta_{\rm CP} > 20°$ for $\theta_{13} \geq 2°$ (99% CL) and measure the sign of Δm^2_{23} [116].

A very recent development of the betabeam concept is the conceptual possibility to have monochromatic, single-flavour neutrino beams thanks to the electron capture process [117, 118]. A suitable ion candidate exists, ^{150}Dy, whose performances have already been delineated [117].

4.4 The neutrino factory[3]

In a Neutrino Factory [120] muons are accelerated from an intense source to energies of several GeV, and injected in a storage ring with long straight sections. The muon decays

$$\mu^+ \rightarrow e^+ \nu_{\rm e} \overline{\nu}_\mu \quad \text{and} \quad \mu^- \rightarrow e^- \overline{\nu}_{\rm e} \nu_\mu$$

[3] Material for this section is taken mainly from Ref. [119].

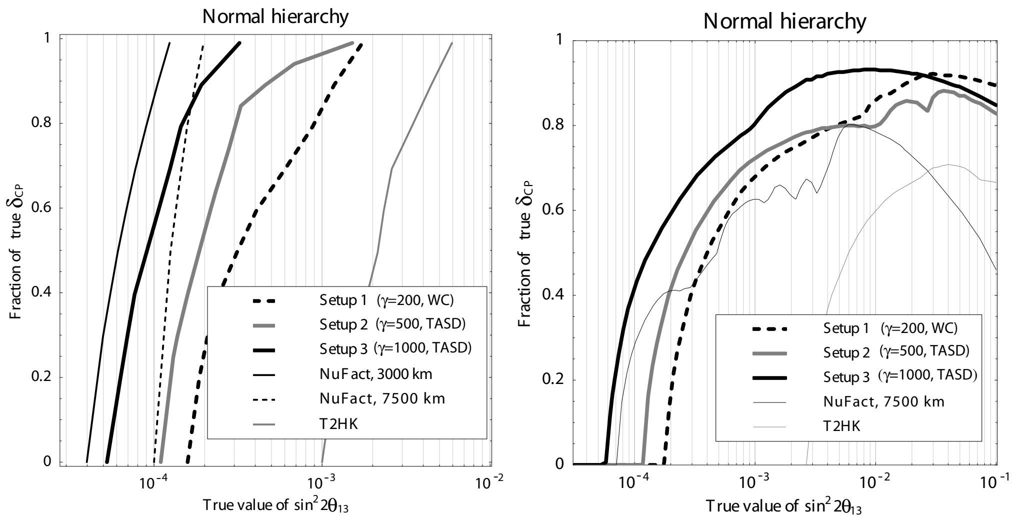

Fig. 12: Left: The $\sin^2 2\theta_{13}$ discovery reach (including systematics and correlations) for different set-ups (the TASD detector is described in Section 4.1) as a function of the true values of $\sin^2 2\theta_{13}$ and δ_{CP} (3σ confidence level). The values of δ_{CP} are 'stacked' to the fraction of δ_{CP}, i.e., $\sin^2 2\theta_{13}$ will be discovered for a certain fraction of all possible values of δ_{CP}. For a uniform probability contribution in δ_{CP}, the fraction of δ_{CP} directly corresponds to the probability to discover $\sin^2 2\theta_{13}$. Taken from Ref. [113]. Right: The sensitivity to CP violation for the normal mass hierarchy for different experiments as a function of the true values of $\sin^2 2\theta_{13}$ and δ_{CP} at the 3σ confidence level. Taken from Ref. [113].

provide a very well known flux with energies up to the muon energy itself. The overall layout is shown in Fig. 13.

Neutrino Factory designs have been proposed in Europe [121, 122], the US [123–125], and Japan [126]. Of these designs, the American one is the most developed, and we shall use it as a general example with a few exceptions. The conclusions of these studies is that, provided sufficient resources are available, an accelerator complex capable of providing about 10^{21} muons per year can be built. The Neutrino Factory consists of the following subsystems:

Proton driver. Provides 1–4 MW of protons on a pion production target. For the Neutrino Factory application, the energy of the beam within 4–30 GeV is not critical, since it has been shown that the production of pions is roughly proportional to beam power. The time structure of the proton beam has to be matched with the time spread induced by pion decay (1–2 ns); for a linac driver such as the SPL, this requires an additional accumulator and compressor ring.

Target, capture and decay. A high-power target sits within a 20 T superconducting solenoid, which captures the pions. The high magnetic field smoothly decreases to 1.75 T downstream of the target, matching into a long solenoid decay channel. A design with horn collection has been proposed at CERN for the Neutrino Factory, with the additional benefit that it can also be used for a superbeam design.

Bunching and phase rotation. The muons from the decaying pions are bunched using a system of RF cavities with frequencies that vary along the channel. A second series of RF cavities with higher gradients is used to rotate the beam in longitudinal phase-space, reducing the energy spread of the muons.

Cooling. A solenoid focusing channel with high-gradient 201 MHz RF cavities and either liquid-hydrogen or liquid-hydrogen absorbers is used to reduce the transverse phase-space occupied by the beam. The muons lose, by d*E*/d*x* losses, both longitudinal and transverse momentum as they pass through the absorbers. The longitudinal momentum is replaced by re-acceleration in the RF cavities.

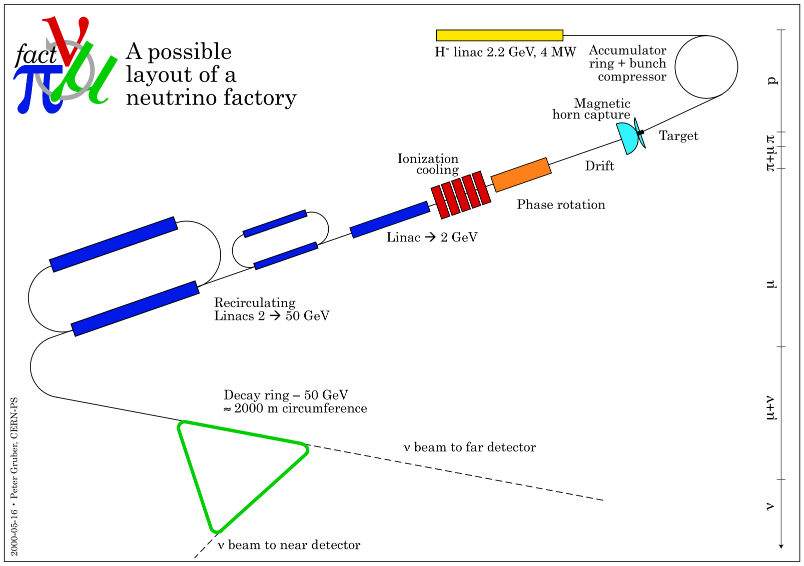

Fig. 13: Schematic layout of a Neutrino Factory

Acceleration. The central momentum of the muons exiting the cooling channel is 220 MeV/c. A superconducting linac with solenoid focusing is used to raise the energy to 1.5 GeV. Thereafter, a recirculating linear accelerator raises the energy to 5 GeV, and a pair of fixed-field alternating-gradient rings accelerate the beam to at least 20 GeV.

Storage ring. A compact racetrack geometry ring is used in which 35% of the muons decay in the neutrino-beam-forming straight section. If both signs are accelerated, one can inject in two superimposed rings or in two parallel straight sections. This scheme produces over 6×10^{20} useful muon decays per operational year and per straight section in a triangular geometry.

The European Neutrino Factory design is similar to the US design, but differs in the technologies chosen to implement the subsystems.

The Japanese design is quite different, and uses very-large-acceptance accelerators. Cooling, although it would improve performance, is not considered mandatory in this scheme.

An important Neutrino Factory R&D effort has been ongoing in Europe, Japan, and the US for a few years. Significant progress has been made towards optimizing the design, developing and testing the required components, and reducing the cost.

To illustrate this progress, the cost estimate for a recent update of the US design [127] is compared in Table 4 with the corresponding cost for the previous 'Study II' US design [125]. In this design the Neutrino Factory would accelerate protons up to 20 GeV/c, with a flux of 1.2×10^{20} muon decays per straight section per year for a proton driver power of 1 MW (4.8×10^{20} μ decays per year at 4 MW).

It should be noted that the Study II design cost was based on a significant amount of engineering input to ensure design feasibility and establish a good cost basis. Neutrino Factory R&D has reached a critical stage in which support is required for two key international experiments (MICE [128] and Targetry [129]) and a third-generation international design study. If this support is forthcoming, a Neutrino Factory could be added to the Neutrino Physics roadmap by the end of the decade.

4.4.1 Oscillations physics at the neutrino factory

Considering a Neutrino Factory with simultaneous beams of positive and negative muons, 12 oscillation processes can in principle be studied, Table 5.

Table 4: Comparison of unloaded Neutrino Factory cost estimates in M$ for the US Study II design and improvement estimated for the latest updated US design (20 GeV/c muons). Costs are shown including A: the whole complex; B: no proton driver; and C: no proton driver and no target station in the estimates. Table from Ref. [127].

	A	B	C
Old estimate from Study II	1832	1641	1538
Multiplicative factor for new estimate	0.67	0.63	0.60

Table 5: Oscillation processes in a Neutrino Factory

$\mu^+ \to e^+\nu_e\overline{\nu}_\mu$	$\mu^- \to e^-\overline{\nu}_e$	
$\overline{\nu}_\mu \to \overline{\nu}_\mu$	$\nu_\mu \to \nu_\mu$	disappearance
$\overline{\nu}_\mu \to \overline{\nu}_e$	$\nu_\mu \to \nu_e$	appearance (challenging)
$\overline{\nu}_\mu \to \overline{\nu}_\tau$	$\nu_\mu \to \nu_\tau$	appearance (atm. oscillation)
$\nu_e \to \nu_e$	$\overline{\nu}_e \to \overline{\nu}_e$	disappearance
$\nu_e \to \nu_\mu$	$\overline{\nu}_e \to \overline{\nu}_\mu$	appearance: 'golden' channel
$\nu_e \to \nu_\tau$	$\overline{\nu}_e \to \overline{\nu}_\tau$	appearance: 'silver' channel

Of course the neutrinos coming from decays of muons of different charge must not be confused with each other; this can be done by timing, provided the storage ring is adequately designed.

One of the most striking features of the Neutrino Factory is the precision with which the characteristics of all components of the beam could be known. This was studied extensively in a CERN Report [130], where the following were considered:

– beam polarization effects, and its measurement with a polarimeter, allowing extraction of the beam energy, energy spread and verification that the polarization effects on the neutrino fluxes average out to zero with high precision;
– beam divergence effects, with the preliminary, conceptual study of a Cherenkov device to monitor the angular distribution of muons in the beam [131];
– radiative effects in muon decay;
– absolute normalization to be obtained both from a beam monitor, with the added possibility of an absolute cross-section normalization using the inverse muon decay reaction, $\nu_\mu e^- \to \mu^-\nu_e$, in the near detector;

with the conclusion that, in principle, a normalization of fluxes and cross-sections with a precision of 10^{-3} can be contemplated. Some of these features should also be present for a betabeam, and for any facility in which a stored beam of well-defined optical properties is used to produce neutrinos. This will be an essential difference with respect to the superbeams, where the knowledge of relative neutrino-vs-antineutrino cross-sections and fluxes will rely on the understanding of the initial particle production.

The Neutrino Factory lends itself naturally to the exploration of neutrino oscillations between ν flavours with high sensitivity. The detector should be able to perform both appearance and disappearance experiments, providing lepton identification and charge discrimination which is a tag for the initial flavour and of the oscillation. In particular the search for $\nu_e \to \nu_\mu$ transitions ('golden channel') [132] appears to be very attractive at the Neutrino Factory, because this transition can be studied in appearance mode looking for μ^- (appearance of wrong-sign μ) in neutrino beams where the neutrino type that is searched for is totally absent (μ^+ beam in a Neutrino Factory).

The emphasis has been placed so far on small mixing angles and small mass differences. With two 40 kt magnetic detectors (MINOS-like) at 700 (or 7000) and 3000 km, with a conservative high-energy muon detection threshold of 5 GeV, exposed to both polarity beams and 10^{21} muon decays, it will be possible to explore the θ_{13} angle down to 0.1° opening the possibility to measure the $\delta_{\rm CP}$ phase [74, 132, 133], as shown by the plots of Fig. 17.

On the other hand, the relative high energies of neutrinos selected by placing such a high threshold on muon energies require very long baselines (several thousand kilometres) for Neutrino Factory experiments, and at these baselines CP asymmetries are dominated by matter effects [134]. Taking advantage of the matter effects, such an experiment will determine unambiguously sign(Δm^2_{23}) for large enough θ_{13} ($\theta_{13} \geq 2^\circ$). However, we recall that, as for other facilities, the determination of (θ_{13}, δ) at the Neutrino Factory is not free of ambiguities: up to eight different regions of the parameter space can fit the same experimental data. In order to solve these ambiguities, a single experimental point on a single neutrino beam is not enough.

One possibility at the Neutrino Factory is to make use of the rich flavour-content of the beam. This implies an optimized network of detectors with different characteristics. Indeed, a specific disadvantage of the considered magnetized iron detector when dealing with degeneracies is the following: the lower part of the Neutrino Factory spectrum (say, $E_\nu \in [0, 10]$ GeV) cannot be used on account of the extremely low efficiency in this region of the detector. This part of the spectrum, on the other hand, is extremely useful to solve degeneracies, as has been shown in several papers [135].

One possibility is to envisage that all betabeams, superbeams, and Neutrino Factories will be available. Several investigations on how to solve this problem have been carried out, as reported in Ref. [136] and references therein. As an example, the result of such an analysis combining the golden and the silver ($\nu_e \rightarrow \nu_\tau$) νF channels with the SPL-SB, taken from Ref. [136], is shown in Fig. 14. It should be stressed, however, that the analysis presented in this figure does not include systematic errors and it is based on a non-updated simulation of the magnetized iron detector [137].

A more interesting but challenging task will be to assume that only one of these facilities will become available (a more economical assumption!) and to investigate its ability to solve these ambiguities.

There are several ways of solving this problem at a Neutrino Factory. Clearly one should use more than just the wrong-sign muons. Such a study was performed assuming the feasibility of a liquid argon detector [138]. By separating the events into several classes: right-sign muon, wrong-sign muon, electron and neutral-current; and by performing a fine energy-binning down to low energies, it was shown that the matter resonance could be neatly measured as shown in Fig. 15. The simultaneous observation of the four aforementioned channels was shown to allow resolution of ambiguities to a large extent.

The tau appearance channel (*silver channel*) [139] has been advocated as a powerful means of solving ambiguities. This can be readily understood since this channel has the opposite-sign dependence on $\delta_{\rm CP}$ than the golden one, while having similar dependence on matter effects and θ_{13}. Another channel to be used is the ν_μ disappearance channel, rather effective for large values of θ_{13} [86]. The principle of degeneracies-solving using several baselines, binning in energies, and both silver and golden channels is explained on Fig. 16. The full demonstration that a Neutrino Factory alone with a complete set of appropriate detectors and two baselines could unambiguously do the job remains, however, to be worked out.

According to Table 5, Neutrino Factory potential could be further improved with a detector capable of measuring the charge of the electrons. R&D efforts for a liquid argon detector embedded in a magnetic field are ongoing [141]; the first curved tracks were recently observed in a 10 litre liquid argon TPC embedded in a magnetic field [142].

5 Preliminary comparison of accelerator facilities

The comparison of the performance of different facilities cannot be considered complete. Several different aspects still need to be clarified before a final comparison can be performed.

– Costs, timescales, fluxes of the different accelerators systems have not yet been fully worked out.

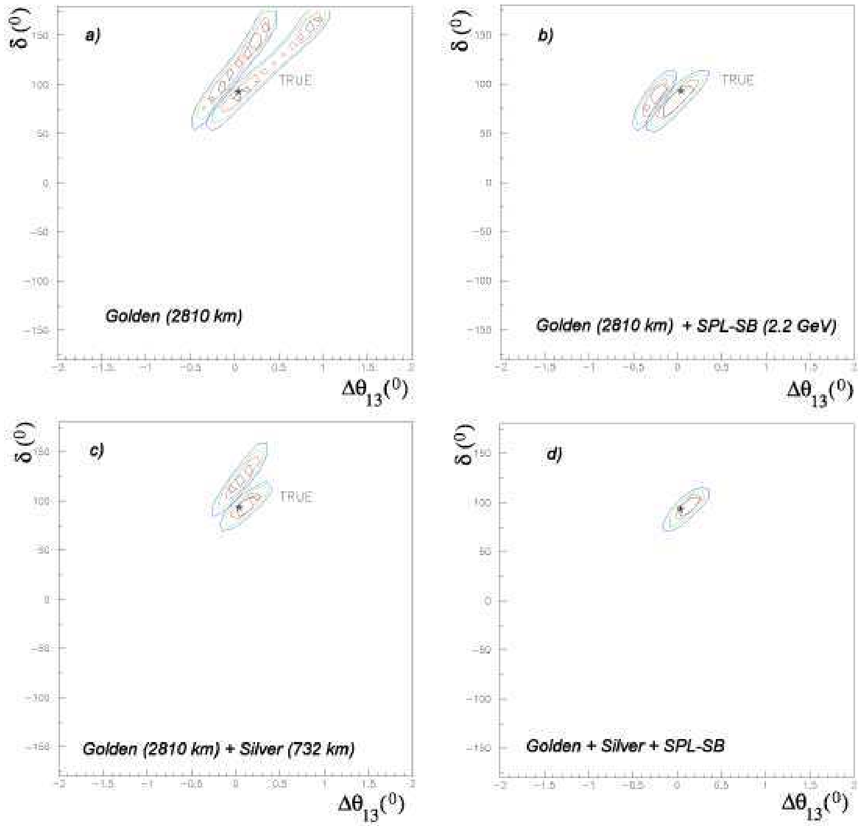

Fig. 14: The results of a χ^2 fit for $\bar{\theta}_{13} = 2°; \bar{\delta}_{\rm CP} = 90°$. Four different combinations of experimental data are presented: a) magnetized iron detector (MID) at a νN; b) MID plus SPL-SB; c) MID plus hybrid emulsion (HE) at νF; d) the three detectors together. Note how in case (d) the eight-fold degeneracy is solved and a good reconstruction of the physical $\theta_{13}, \delta_{\rm CP}$ values is achieved. From Ref. [136].

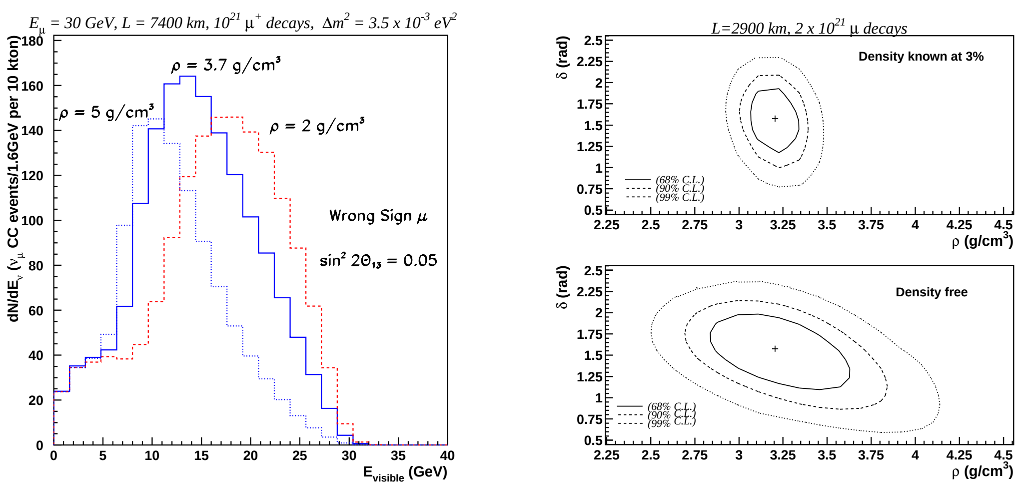

Fig. 15: Left: variation of the MSW resonance peak for wrong-sign muons as a function of Earth density. The plot is normalized to $10^{21}\mu^+$ decays. Right: result of a simultaneous fit to the matter density and to the CP phase for a 10 kt detector situated 7000 km away from a 30 GeV muon storage ring Neutrino Factory. Both plots are from Ref. [138].

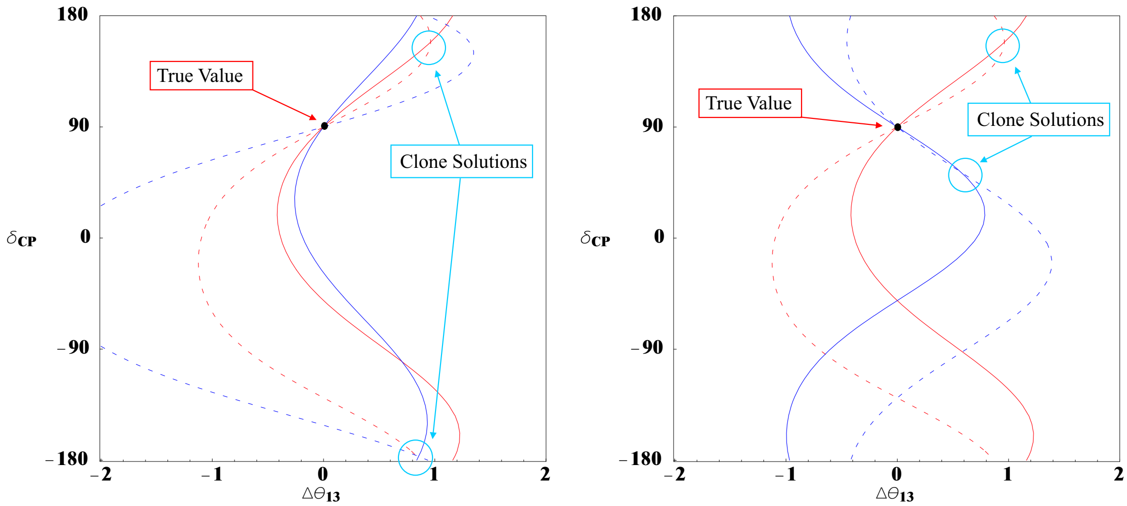

Fig. 16: Solving the intrinsic degeneracy: two baselines $L = 730$ and 3500 km, same channel example on the left, vs. two channels $\nu_e \to \nu_\mu$ vs. $\nu_e \to \nu_\tau$ same baseline example on the right. From Ref. [140].

- The performance and optimization of the detectors are not known at the same level: for water Cherenkov detectors full simulation and full reconstructions of the events are available, based on the experience of Super-Kamiokande, but the optimization in terms of photodetector coverage is still to be performed. The optimization of the magnetic detector (and of the assumed cuts) for the Neutrino Factory was performed for very small values of θ_{13}, and the performance is for the moment based on parametrization of the MINOS performance, and very low values of backgrounds from hadron decays (pions, kaons, and charm) are claimed possible. The performances of the emulsion detector for the silver channel of Nufact or of the liquid argon detector are based on full simulations, but will need to be benchmarked using the performances of OPERA and ICARUS, respectively.
- Several different measurements can be defined as significant for the facility, and they cannot be optimized all together (see also Ref. [113]). For instance, the following measurements bring different optimizations: sensitivity to θ_{13}, discovery of subleading $\nu_\mu \to \nu_e$ oscillations, unambiguous measurement of θ_{13}, measure of sign(Δm^2_{23}), discovery of leptonic CP violation, unambiguous measurement of $\delta_{\rm CP}$.
- The final extraction of the oscillation parameters can significantly change based on technical aspects of the fitting programs (like choice of the input parameters, treatment of the errors on the neutrino oscillation parameters, treatment of degeneracies etc.).

  The GLoBES program [108] represents a major improvement: it allows one to compare different facilities keeping the same fitting program, and it makes explicit the description of the performances of the detectors. We strongly recommend that new developments in this field make use of GLoBES, in view of a more transparent comparison of the different proposals.
- Systematic errors that strongly influence performances, for instance sensitivity to leptonic CP violation for large values of θ_{13}, are not substantially discussed in the literature. We are confident that facilities where neutrino fluxes can be known *a priori,* as in the case of betabeams and Neutrino Factories, will have smaller systematic errors (and smaller backgrounds) than, for example, neutrino superbeams. This difference is not known quantitatively today.

  The concept of the near-detector station(s) and flux monitoring systems has to be proposed together with the facility, in particular for low-energy (few 100 MeV) betabeams and superbeams where the issues of muon mass effect, Fermi motion and binding energy uncertainty are highly non-trivial.

Finally, for the Neutrino Factory, the question of systematics on the prediction of matter effects is essential for the performance at large values of θ_{13}.

– Overall performances will depend on the combination of several different inputs. For instance, low-energy superbeams and betabeams can profit from atmospheric neutrino oscillations, detected with a large statistics in the gigantic water Cherenkov detector, to solve degeneracies and measure sign(Δm^2_{23}), as shown in Ref. [109]. A Neutrino Factory can take advantage of the combination of different channels such as the golden and the silver one (see Section 4.4), detectors at different baselines, atmospheric neutrinos collected in the the iron magnetized detector [143]. A full exploration of these possibilities is an ongoing process and the results available today cannot be considered final.

Having said that, a comparison of the facilities that at present are described in the GLoBES library [144], as far as concerns and leptonic CP violation discovery potential, is shown in Fig. 17.

The plots show the sensitivity to CP violation at 3σ CL ($\Delta\chi^2 = 9$). Sensitivity to CP violation is defined, for a given point in the θ_{13}–$\delta_{\rm CP}$ plane, by being able to exclude $\delta_{\rm CP}$ = 0 and $\delta_{\rm CP} = \pi$ at the given confidence level. All plots have been prepared with GLoBES [108].

Degeneracies and correlations are fully taken into account. For all set-ups the appropriate disappearance channels have been included. The betabeam is lacking muon neutrino disappearance, but the result does not change if T2K disappearance information is included in the analysis. In all cases systematics between neutrinos, antineutrinos, appearance and disappearance is uncorrelated. For all set-ups with a water Cherenkov detector the systematics applies both to background and signal, uncorrelated.

The Neutrino Factory assumes $3.1\times10^{20}\mu^+$ decays per year for 10 years and $3.1\times10^{20}\mu^-$ decays for 10 years. It has one detector with m = 100 kt at 3000 km and another 30 kt detector at 7000 km. The density errors between the two baselines are uncorrelated, sensitivities are computed for 2% and 5% systematic error on matter density. The systematics are 0.1% on the signal and 20% on the background, uncorrelated. The detector threshold and the other parameters are taken from Ref. [135] and approximate the results of Ref. [137].

The betabeam assumes 5.8×10^{18} ^{6}He decays per year for five years and 2.2×10^{18} ^{18}Ne decays per year for five years. The detector mass is 500 kt. The detector description and the globes-file is from Ref. [106].

The SPL set-up is taken from Ref. [97], and the detector mass is 500 kt.

The T2HK set-up is taken from Ref. [135] and closely follows the LoI [81]. The detector mass is 1000 kt and it runs with 4 MW beam power, six years with antineutrinos and two years with neutrinos. The systematic error on both background and signal is 5%.

The oscillation parameters were [145, 146]: $\delta m^2_{23} = 0.0024\,{\rm eV}^2$, $\delta m^2_{12} = 0.00079\,{\rm eV}^2$, $\theta_{23} = \pi/4$, $\theta_{12} = 0.578$. The input errors are (at 1σ) 10% on δm^2_{23}, 10% on θ_{23}, 10% on θ_{12}, 4% on δm^2_{12}, 5% on ρ (unless otherwise stated).

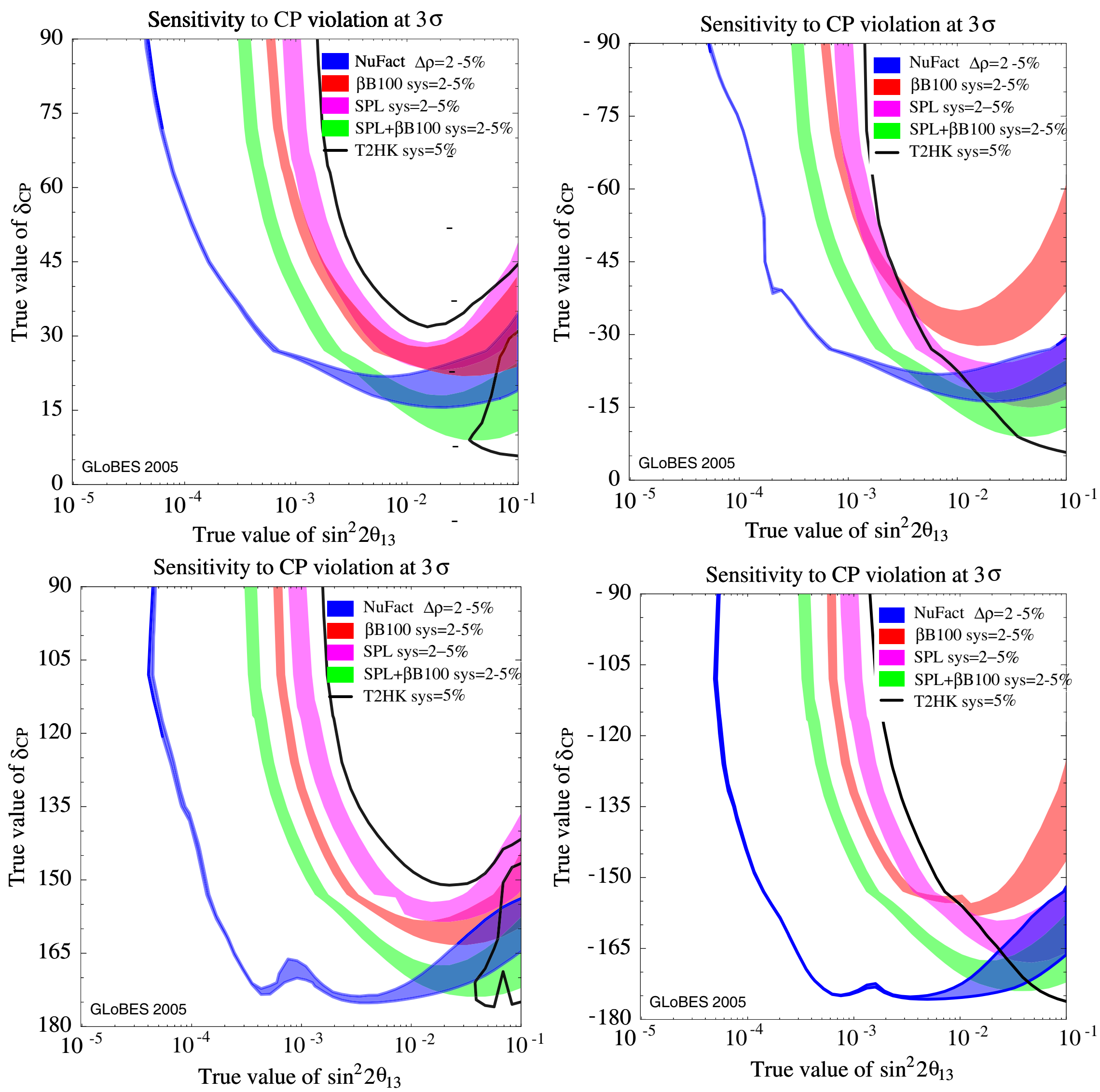

Fig. 17: The $\delta_{\rm CP}$ discovery potential at 3σ (see text) computed for 10 years of running time. For an explanation of the facilities see the text. The four plots represent the four possible quadrants of $\delta_{\rm CP}$ values; performances of the different facilities are not at all the same in the different quadrants. The width of the curves reflects the range of systematic errors: 2% and 5% on signal and background errors for SPL-SB and betabeam, 2% and 5% for the matter density. Other systematic errors are 5% on signal and background of T2HK, 0.1% for the nufact signal, 20% for nufact backgrounds. A description of the facilities can be found in Ref. [144].

References

[1] C. Weinheimer, *Nucl. Phys. Proc. Suppl.* **118** (2003) 279.

[2] V.M. Lobashev *et al., Nucl. Phys. Proc. Suppl.* **91** (2001) 280; V.M. Lobashev, in Proceedings of Neutrino Telescopes 2005, Venice, pp. 507–517.

[3] KATRIN Collaboration, hep-ex/0109033.

[4] A. Monfardini *et al.*, arXiv:hep-ex/0509038.

[5] H.V. Klapdor-Kleingrothaus, A. Dietz and I.V. Krivosheina, *Found. Phys.* **32** (2002) 1181 [Erratum *ibid.* **33** (2003) 679] [arXiv:hep-ph/0302248].

[6] Y.G. Zdesenko, F.A. Danevich and V.I. Tretyak, *Phys. Lett. B* **546** (2002) 206.

[7] A.M. Bakalyarov, A.Y. Balysh, S.T. Belyaev, V.I. Lebedev and S.V. Zhukov [C03-06-23.1 Collaboration], *Phys. Part. Nucl. Lett.* **2** (2005) 77 [*Pisma Fiz. Elem. Chast. Atom. Yadra* **2** (2005) 21] [arXiv:hep-ex/0309016].

[8] C. Arnaboldi *et al., Phys. Rev. Lett.* **95** (2005) 142501 [arXiv:hep-ex/0501034].

[9] R. Arnold *et al.* [NEMO Collaboration], arXiv:hep-ex/0507083.

[10] R. Ardito *et al.*, arXiv:hep-ex/0501010.

[11] S. Schonert *et al.* [GERDA Collaboration], *Nucl. Phys. Proc. Suppl.* **145** (2005) 242.

[12] M. Fukugita, arXiv:hep-ph/0511068.

[13] M. Fukugita and T. Yanagida, *Phys. Lett. B* **174** (1986) 45.

[14] W. Buchmüller, P. Di Bari and M. Plümacher, *Nucl. Phys. B* **665** (2003) 445.

[15] G.F. Giudice, A. Notari, A. Riotto and A. Strumia, *Nucl. Phys. B* **685** (2004) 89.

[16] W. Buchmüller, P. Di Bari and M. Plümacher, *Ann. Phys.* **315** (2005) 303.

[17] C.L. Bennett *et al., Astrophys. J. Suppl.* **148** 2003) 1.

[18] D.G. York *et al., Astron. J.* **120** (2000) 159.

[19] D.N. Spergel *et al., Astrophys. J. Suppl.* **148** (2003) 175.

[20] M. Tegmark *et al., Phys. Rev. D* **69** (2004) 103501.

[21] D. Eisenstein *et al.,* arXiv:astro-ph/0501171.

[22] M. Tegmark *et al., Astrophys. J.* **606** (2004) 702.

[23] S. Cole *et al., Mon. Not. R. Astron. Soc.* **362** (2005) 505.

[24] W. Hu, D.J. Eisenstein and M. Tegmark, *Phys. Rev. Lett.* **80** (1998) 5255.

[25] R. Valdarnini, T. Kahniashvili and B. Novosyadlyj, *Astron. Astrophys.* **336** (1998) 11.

[26] S. Hannestad, *JCAP* **5** (2003) 004.

[27] S.W. Allen, R.W. Schmidt and S.L. Bridle, *Mon. Not. R. Astron. Soc.* **346** (2003) 593.

[28] V. Barger, D. Marfatia and A. Tregre, *Phys. Lett. B* **595** (2004) 55.

[29] R.A.C. Croft, D.H. Weinberg, N. Katz and L. Hernquist, *Astrophys. J.* **495** (1998) 44.

[30] P. McDonald *et al.,* arXiv:astro-ph/0405013.

[31] U. Seljak *et al.,* arXiv:astro-ph/0407372.

[32] R.A.C. Croft, W. Hu and R. Davé, *Phys. Rev. Lett.* **83** (1999) 1092.

[33] Ø. Elgarøy and O. Lahav, *New J. Phys.* **7** (2005) 61.

[34] Precision electroweak measurements on the Z resonance, The LEP Collaborations, hep-ex/0509008, to appear in Physics Reports.

[35] B.T. Cleveland *et al., Astrophys. J.* **496** (1998) 505.

[36] M. Altmann *et al.* [GNO Collaboration], *Phys. Lett. B* **490** (2000) 16 [arXiv:hep-ex/0006034].

[37] J.N. Abdurashitov *et al.* [SAGE Collaboration], *J. Exp. Theor. Phys.* **95** (2002) 181 [*Zh. Eksp. Teor. Fiz.* **122** (2002) 211] [arXiv:astro-ph/0204245].

[38] S. Fukuda *et al.* [Super-Kamiokande Collaboration], *Phys. Lett. B* **539** (2002) 179 [arXiv:hep-

ex/0205075].

[39] S.R. Ahmad *et al.* [SNO Collaboration], nucl-ex/0204008; S.N. Ahmed *et al.* [SNO Collaboration], *Phys. Rev. Lett.* **92** (2004) 181301 [arXiv:nucl-ex/0309004].

[40] K. Eguchi *et al.* [KamLAND Collaboration], *Phys. Rev. Lett.* **90** (2003) 021802 [arXiv:hep-ex/0212021]; T. Araki *et al.* [KamLAND Collaboration], *Phys. Rev. Lett.* **94** (2005) 081801 [arXiv:hep-ex/0406035].

[41] Y. Fukuda *et al.* [Super-Kamiokande Collaboration], *Phys. Rev. Lett.* **81** (1998) 1562 [arXiv:hep-ex/9807003].

[42] M.C. Sanchez *et al.* [Soudan 2 Collaboration], *Phys. Rev. D* **68** (2003) 113004 [arXiv:hep-ex/0307069].

[43] M. Ambrosio *et al.* [MACRO Collaboration], *Phys. Lett. B* **566** (2003) 35 [arXiv:hep-ex/0304037].

[44] Y. Ashie *et al.* [Super-Kamiokande Collaboration], *Phys. Rev. Lett.* **93** (2004) 101801 [arXiv:hep-ex/0404034].

[45] M. Apollonio *et al.* [CHOOZ Collaboration], *Eur. Phys. J. C* **27** (2003) 331 [arXiv:hep-ex/0301017].

[46] E. Aliu *et al.* [K2K Collaboration], *Phys. Rev. Lett.* **94** (2005) 081802 [arXiv:hep-ex/0411038].

[47] See for instance P. Lipari, *Phys. Rev. D* **64** (2001) 033002 [arXiv:hep-ph/0102046].

[48] G.L. Fogli, E. Lisi, A. Marrone and A. Palazzo, arXiv:hep-ph/0506083.

[49] A. Aguilar *et al.* [LSND Collaboration], *Phys. Rev. D* **64** (2001) 112007 [arXiv:hep-ex/0104049].

[50] B. Armbruster *et al.* [KARMEN Collaboration], *Phys. Rev. D* **65** (2002) 112001 [arXiv:hep-ex/0203021].

[51] P. Astier *et al.* [NOMAD Collaboration], *Phys. Lett. B* **570** (2003) 19 [arXiv:hep-ex/0306037].

[52] E. Church *et al.* [BooNe Collaboration], arXiv:nucl-ex/9706011.

[53] A. Guglielmi, M. Mezzetto, P. Migliozzi and F. Terranova, arXiv:hep-ph/0508034.

[54] E. Ables *et al.* [MINOS Collaboration], Fermilab-proposal-0875; G. S. Tzanakos [MINOS Collaboration], *AIP Conf. Proc.* **721** (2004) 179.

[55] The Fermilab NuMI Group, *NumI Facility Technical Design Report*, Fermilab Report NuMI-346 (1998).

[56] F. Arneodo *et al.* [ICARUS Collaboration], *Nucl. Instrum. Meth. A* **461** (2001) 324; P. Aprili *et al., The ICARUS Experiment*, CERN-SPSC/2002-27, SPSC-P-323.

[57] OPERA Collaboration, CERN-SPSC-P-318, LNGS-P25-00; H. Pessard [OPERA Collaboration], arXiv:hep-ex/0504033; M. Guler *et al.* [OPERA Collaboration], *OPERA: An Appearance Experiment to Search for $\nu_\mu \rightarrow \nu_\tau$ Oscillations in the CNGS Beam,* Experimental proposal, CERN-SPSC-2000-028.

[58] G. Acquistapace *et al., The CERN Neutrino Beam to Gran Sasso,* report CERN 98-02, INFN/AE-98/05 (1998); CERN-SL/99-034(DI), INFN/AE-99/05 Addendum.

[59] H.W. Atherton *et al., Precise Measurements of Particle Production by 400 GeV/c Protons on Beryllium Targets,* report CERN-80-07.

[60] G. Ambrosini *et al.* [NA56/SPY Collaboration], *Eur. Phys. J. C* **10** (1999) 605.

[61] L. Casagrande *et al., The Alignment of the CERN West Area Neutrino Facility,* report CERN 96-06.

[62] A. Guglielmi and G. Collazuol, *Monte Carlo Simulation of the SPS WANF Neutrino Flux,* INFN/AE-03/05 (2003);
P. Astier *et al.* [NOMAD Collaboration], *Nucl. Instrum. Meth. A* **515** (2003) 800 [arXiv:hep-ex/0306022].

[63] A. Ferrari, A. Guglielmi and P.R. Sala, *Nucl. Phys. Proc. Suppl.* **145** (2005) 93 [arXiv:hep-ph/0501283].

[64] Report to the Fermilab Director by the Proton Committee, November 9, 2004,

http://www.fnal.gov/directorate/program_planning/Nov2004PACPublic/Draft_Proton_Plan_v2.pdf.

[65] M. Komatsu, P. Migliozzi and F. Terranova, *J. Phys. G* **29** (2003) 443 [arXiv:hep-ph/0210043].

[66] P. Migliozzi and F. Terranova, *Phys. Lett. B* **563** (2003) 73 [arXiv:hep-ph/0302274].

[67] M. Benedikt, K. Cornelis, R. Garoby, E. Metral, F. Ruggiero and M. Vretenar, Report of the High Intensity Protons Working Group, CERN-AB-2004-022-OP-RF.

[68] F. Ardellier *et al.* [Double-CHOOZ Collaboration], arXiv:hep-ex/0405032.

[69] A. De Rújula, M.B. Gavela, P. Hernandez, *Nucl. Phys. B* **547** (1999) 21, arXiv: hep-ph/9811390.

[70] *ECFA/CERN Studies of a European Neutrino Factory Complex,* A. Blondel *et al.,* Eds., report CERN 2004-002 (2004) http://preprints.cern.ch/cernrep/2004/2004-002/2004-002.html

[71] Beams for European Neutrino Experiments is a Networking Activity (http://bene.na.infn.it/) supported by the EC and most major European Agencies in the framework of the FP6 Integrated Activity CARE (Coordinated Accelerator R&D in Europe) http://esgard.lal.in2p3.fr/Project/Activities/Current/. The scope of BENE is also described in more detail in the following document: http://esgard.lal.in2p3.fr/Project/Activities/Current/Networking/N3/BENE-downsized-11.doc.

[72] Summary of the Workshop on Physics with a Multimegawatt Proton Source, CERN, 2004; CERN-SPSC-2004–024; SPSC-M-722.

[73] B. Richter, SLAC-PUB-8587 [arXiv:hep-ph/0008222], and references therein.

[74] J. Burguet-Castell, M.B. Gavela, J.J. Gomez-Cadenas, P. Hernandez and O. Mena, *Nucl. Phys. B* **608** (2001) 301 [arXiv:hep-ph/0103258].

[75] K. Kimura, A. Takamura and H. Yokomakura, *Phys. Rev. D* **66** (2002) 073005 [arXiv:hep-ph/0205295]; E.K. Akhmedov, R. Johansson, M. Lindner, T. Ohlsson and T. Schwetz, *JHEP* **0404** (2004) 078 [arXiv:hep-ph/0402175]; M. Freund, *Phys. Rev. D* **64** (2001) 053003 [arXiv:hep-ph/0103300].

[76] H. Minakata and H. Nunokawa, *JHEP* **0110** (2001) 001 [arXiv:hep-ph/0108085].

[77] V. Barger, D. Marfatia and K. Whisnant, *Phys. Rev. D* **65** (2002) 073023 [arXiv:hep-ph/0112119].

[78] G.L. Fogli and E. Lisi, *Phys. Rev. D* **54** (1996) 3667 [arXiv:hep-ph/9604415].

[79] M.G. Catanesi *et al.* [HARP Collaboration], CERN-SPSC/2001-017, SPSC/P322, May 2001.

[80] M.G. Catanesi *et al.* [HARP Collaboration], arXiv:hep-ex/0510039.

[81] Y. Itow *et al.*, The JHF-Kamiokande neutrino project, arXiv:hep-ex/0106019.

[82] The E889 Collaboration, *Long Baseline Neutrino Oscillation Experiment at the AGS,* Brookhaven National Laboratory Report BNL 52459, April 1995; A. Para and M. Szleper, arXiv:hep-ex/0110032.

[83] S. Geer, *Phys. Rev. D* **57** (1998) 6989 [Erratum *ibid. D* **59** (1999) 039903], [hep-ph/9712290].

[84] P. Zucchelli, *Phys. Lett. B* **532** (2002) 166.

[85] H. Minakata, M. Sonoyama and H. Sugiyama, *Phys. Rev. D* **70** (2004) 113012; hep-ph/0406073; A. Donini, D. Meloni and S. Rigolin, hep-ph/0506100.

[86] A. Donini, E. Fernandez-Martinez, D. Meloni and S. Rigolin, arXiv:hep-ph/0512038.

[87] D. S. Ayres *et al.* [NOνA Collaboration], arXiv:hep-ex/0503053.

[88] B. Autin *et al.*, report CERN-2000-012.

[89] J.J. Gomez-Cadenas *et al.*, Proceedings of Venice 2001, Neutrino Telescopes, vol. 2*, 463–481, arXiv:hep-ph/0105297; A. Blondel *et al.*, *Nucl. Instrum. Meth. A* **503** (2001) 173; M. Mezzetto, *J. Phys. G* **29** (2003) 1771 [arXiv:hep-ex/0302005].

[90] M. Apollonio *et al.*, arXiv:hep-ph/0210192.

[91] L. Mosca, *Nucl. Phys. Proc. Suppl.* **138** (2005) 203.

[92] J.E. Campagne and A. Cazes, arXiv:hep-ex/0411062.

[93] R. Garoby, The SPL at CERN, CERN-AB-2005-007.

[94] S. Gilardoni *et al., AIP Conf. Proc.* **721** (2004) 334.

[95] A. Blondel *et al.,* CERN-NUFACT-Note-78 (2001).

[96] M. Mezzetto, *Nucl. Phys. Proc. Suppl.* **149** (2005) 179.

[97] J.E. Campagne, hep-ex/0511005.

[98] C. K. Jung [UNO Collaboration], arXiv:hep-ex/0005046.

[99] `http://www.ganil.fr/eurisol/`.

[100] J. Nolen, *Nucl. Phys. A* **701** (2002) 312c.

[101] P. Sortais, presentations at the Moriond Workshop on Radioactive Beams, Les Arcs (France), 2003, ECR technology, `http://moriond.in2p3.fr/radio`.

[102] M. Benedikt, S. Hancock and J.-L. Vallet, CERN note AB-Note-2003-080 MD.

[103] B. Autin *et al.*, arXiv:physics/0306106; M. Benedikt, S. Hancock and M. Lindroos, Proceedings of EPAC 2004, `http://accelconf.web.cern.ch/AccelConf/e04`.

[104] M. Mezzetto, *J. Phys. G* **29** (2003) 1781 [arXiv:hep-ex/0302007]; J. Bouchez, M. Lindroos and M. Mezzetto, *AIP Conf. Proc.* **721** (2003) 37 [arXiv:hep-ex/0310059]; M. Mezzetto, *Nucl. Phys. Proc. Suppl.* **143** (2005) 309 [arXiv:hep-ex/0410083].

[105] A. Donini, E. Fernandez-Martinez, P. Migliozzi, S. Rigolin and L. Scotto Lavina, *Nucl. Phys. B* **710** (2005) 402 [arXiv:hep-ph/0406132].

[106] M. Mezzetto, arXiv:hep-ex/0511005.

[107] A. Donini, E. Fernandez-Martinez and S. Rigolin, *Phys. Lett. B* **621** (2005) 276 [arXiv:hep-ph/0411402].

[108] P. Huber, M. Lindner and W. Winter, *Comput. Phys. Commun.* **167** (2005) 195 [arXiv:hep-ph/0407333].

[109] P. Huber, M. Maltoni and T. Schwetz, *Phys. Rev. D* **71** (2005) 053006 [arXiv:hep-ph/0501037]; R. Gandhi, P. Ghoshal, S. Goswami, P. Mehta and S. Uma Sankar, arXiv:hep-ph/0506145.

[110] J. Burguet-Castell, D. Casper, E. Couce, J.J. Gomez-Cadenas and P. Hernandez, arXiv:hep-ph/0503021.

[111] J. Burguet-Castell *et al., Nucl. Phys. B* **695** (2004) 217 [arXiv:hep-ph/0312068].

[112] F. Terranova, A. Marotta, P. Migliozzi and M. Spinetti, *Eur. Phys. J. C* **38** (2004) 69 [arXiv:hep-ph/0405081].

[113] P. Huber *et al.*, arXiv:hep-ph/0506237.

[114] M. Lindroos, EURISOL DS/TASK12/TN-05-02, M. Lindroos, Proceedings of Nufact 05.

[115] O. Bruning *et al.*, LHC luminosity and energy upgrade: A feasibility study, CERN-LHC-PROJECT-REPORT-626.

[116] A. Donini, E. Fernandez, P. Migliozzi, S. Rigolin, T.T. de Fatis and F. Terranova, arXiv:hep-ph/0511134.

[117] J. Bernabeu, J. Burguet-Castell, C. Espinoza and M. Lindroos, hep-ph/0505054.

[118] J. Sato, hep-ph/0503144.

[119] A. Blondel, Proceedings of Nufact 05, in press.

[120] S. Geer, *Phys. Rev. D* **57** (1998) 6989; A. De Rújula, M.B. Gavela and P. Hernandez, *Nucl. Phys. B* **547** (1999) 21; A. Blondel *et al., Nucl. Instrum. Methods Phys. Res. A* **451** (2000) 102; J.J. Gomez-Cadenas and D.A. Harris, Physics opportunities at neutrino factories, *Annu. Rev. Nucl. Part. Sci.* **52** (2002) 253 and the annual proceedings of the International Nufact Workshop.

[121] B. Autin, A. Blondel and J. Ellis (Eds), CERN Report CERN 99-02, ECFA 99-197.

[122] P. Gruber *et al.,* The Study of a European Neutrino Factory Complex, Neutrino Factory Note 103 (2002) CERN/PS/2002-080(PP), in *ECFA/CERN Studies of a European Neutrino Factory Complex*, A. Blondel *et al.,* Eds., CERN-2004-002, ECFA-04-230, p. 7.

[123] The Muon Collider and Neutrino Factory Collaboration, see the web site http://www.cap.bnl.gov/mumu/ which also contains references to several physics studies.

[124] *Feasibility Study on a Neutrino Source Based on a Muon Storage Ring,* D. Finley and N. Holtkamp, Eds. (2000), http://www.fnal.gov/projects/muon_collider/reports.html.

[125] *Feasibility Study-II of a Muon-Based Neutrino Source,* S. Ozaki, R. Palmer, M. Zisman and J. Gallardo, Eds., BNL-52623, June 2001, available at http://www.cap.bnl.gov/mumu/studyii/FS2-report.html; M.M. Alsharo'a *et al., Phys. Rev. ST Accel. Beams* **6** (2003) 081001.

[126] *A Feasibility Study of A Neutrino Factory in Japan,* Y. Kuno, Ed., http://www-prism.kek.jp/nufactj/index.html.

[127] *Neutrino Factory and Beta Beam Experiments and Developments,* (Eds. S. Geer and M. Zisman), Report of the Neutrino Factory and Beta Beam Working Group, APS Multi-Divisional Study of the Physics of Neutrinos, July 2004.

[128] The International Muon Ionization Experiment MICE, http://hep04.phys.iit.edu/cooldemo.

[129] R.J. Bennett *et al.,* Studies of a target system for a 4 MW 24 GeV proton beam, CERN-INTC proposal 2003-033, April 2004.

[130] A. Blondel *et al.,* Eds., *ECFA/CERN Studies of a European Neutrino Factory Complex*, report CERN-2004-002 (2004) http://preprints.cern.ch/cernrep/2004/2004-002/2004-002.html.

[131] A. Broncano and O. Mena, *Eur. Phys. J. C* **29** (2003) 197-206; hep-ph/0203052.

[132] A. Cervera *et al., Nucl. Phys. B* **579** (2000) 17-55, Erratum *ibid.B* **593** (2001) 731-732; hep-ph/0002108.

[133] P. Huber and W. Winter, *Phys. Rev. D* **68** (2003) 037301; hep/ph-0301257.

[134] S. Geer, *Comments Nucl. Part. Phys. A* **2** (2002) 284 [arXiv:hep-ph/0008155].

[135] P. Huber, M. Lindner and W. Winter, *Nucl. Phys. B* **645** (2002) 3-48; hep-ph/0204352.

[136] A. Donini, *AIP Conf. Proc.* **721** (2004) F219 [arXiv:hep-ph/0310014].

[137] A. Cervera, F. Dydak and J. Gomez Cadenas, *Nucl. Instrum. Meth. A* **451** (2000) 123.

[138] A. Bueno, M. Campanelli, A. Rubbia, *Nucl. Phys. B* **589** (2000) 577 [arXiv:hep-ph/0005007].

[139] A. Donini, D. Meloni, P. Migliozzi, *Nucl. Phys. B* **646** (2002) 321, hep-ph/0206034; D. Autiero *et al., Eur. Phys. J. C* **33** (2004) 243 [arXiv:hep-ph/0305185]

[140] S. Rigolin, Rencontres de Moriond 2004, hep-ph/0407009.

[141] A. Ereditato and A. Rubbia, arXiv:hep-ph/0510131.

[142] A. Badertscher *et al.,* arXiv:physics/0505151.

[143] R. Gandhi, P. Ghoshal, S. Goswami, P. Mehta and S. Uma Sankar, arXiv:hep-ph/0411252; S. Choubey and P. Roy, *Phys. Rev. D* **73** (2006) 013006 [arXiv:hep-ph/0509197].

[144] http://www.hep.ph.ic.ac.uk/%7Elongkr/UKNF/Scoping-study/ISS-www-site/WG1-PhysPhen/Workshops/2005-11/AEDL/AEDL-Catalogue.htm.

[145] M. Maltoni, T. Schwetz, M.A. Tortola and J.W.F. Valle, *New J. Phys.* **6** (2004) 122 [hep-ph/0405172].

[146] G.L. Fogli, E. Lisi, A. Marrone, A. Palazzo and A.M. Rotunno, hep-ph/0506307.

Superior neutrino beams: overview and recommendations

As described in the previous sections, the discovery of neutrino oscillations forms one of the most important results in particle physics in the last decade [1]. It has led to the creation of many new projects to investigate oscillations in more detail. For example, a number of so-called long-baseline neutrino oscillation facilities, in which the neutrinos are produced by an accelerator and detected several hundred kilometres away, have recently started taking data or are under construction: MINOS [2], CNGS [3] and T2K [4]. However, these projects are unlikely to have much impact on the so far unmeasured parameters of neutrino oscillations, θ_{13}, the CP-violation angle δ, and the sign of Δm_{23}^2. For these, new, more advanced neutrino beams will be required and these are the subject of this section.

There are three candidate facilities to provide these advanced beams: superbeams, a Neutrino Factory (see Fig. 1) and a betabeam (see Fig. 2). In a superbeam facility, e.g. an upgraded T2K or CERN to Fréjus, the neutrinos are produced in the 'standard' manner, by bombarding a target with a proton beam and focusing the pions created. However, the superbeam projects are different in two respects from the long-baseline facilities currently under construction: (1) the proton beam power is higher, around 4 MW, and (2) the neutrino detector is much bigger, typically around 1 Mt. Some will also employ the so-called off-axis technique, in which the pion beam is pointed a few degrees away from the detector. This has the effect of kinematically suppressing the high-energy neutrino tails and producing more neutrinos of a useful energy. In a Neutrino Factory, the neutrinos come from the decay of muons in a storage ring at an energy of between 20 and 50 GeV. This has many advantages over a conventional neutrino beam, in particular the composition, intensity, and energy spectra of the neutrino beams are precisely known and high intensities are possible. A betabeam has a number of benefits in common with a Neutrino Factory. However, the stored particles in this case are beta-emitters, in particular ^{6}He and ^{18}Ne which produce electron anti-neutrinos and neutrinos, respectively. As for the Neutrino Factory, the result is a neutrino beam of precisely known composition, intensity, and energy spectra.

As current preliminary simulations indicate that the Neutrino Factory has the best sensitivity to the three unmeasured parameters of neutrino oscillations [5], this section will concentrate on this machine. It will give an overview of the facility, introduce the main technical challenges, and describe the theoretical and experimental work that is or should be undertaken to solve these. It should be noted that a superbeam could form the first stage in a Neutrino Factory project. A possible betabeam facility is described later in this report.

1 Neutrino Factory layout

A possible layout for a Neutrino Factory is shown in Fig. 1. As outlined above, the primary aim is the production of intense neutrino beams for precise, long-baseline, neutrino oscillation measurements from the decay of muons in a storage ring. The muons are made by firing an intense proton beam into a target to make pions. As many of these pions as possible are focused magnetically into a decay channel in which they decay to give muons. The muons produced have a large spread in energy and this must be reduced to increase the fraction captured in the subsequent accelerators. This compression takes place in two stages: phase rotation and cooling. The muons are then accelerated in a number of steps before injection into the storage ring.

Theoretical studies suggest that the muons must have an energy of at least 20 GeV and that two different baselines are desirable, preferably one around 3000 km and another of the order of either 1000 or 7000 km [6]. Typically these studies assume a total of 10^{21} muon decays per year in the storage ring, with up to 40% being in a straight-section and hence useful for physics. These parameters determine the performance of rest of the elements of the accelerator complex and lead to many challenges in their design and construction. These, and the R&D being undertaken to solve the problems, are described in the following sections. Recommendations for additional work that must be carried out over the next few years to enable the production of a conceptual design are also given

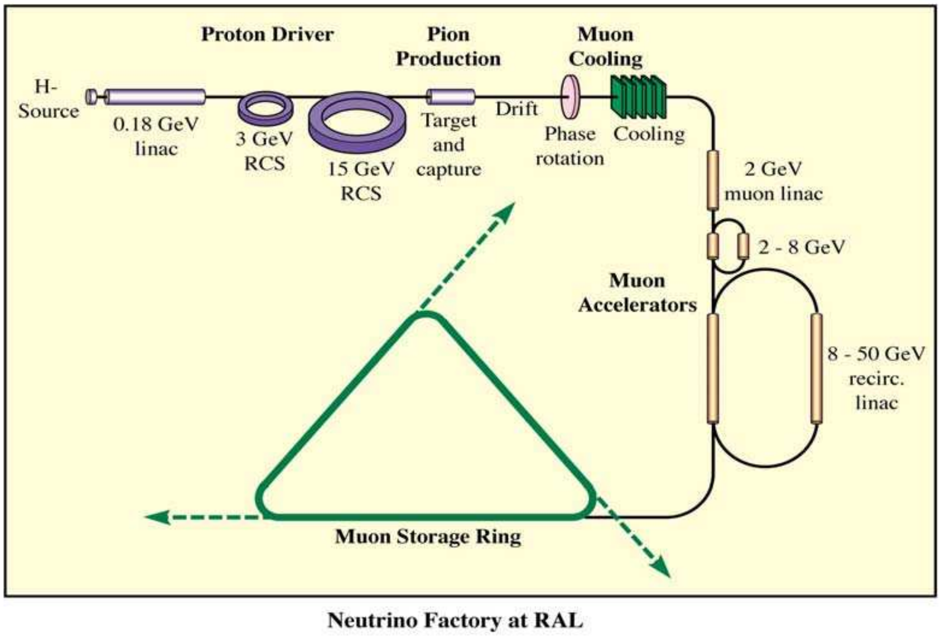

Fig. 1: The layout of a Neutrino Factory, consisting of a proton driver, target, pion collection channel, muon front-end, muon accelerators, and a storage ring

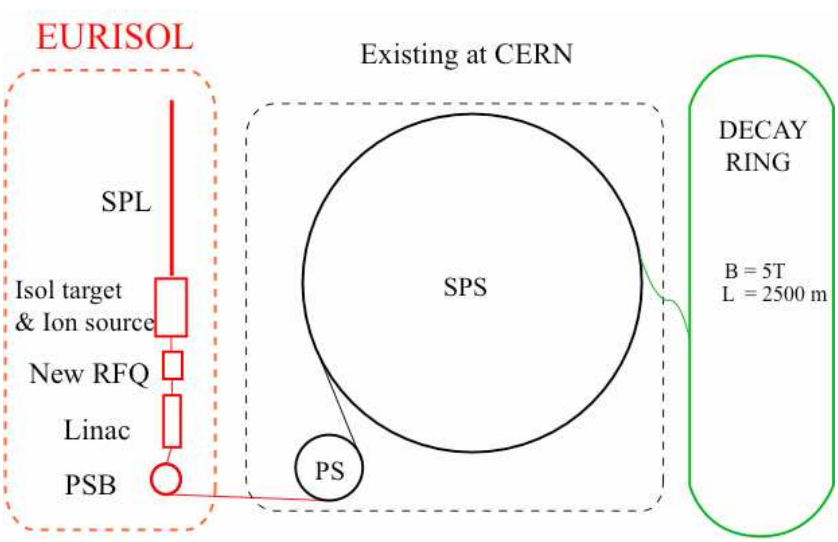

Fig. 2: Layout of a betabeam facility at CERN, consisting of a proton driver (the SPL), an ion source, an ion acceleration system, and the storage ring

1.1 Proton driver

To produce a sufficient number of muons, the proton driver should have a beam power of 4 MW, bigger than any equivalent existing machine. At this power level it is essential to minimize beam losses at higher energies where they would cause significant activation, resulting in problems with access. This imposes stringent requirements on the preparation and handling of the beam. In addition, to aid in the compression of the energy spread of the muons via phase rotation, the proton bunch should be about 1 ns long. Thus, the large proton current required to achieve 4 MW must be compressed into a very short bunch.

In Europe, two different approaches have been taken for the proton driver. In the CERN layout, a linac is used for acceleration, while buncher and compressor rings are used to produce the correct bunch structure and bunch length. At RAL, synchrotron rings are used for the bulk of the acceleration, while a linac is used only for injection. A number of designs have been studied for a variety of proton energies.

The R&D activity on the proton driver is currently focused on the low-energy components of the linac injector (see Fig. 3). This is because these are crucial for the preparation of the beam to avoid losses at higher energy and it is essential to check their performance at the high beam currents required. Two test stands are being constructed as part of the HIPPI project [7]: one primarily intended for HEP uses at CERN and a more generic version at RAL. Both will consist of a H^- ion source, low-energy beam transport, RFQ, and chopper and will have the necessary diagnostics to check their operation. Both should be operational within the next couple of years.

Along with this R&D, work is continuing on the design of the higher-energy sections of the driver. In particular, a second conceptual design of the linac proposed at CERN, the SPL, is being undertaken and a new design using a non-scaling FFAG has recently been produced at RAL.

Recent studies of pion production in the target with MARS and Geant 4 indicate that the optimum proton energy might be somewhat above the current 3.5 GeV of the SPL, in the range 6–10 GeV, and give a substantial improvement in the captured pion flux, a factor of 2 or more. Thus the practicality of a higher-energy proton driver at CERN needs to be investigated. In addition, studies of shock in the target show that this can be significantly reduced if the proton beam is split into a number of bunches, with a bunch spacing of about 10 s or more. As a result of this and a potentially higher energy proton beam, the accumulator and compressor rings in the CERN layout also need further study.

1.2 Target and pion collection

The target is probably the most difficult problem for a Neutrino Factory and the area that should receive the highest priority for R&D. As described above, the large proton power has to be compressed into a short bunch. In addition, to maximize the production of pions, the target cannot be too large transversely to prevent large losses from re-interactions. Thus, the energy density from the beam in the target is very large. This causes sudden heating, leading to severe stress in a solid target, and huge activation. Although targets of similar energy density already exist, they are run at a much lower frequency (~1 Hz compared with up to 50 Hz) and there are indications that they are damaged by the beam [8]. In addition, the activation of the target and surroundings will be huge and it is likely that the target area will require the same safety precautions as for a nuclear reactor. Safety is probably the single most difficult problem in the design of the target station and a potential 'show-stopper' for the whole project.

As a result, R&D on the target is essential. Two types of target have been proposed and are currently under study: a liquid metal (mercury) jet and a solid, replaced frequently. For the former, a liquid mercury jet has been tested, but separately, by impinging a high-intensity beam on to it and passing it through a strong magnetic field to simulate that used to capture the pions [9]. However, the effect of a beam and the magnetic field have not been tested together and, in general, the parameters of the tests have been less stringent than required for the Neutrino Factory. An experiment, MERIT, is now under development to perform the beam and magnet tests simultaneously and will use parameters closer to those of the real situation. This will be housed in the TT2A beamline at CERN and use a beam from the PS with approximately the right energy density. It should demonstrate the feasibility of a liquid mercury jet as a high-power target.

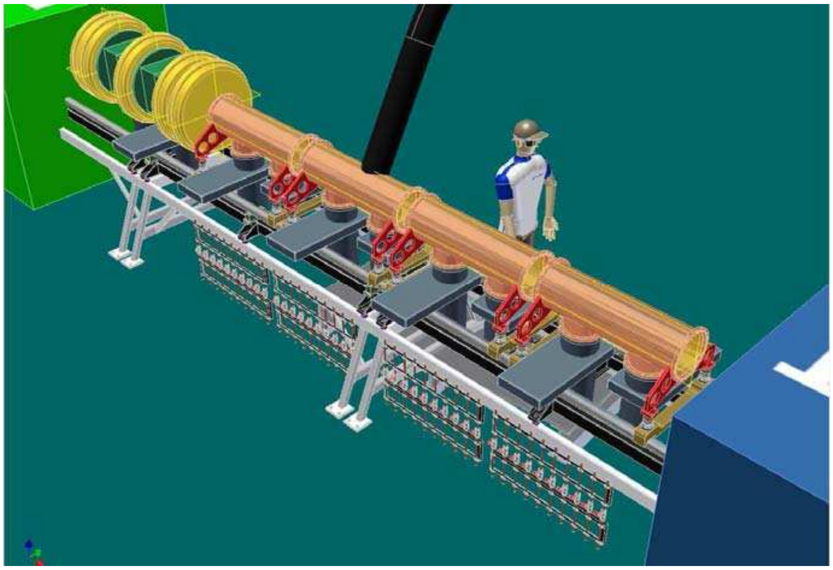

Fig. 3: Drawing of the radio-frequency quadrupole and chopper for the RAL proton front-end test stand

For solid targets, the most important problems are the lifetime due to shock induced by the sudden heating from the proton beam, and the resulting temperature. Both of these are eased by changing the target between proton pulses in some way, so that different targets are exposed to different proton bunches. Nevertheless, it is important to determine what the lifetime of such a target would be. Theoretical simulations suggest this could only be one proton pulse, though the existence of higher energy density targets implies this is not the whole story. A programme of tests on a number of materials, including tantalum, graphite and tungsten, has already started. This will use proton beams, lasers and large electric currents to induce shock and use a variety of techniques to measure the effect and determine the target lifetime.

It is hoped that these programmes will demonstrate the feasibility of at least one target technology. What will still be missing is the practical incorporation of the selected target technology in the target station, including a method of rapidly changing the solid targets. In addition, the design of a target station that will satisfy all the relevant safety requirements will be a major issue.

There are two possible methods for pion collection. The default is to use a 20 T solenoidal magnetic field around the target which is adiabatically ramped down to match the pion decay channel. The radius of the channel is increased to ensure that no captured pions are lost. The magnet has a superconducting outer core which is shielded from radiation by a normally conducting inner core. The alternative method is to use a magnetic horn.

The main problems for the solenoid are the heating and long-term damage from radiation and its incorporation in the target station, particularly in relation to the beam dump. For the horn, there are additional problems arising from a huge current requirement, ~300 kA, and the need to pulse it at up to 50 Hz.

1.3 Muon front-end

The 'muon front-end' is the section of the machine from the start of the pion decay channel to the first muon accelerator. A solenoidal decay channel is envisaged to transport the pion beam captured from the target and the large emittance muon beam resulting from the pion decay. The remainder of the front-end is used to prepare the muon beam for acceleration. In particular, the muon energy spread, and possibly emittance, must be reduced. The energy compression is performed using phase rotation, in which RF accelerating cavities are used to speed up the slower muons and to slow down the faster muons.

The emittance reduction would be performed by ionization cooling. In this, the muons are passed through some material, called an absorber, in which they will lose both longitudinal and transverse momentum via standard ionization energy loss. The lost longitudinal momentum is restored with RF cavities after the absorber, resulting in a net reduction in transverse momentum and a net transverse cooling. Of course, things are never that simple and as well as cooling coming from the energy loss there is also heating coming from multiple scattering. The net cooling is a balance between the cooling and heating effects. This balance is tilted in favour of cooling by using a low-Z absorber and creating a highly convergent or divergent beam using a strong magnetic field. As a result, a cooling cell would be a technically complicated device.

On account of this complication, the Muon Ionization Cooling Experiment (MICE) is being built at RAL to show that ionization cooling really works and to learn about it in detail.

Over recent years, the amount of cooling included in Neutrino Factory designs has decreased from more than a factor of 10 to 1.7 in the most recent study in the US, primarily due to the use of larger acceptance FFAGs for muon acceleration. As a result, one of the most important questions concerning the front-end is whether cooling is actually necessary. As well as the simplification and cost reduction coming from not having this channel, the rest of the front-end will also become easier and cheaper as it will be unnecessary to transmit such a large-emittance muon beam. In addition, the existing front-end designs in Europe have fallen behind the US and, in particular, have not developed in line with the changes in muon accelerators. It is important that this problem be addressed in the near future**.**

1.4 Muon acceleration

The acceleration of the muons needs to be fast, because of the muon lifetime, but the cost has to be kept under control. The requirement for rapid acceleration essentially eliminates conventional synchrotrons because of the time required to cycle the magnets (the current fastest cycling synchrotron is ISIS at RAL [10], which has a frequency of 50 Hz and hence a cycle time of 20 ms). On the other hand, although acceleration via linear accelerators is fast, it is expensive for the muon energies required. As a result, two other techniques are under study: re-circulating linear accelerators [11] and Fixed Field Alternating Gradient synchrotrons (FFAGs) [12]. The former comprises a linac injector into a ring consisting of two linacs connected together with a number of separate magnetic arcs, each set for a different momentum. This re-uses each linac a number of times (4) and avoids the need to ramp the magnets in the arcs. Nevertheless, the second US Feasibility Study showed this to be an expensive option. On the other hand, an FFAG, as originally envisaged, employs large-aperture magnets with a strong gradient in the magnetic field as a function of radius (see Fig. 4) so that as they are accelerated, the muons move to a larger radius and see a stronger magnetic field. It again has the advantage that the magnets do not have to be ramped and that the RF cavities are passed through many times (typically 10). In addition, a FFAG naturally has a large transverse acceptance and, if low-enough-frequency RF is used, it can also have a large longitudinal acceptance. As a result, it may be unnecessary to cool the muons if FFAGs are used for the acceleration. In fact, the Japanese Neutrino Factory layout utilizes four FFAG rings, accelerating in steps from 300 MeV/c to 20 GeV/c, without cooling.

Fig. 4: The 150 MeV scaling FFAG built at the KEK laboratory in Japan

The FFAGs used in the Japanese layout are called scaling FFAGs. Recently, an alternative type, called non-scaling, has been invented. These have a number of advantages over their scaling cousins for the acceleration of muons. In particular:

– the non-scaling optics allows a much smaller magnet aperture;

– the magnetic field variation is a linear function of the magnet radius rather than being a high power of it;

– higher frequency RF can be used, ~200 MHz, rather than ~6–30 MHz;

– it is possible to run the RF at a fixed frequency, rather than having to modulate it during acceleration, resulting in very fast acceleration;

– there is a large transverse acceptance;

– the accelerators are more compact.

In short, non-scaling FFAGs are ideal for muon acceleration and are rapidly becoming the default for a Neutrino Factory.

Non-scaling FFAGs are **not**, however, without problems. None have ever been built and they have a number of unique features which have never been tested before. Therefore, it is now essential that a proof-of-principle machine be built to show that non-scaling optics work, to study these features in detail, and to learn how to build the optimum accelerators for a Neutrino Factory. It is planned to construct an electron model of the muon accelerators at the Daresbury Laboratory in the UK to do this.

2 Recommendations

As noted above, the following are the areas that most urgently need addressing by the European Neutrino Factory community. All currently require additional resources. They are split into accelerator design work and R&D activities.

Design studies

1) FFAGs: non-scaling FFAGs have become the baseline for the acceleration of muons for a Neutrino Factory. Currently, no work has been done to incorporate them into a European layout. It is essential for such work to start soon, as Europe is already far behind the US and Japan in this and they are likely to bring a significant reduction in the cost of the facility.
2) Muon front-end: this is another area in which little work has been done in Europe for a number of years and we are again far behind the US and Japan. The existing designs need urgent development to allow for the large-acceptance FFAGs for acceleration.
3) Proton driver: because of the emerging information about pion production and shock in the targets, the higher energy parts of the proton driver in the CERN layout require further study. In addition, the potential of non-scaling FFAGs for proton acceleration needs understanding.
4) Storage ring: there has also been little work on this for a number of years. It is clearly the most crucial part of the facility as far as neutrino oscillations are concerned. The existing studies need to be updated to take into account recent requirements coming from the physics.
5) Once the investigations of the individual sections of the accelerator are more advanced, detailed end-to-end studies must be performed. These should lead to an overall cost optimization of the entire complex, including the neutrino detectors.

R&D activities

1) Target and the target station: this is the most critical item for R&D for a Neutrino Factory and other high-power proton projects. It is essential that the feasibility of at least one target technology be demonstrated over the next few years and the work currently being undertaken should do this, though additional resources are required to do a thorough job. It is also critical that a serious engineering study of a target station be undertaken to show that this target can be incorporated within the station and to investigate all aspects of safety. At the moment, no work is being done on this.
2) FFAGs: it is essential to build and successfully operate a non-scaling FFAG to show that it works and to demonstrate the applicability to a Neutrino Factory.
3) Proton front-end test stands: these are essential for preparing the intense proton beam for acceleration and their successful operation is very important. The resources are in place to do this.
4) RF cavities and kicker magnets: these have potential application in several parts of the machine and require common R&D. In particular, on account of the muon lifetime and beam emittance, large-aperture, 200 MHz cavities with large gradients need to be developed for rapid muon acceleration. If the muons are to be injected into a ring, e.g. for cooling or acceleration, substantial kickers will be required because of the large emittance and relatively small ring circumference. Similar R&D for other components of the machine is likely to be identified as work advances.
5) MICE: if ionization cooling is used in a Neutrino Factory, it will be important to have a good understanding of how it works and how to build the cooling channel. Currently only the first phase of MICE, which will not demonstrate cooling, is funded.
6) Horns: if magnetic horns are used for the pion focusing, it needs to be demonstrated that they have a high enough lifetime resulting from the current and high pulsing rate and from radiation damage. There are insufficient resources do this at full current and at 50 Hz.

References

[1] M. Mezzetto, talk at European Neutrino Group meeting, see http://cern.ch/psdata/www/nfwg/minutes/ENG-1/mezzetto.pdf
[2] MINOS Collaboration, NuMI-L-375 (1998).
[3] D. Duchesneau, hep-ex/0209082 (2002).
[4] Y. Itow *et al.*, hep-ex/0106019 (2001).
[5] P. Huber *et al.*, *Nucl. Phys. B* **645** (2002) 3–48.
[6] A. Cervera *et al.*, *Nucl. Phys. B* **579** (2000) 17–55.
[7] See http://cern.ch/mgt-hippi/.
[8] http://www.cap.bnl.gov/mumu/conf/target-030908/tuesday_pm/Morgan.pdf.
[9] A. Fabich and J. Lettry, *Nucl. Instrum. Methods Phys. Res. A* **503** (2003) 336–339.
[10] D.J. Adams *et al.*, see http://cern.ch/accelconf/e00/PAPERS/THP4A08.pdf.
[11] S.A. Bogacz, *J. Phys. G* **29** (2003) 1723–1726.
[12] S. Machida *et al.*, see http://cern.ch/accelconf/e00/PAPERS/MOP1B20.pdf.

Multimegawatt proton drivers

A high-power proton driver is the backbone of any future neutrino facility. Two main technical options are being studied in Europe, the USA and Japan:

– Superconducting Proton Linacs (SPL)

– Rapid Cycling Cyclotrons (RCS)

In addition, recently, Fixed-Field Alternating Gradient (FFAG) accelerators have been proposed as an attractive alternative [1].

The selection of the optimum technology for the proton driver producing intense neutrino beams is strongly correlated with the method of neutrino production that will be selected. Following the recent SPSC recommendations [2] (Villars04), Europe is pursuing its R&D on two neutrino production techniques:

– betabeam, or neutrinos from a beta-emitter beam, where beta emitters (^{6}He and ^{18}Ne) produced by a third-generation radioactive ion beam (RIB) facility (driven by a 1–2 GeV SPL) are accelerated in the CERN SPS to $\gamma = 100$ and sent to a decay ring to produce electron neutrinos.

– Neutrino Factory, or neutrinos from a muon beam[1] [3], where muons originating from the decay of pions produced from the interaction of a high-power proton driver on a mercury target are accelerated up to an energy greater than 20 GeV, and sent to a decay ring to produce muon and electron neutrinos.

The availability of a superbeam (neutrinos originating from decays of parents (pions and kaon) without reacceleration, produced from the interaction of a high-power proton driver on a mercury target) would benefit both options.

In terms of proton energy, neutrinos from a betabeam would require only a modest energy (1–2 GeV), a moderate energy will be optimal for a superbeam proton driver (3–4 GeV), whereas a neutrino factory would require an energy greater than or equal to 5 GeV. In addition, the proton driver parameters will have to be defined through a global optimization including RIB or pion and/or muon capture and muon front-end.

We review in this paper the R&D activities regarding high-power proton drivers for intense neutrino beams in Europe, the USA and Japan, as they were presented at the most recent relevant conference, NUFACT05 [3].

1 Proton driver activities in Europe

1.1 Accelerator R&D for a proton driver of a neutrino complex in the UK

The UK is actively supporting accelerator studies and developments aiming both at the upgrade of the ISIS facility and at a UK-based neutrino factory (Fig. 1).

[1] Muons decay weakly into an electron, a muon neutrino and an electron antineutrino.

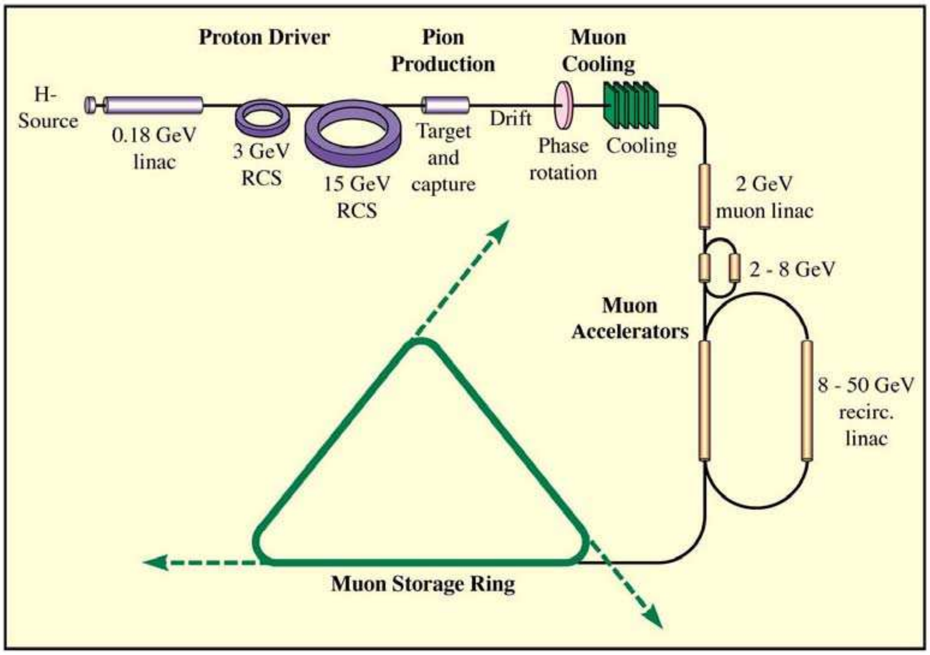

Fig. 1: Neutrino Factory at RAL

A classical means of accelerating particles to high energy is through the use of synchrotrons. To reach high beam power, they must be 'Rapid Cycling Synchrotrons' (RCSs), equipped with fast ramping magnets and power supplies, ceramic vacuum chambers to avoid eddy current and unusually high RF power for acceleration.

Such proton drivers for a neutrino factory are under study at the Rutherford Appleton Laboratory, complementing a similar investigation using a high-energy linac plus accumulator and compressor rings at CERN (see below). Two models are being considered:

– Driver I: a 5 GeV, 4 MW driver with four bunches of $2.5 \quad 10^{13}$ protons per pulse at 50 Hz (Fig. 2).

– Driver II: a 15 GeV, 4 MW driver (upgradable to 5 MW) with six bunches of $1.11 \quad 10^{13}$ protons per pulse at 25 Hz (Fig. 3).

The linac is common to both designs. In both cases, the 180 MeV linac beam of negative hydrogen ions is accumulated into the first RCS using charge exchange injection.

The main requirement of the driver is to produce bunches with a longitudinal emittance of ε_L~ 1 eV.s and of 1 ns r.m.s. duration at ejection. The low emittance is best obtained with a linac energy in the range 150–200 MeV. Injection presents different problems than compression and is carried out in separate booster rings. The design of the high-energy synchrotrons is determined by the method of final bunch compression. An energy of 5 GeV is considered the lowest practical at which compression can be achieved. However, a crude figure of merit for the pion target is given by the product of output energy   repetition rate for a fixed driver power, and this suggests some bias towards the 15 GeV option.

The main design issues to be addressed in an RCS proton driver are

– getting 4 MW of beam power at a repetition rate appropriate for the pion target;

– minimization of beam loss, keeping uncontrolled loss below 1 W/m:

beam instabilities (electron cloud)
space charge effects;

- beam accumulation, namely:

  balance between linac current and number of injection turns
  design of the charge exchange injection (phase space painting, foil heating and lifetime, H0 dump);

- bunch compression at the nanosecond level.

The initial design of the UK Neutrino Factory linac was based on the low-energy part of European Spallation Source linac, with an additional DTL section to 180 MeV. A subsequent design made in 2004 was based on a DTL to 90 MeV at a frequency of 234.8 MHz, followed by a Side-Coupled Linac (SCL) section operating on the third harmonic (704.4 MHz). This SCL is common to the CERN scheme for its linac4 (see below). In the most recent design, the Japanese JPARC accelerator frequency of 324 MHz is preferred at low energy, and its third harmonic (972 MHz) is used at high energy, with commercial Toshiba klystrons as RF sources.

The injector linac has a length of 129 m and accelerates a 57 mA H^- beam to 180 MeV. The transfer line to the rings includes a four-period 180 degrees achromatic arc with reverse bends to give a high peak dispersion for momentum collimation in a limited space. Two buncher cavities provide momentum ramping for injection painting.

Some details of the two RCS designs are given below.

In both designs, the H^- linac beam is chopped with a 70% duty factor at the ring revolution frequency. It is stripped when passing through an Al_2O_3 foil and painting is done in all phase planes of the booster synchrotron. The linac beam pulse to fill one ring is 200 s long (Driver I) or 134 s long (Driver II), and the second ring is filled immediately after the first one. A normalized dispersion $\Delta x/\beta\sqrt{x}$ = 1.8 couples the painting into transverse horizontal phase space, while vertical orbit bump magnets help reduce foil traversals by the circulating beam.

In both designs, the bunches from the two vertically-stacked booster synchrotrons are extracted and transferred together to either the upper or lower of the two main synchrotrons. They are then accelerated to top energy (5 GeV or 15 GeV) and, as soon as compressed, ejected onto the pion target which is then supplied with beam at twice the repetition rate of a single ring.

1.1.1 5 GeV, 50 Hz 4 MW RCS design

Beam from the linear accelerator is injected into two 50 Hz, 1.2 GeV, 200 m circumference synchrotrons, operating almost in phase and stacked one above the other. The synchrotrons accelerate the beam with a peak RF voltage of 0.25 MV on $h = 2$. This generates two bunches per ring which are extracted sequentially and injected in alternate cycles into a pair of 5 GeV synchrotrons operating at 25 Hz and $h = 8$. The 5 GeV rings are also vertically stacked, but operate in phase opposition. The beam is accelerated to 5 GeV with maximum voltages of 0.575 MV. In the final stages of the acceleration process, the beam is compressed in time by the addition of 0.5 MV on $h = 24$. The combined output of the latter two rings is (on target) 5 GeV at 50 Hz.

1.1.2 15 GeV, 25 Hz, 4 MW RCS driver

The scheme is similar to the 5 GeV design but with half the repetition rate. The linac beam is injected into the first pair of rings which simultaneously accelerate to 3 GeV on $h = 3$. The 3 GeV beam is alternately sent to the 15 GeV rings which operate in phase opposition at 12.5 Hz. They accelerate on $h = 36$ and their combined outputs are sent onto the target at 25 Hz. The required short bunch duration results from adiabatic compression of the bunch. This design can be upgraded to 5 MW.

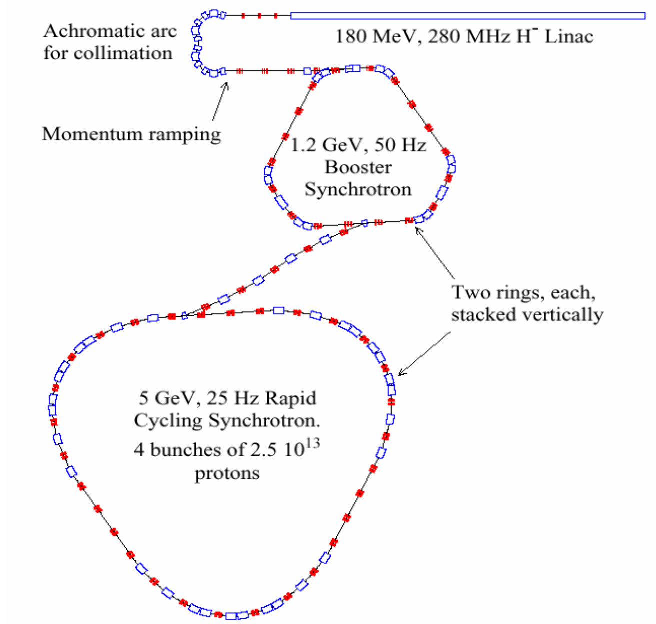

Fig. 2: Schematic of the 5 GeV, 50 Hz RCS design

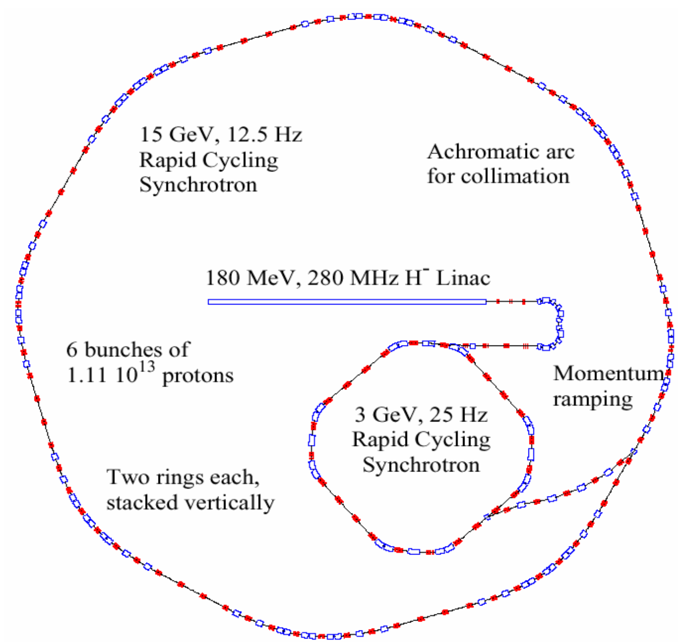

Fig. 3: Layout of the 15 GeV, 25 Hz RCS design

Final bunch compression to 1 ns (r.m.s.) is carried out over the last 500 revolutions of the accelerating cycle. At top energy the rings are close to, but just below, transition energy, and the lattices are designed so as to minimize the depression in γ_t under transverse space charge. Longitudinal inductive impedances of 5–10 Ω for *Z*/*n* are envisaged for the metallic and ceramic vacuum chambers to reduce longitudinal space charge effects. In Driver I, a higher order harmonic voltage (*h* = 24) is raised progressively to assist the compression, which is achieved with a peak voltage of ~0.6 MV. Driver II relies on adiabatic bunch compression at a single harmonic (*h* = 36) to achieve similar results. The final longitudinal emittance is ε_L~1.0 eV.s, with $\Delta p/p$ ~1.6% or 1.0% in the 5 and 15 GeV rings, respectively. Chromaticity is corrected with an arrangement of sextupoles and these can also be used to reduce second-order momentum effects.

1.2 Accelerator R&D for a proton driver of a neutrino complex at CERN [4]

During the CERN council meeting in December 2004, the Director-General of CERN outlined the ‘seven-point CERN strategy’:

1. Completion of the LHC project on schedule.
2. Consolidation of existing infrastructure at CERN to guarantee reliable operation of the LHC.
3. An examination of a possible future experimental programme apart from the LHC.
4. A role for CERN in the growing coordination of research in Europe.
5. The construction of a linear accelerator injector at CERN to provide more intense beams for the LHC.
6. An accelerated R&D effort towards CLIC, CERN’s novel new accelerator technology, which could open the way to much higher energies than are available today.
7. A comprehensive review of CERN’s long-term activity to be available by 2010, when results from the LHC will have given a first description of the particle physics landscape for years to come.

The following events that happened in 2005 are also relevant for the proton driver activity devoted to a neutrino complex at CERN:

- Publication of the SPSC Villars report [5].
- Continuation of the negotiation for additional resources from non-member states (India and China) in favour of Linac4, the low-energy front-end of the SPL, which should replace the existing CERN Linac2.
- Announcement of a special INTC meeting (NuPAC [6] – Geneva, Oct. 2005) about the needs of ISOLDE and nToF for the next decade, which will provide a new set of recommendations, including on proton drivers for such facilities.
- Creation of two CERN working groups [7] (POFPA: Physics Opportunities with Future Proton Accelerators and PAF: Proton Accelerators of the Future) to analyse scenarios and contribute to the definition of a baseline scheme for 2010. Relevant excerpts of the PAF mandate are given in the Appendix.

1.2.1 R&D activities for the SPL at CERN

R&D activities related to the Super Proton Linac (SPL, Fig. 4) as a proton driver for a neutrino complex at CERN are organized around four main projects:

- The SPL Study, with contributions from KFZ Juelich, CERN, RAL, GSI, Tokyo Univ., LANL.
- The IPHI–SPL Collaboration: CEA (DSM/DAPNIA at Saclay) and CNRS (IN2P3 at Orsay and Grenoble).

– The HIPPI JRA (inside CARE, supported by the European Union): CEA (F), CERN (CH), Frankfurt University (D), GSI (D), INFN-Milano (I), IN2P3 (F), RAL (GB), KFZ Juelich (D).

– ISTC projects #2875, 2888 and 2889: BINP (Novosibirsk), IHEP (Protvino), IHEP (Moscow), VNIIEF (Sarov), VNIITF (Snezinsk).

The original characteristics of the SPL, as published in the Conceptual Design Report [8], were ‘optimized’ for a neutrino factory and assumed the use of LEP cavities and klystrons up to the highest energy. They have been revised (Table 1) taking into account the latest physics requests, and assuming the use of state-of-the-art bulk niobium cavities above 180 MeV. A second conceptual design report is therefore in preparation (CDR-2) in collaboration with scientists from CEA-Saclay and INFN-Milano. It should be published in spring 2006. Up-to-date information is available at http://project-spl.web.cern.ch/project-spl/.

The RF system will be based on 704 MHz bulk niobium cavities. Three families of cavities will be used, centred at $\beta = 0.5, 0.85, 1.0$, with accelerating gradients of 15, 18, 30 MV/m and using five, six, and seven cells per cavity.

To minimize cold/warm transitions and maximize real-estate gradient, quadrupoles will be cold (2 K) because imbedded in the cryomodules, and independently aligned from the cavities. The design assumes cryomodules of maximum length (between 10 and 15 m), containing n cavities and $(n + 1)$ quadrupoles. Beam diagnostics, steering etc. will be located between cryomodules. The length of the cavities is limited by fabrication and handling considerations. The proposed number of cells per cavity is therefore five, six, and seven for the three sections. The SPL will be built assuming 2 MW maximum power per coupler.

Table 1: The CDR2 SPL characteristics

Ion species	H^-
Kinetic energy	3.5 GeV
Mean current during the pulse	40 mA
Mean beam power	4 MW
Pulse repetition rate	50 Hz
Pulse duration	0.57 ms (0.76 ms?)
Bunch frequency	352.2 MHz
Duty cycle during the pulse	62 (5/8)%
r.m.s. transverse emittances	0.4 π mm mrad
Longitudinal r.m.s. emittance	0.3π deg MeV

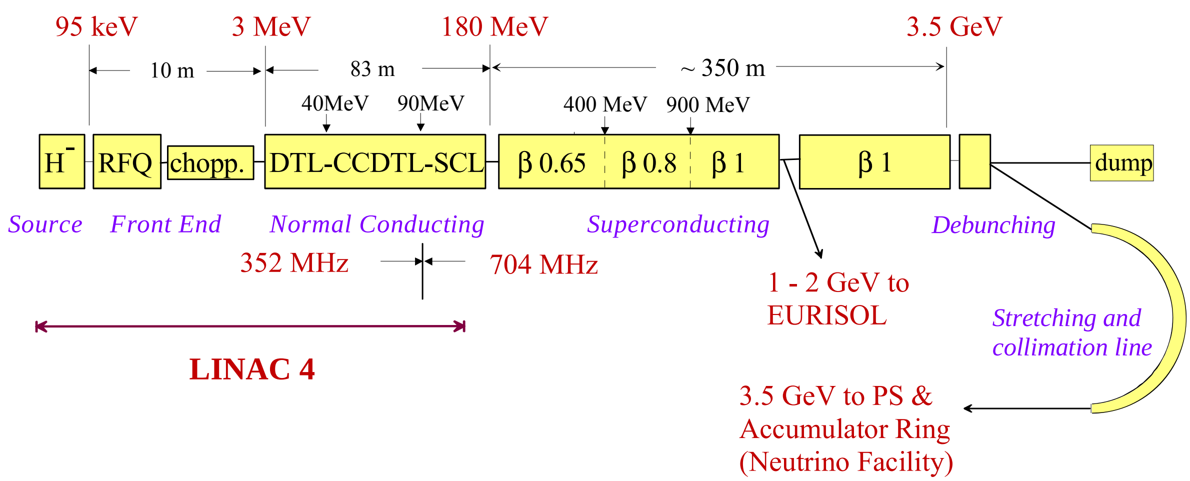

Fig. 4: The SPL

The main goals of the SPL at CERN are to

– increase the performance of the CERN high-energy accelerators (PS, SPS & LHC),

– address the needs of future experiments with neutrinos and radioactive ion beams.

The present R&D programme concentrates on the low-energy items (Linac4), wherever possible in collaboration with other laboratories.

1.2.2 Linac4-related activities

In this context, Linac4 (Fig. 5), a new injector for the CERN booster synchrotron, is proposed to improve the beam delivered to the LHC, ease operation, help reach the ultimate luminosity, and increase the flux to ISOLDE. With a length of ~90 m, it will be located in an existing experimental hall and will extensively re-use LEP RF equipment (klystrons etc.).

The main collaborations related to Linac4 are

– IPHI Collaboration: between CEA, CERN and IN2P3 whose main goal is the construction of the 3 MeV, high-duty-factor RFQ to be delivered at the end of 2007.

– ISTC project #2875 [9]: collaboration between BINP (Novosibirsk), VNIITF (Snezinsk), and CERN whose aims are

  – The development of the technological basis for serial production of CCDTL structures in the energy range of 40–100 MeV for the SPL project.

  – The feasibility study of the effective application of normal-conducting SCL structures up to the energy of 150–180 MeV.

This ISTC project, costing k$ 550, started in July 2004. The prototype of the CCDTL structure should be delivered to CERN for high-power testing by mid-2006, whereas the technological model of the SCL structure is to be tested in 2006.

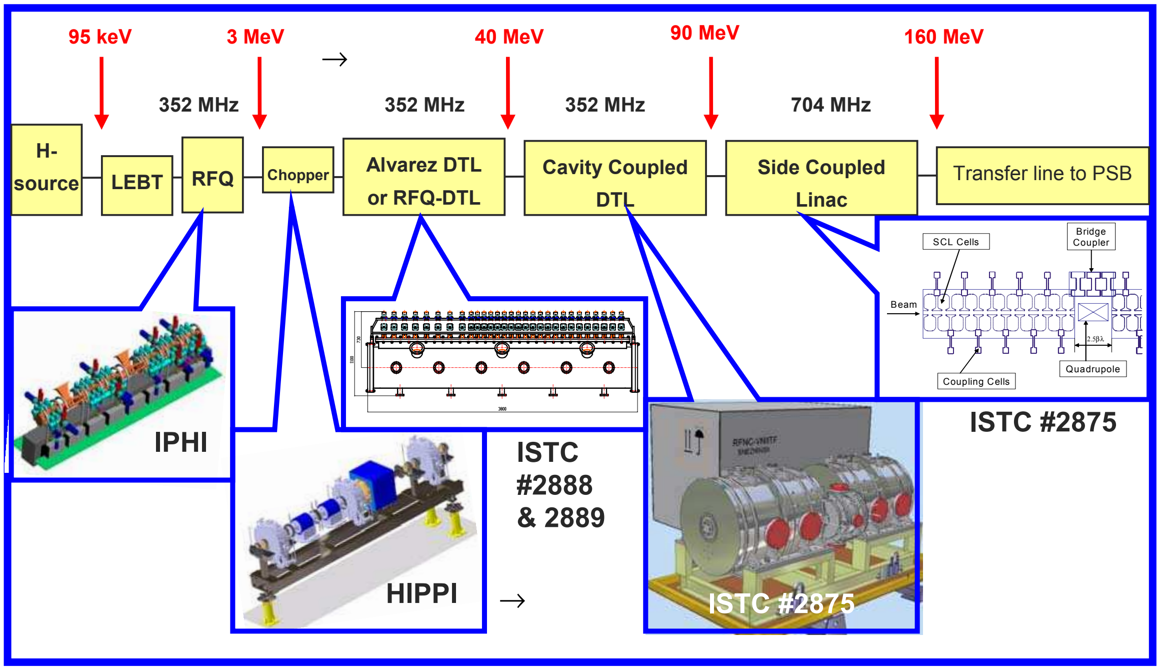

Fig. 5: LINAC4

– ISTC project #2888 [10]: collaboration between ITEP (Moscow), VNIIEF (Sarov), and CERN for the development of the technological basis for construction of Alvarez-type structures for the room-temperature part of the CERN SPL. After approval in February 2005 (for a cost of k$ 460), the prototype of the first DTL tank (3–10 MeV) should be delivered to CERN for high-power testing by the end of 2006. In the frame of this project, only one drift tube will be equipped with a Permanent Magnet Quadrupole (PMQ) and the prototype will not be capable of accelerating beam.

– ISTC project #2889 [11]: collaboration between IHEP (Protvino), VNIIEF (Sarov), and CERN to design and manufacture a DTL-RFQ accelerating structure prototype for a 3–40 MeV H^- linac of the SPL project. At a cost of k$ 477, this project was also approved in February 2005. A prototype of the RFQ-DTL structure is expected at CERN for high-power testing by the end of 2006.

Other collaborations are currently under negotiation:

– with China (IHEP-Beijing), concerning a 352 MHz buncher, Linac4 quadrupoles, and Linac4–PSB transfer line magnets;

– with India (BARC-Bombay and CAT-Indore) concerning pulsed power supplies for the LEP klystrons.

1.2.3 *Other potential applications of SPL R&D*

Nuclear physics application: there exists a strong demand to establish Radioactive Ion Beam (RIB) facilities in Europe, with intensities 3 orders of magnitude higher than currently available, for nuclear and solid-state physics, biophysics, nuclear astrophysics, etc. Two parallel programmes are under study: in-flight at GSI and Ion Separation On-Line (ISOL) in a new laboratory. In the ISOL-type facility, radioactive ions will be produced by a high-intensity 1–2 GeV proton beam hitting either a direct production target or a converter target irradiating the production material with spallation neutrons. For direct production, 100 kW of proton beam power are sufficient, while up to 5 MW are required when using a converter. The driver would operate in a CW or pulsed mode, at a frequency higher than 50 Hz.

In the frame of the EU-funded R&D for a European third-generation RIB machine (EURISOL Design Study) the preferred option is to have a dedicated driver, which would then operate continuously, with a normal-conducting 5 MeV front-end at 352 MHz followed by an intermediate-energy superconducting part at 704 MHz. The alternative option of using a pulsed linac like the SPL is also being analysed (Fig. 6).

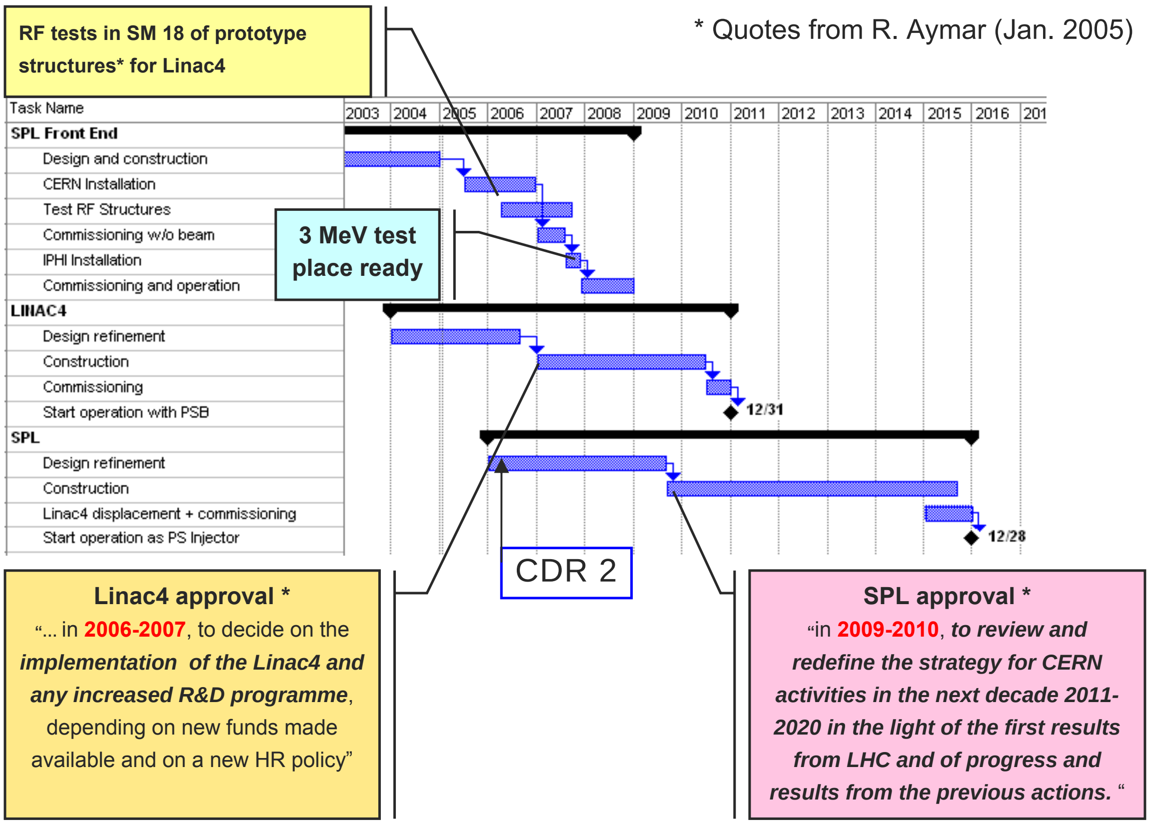

Fig. 6: The Linac4 and SPL planning

In neutron production applications, superconducting linacs are the preferred sources of protons to produce intense fluxes of neutrons for:

– basic science and condensed-matter studies (as in the US SNS project (Fig. 7), see www.sns.gov, that is hosting the highest power (1.4 MW), proton linac),

– driving subcritical reactors and 'burn' nuclear waste and possibly generating electricity (Accelerator Driven Systems).

Fig. 7: The US SNS proton linac

Regarding ADS, the accelerator group working for the EU programme, XADS, has investigated the characteristics of a transmutation driver for 600 MeV, 6 mA, and less than 5 trips/year. The conclusion is that CW SC linacs are preferred to cyclotrons because of their stronger reliability and upgradability. An Integrated Project, EUROTRANS now submitted to EU, to study reliability and build a demonstrator will seek funding for construction in the next FP (2008).

2 Proton driver activities in the USA [12]

In terms of neutrino physics, the recent US events are on one side the publication of the results of the American Physical Society study on the physics of neutrinos. The report made public at the end of 2004, 'the neutrino matrix' [13], underlines clear recommendations for the future:

"*We recommend, as a high priority, a phased program of sensitive searches for neutrinoless nuclear double beta decay". [..]We recommend, as a high priority, a comprehensive U.S. program to complete our understanding of neutrino mixing, to determine the character of the neutrino mass spectrum and to search for CP violation among neutrinos.*
This comprehensive program would have several components: an experiment built a few kilometers from a nuclear reactor, a beam of accelerator-generated neutrinos aimed towards a detector hundreds of kilometers away, and, in the future, a neutrino 'superbeam' program utilizing a megawatt-class proton accelerator. […]

On the other side, we had the launching in March 2005 by the DOE and the NSF of a subcommittee of HEPAP and NSAC on neutrino physics, NUSAG, for a duration of two years, whose charge is to "*make recommendations on the specific experiments that should form part of the broad US neutrino science program*".

In the USA, two neutrino superbeam proposals have been made: at Brookhaven (Fig. 8), based on the AGS and a 1.2 GeV superconducting proton linac, and at Fermilab (Fig. 9), based on a new 8 GeV superconducting proton linac.

It is based on upgrading the existing (in red) facilities at Brookhaven by adding a Coupled Cavity Linac (CCL) to the existing 116 MeV linac, and bring the energy up to 400 MeV, and continue with a superconducting linac to reach 1.5 GeV. Only one type of cavity, cryomodule and klystron, similar to the one in operation for SNS, will be used. The AGS repetition rate has to be increased from 1/3 Hz to 2.5 Hz, which implies tripling the existing main magnet power supply and current feeds and doubling the RF power and accelerating gradient. More details are given in Tables 2 and 3.

According to the Fermilab management [14], FNAL will be the centre of US HEP in ~2010. The strategy will depend strongly on the output of the ongoing Global Design Effort for the International Linear Collider (ILC). If the ILC cost published in the CDR in 2006 is considered affordable, construction could start at FNAL as soon as 2010, together with a neutrino programme based on the main injector (120 GeV/1 MW). If not, the construction of a superconducting 8 GeV proton driver could start as early as 2008. It would be followed by implementation of 30–120 GeV and 8 GeV beams of 2–4 MW after 2012. This would constitute a stepping-stone to a delayed construction of the ILC, starting in ~2012.

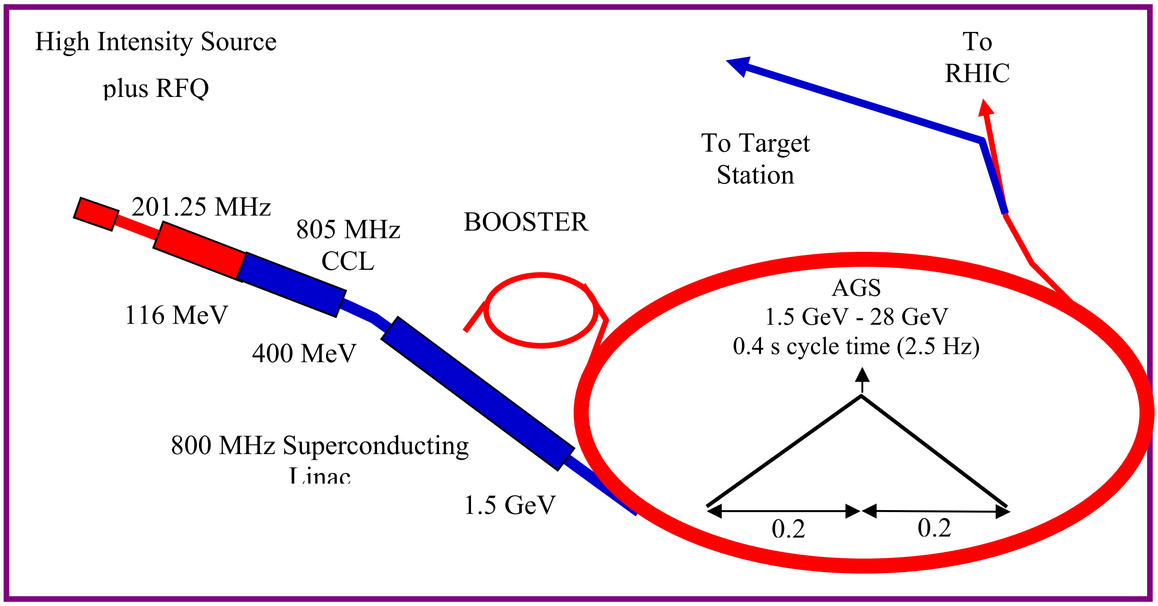

Fig. 8: Upgrade plans at BNL

Table 2: Comparison between existing AGS parameters, the upgraded AGS, and the Japanese JPARC project

	AGS (now)	AGS (1 MW)	JPARC
Total beam power [MW]	0.14	1.00	0.75
Injector energy [GeV]	1.5	1.2	3
Beam energy [GeV]	24	28	50
Average current [A]	6	36	15
Cycle time [s]	2	0.4	3.4
No. of protons per fill	0.7 10^{14}	0.9 10^{14}	3.3 10^{14}
Avg. circulating current [A]	4.2	5.0	12
No. of bunches at extraction	6	23	8
No. of protons per bunch	1 10^{13}	0.4 10^{13}	4 10^{13}
No. of protons per 10^7 s	3.5 10^{20}	23 10^{20}	10 10^{20}

Table 3: Characteristics of the 1.2 GeV BNL superconducting linac, based on the SNS experience

Beam energy	0.2 → 0.4 GeV	0.4 → 0.8 GeV	0.8 → 1.2 GeV
RF frequency	805 MHz	1610 MHz	1610 MHz
Acc. gradient	10.8 MeV/m	23.5 MeV/m	23.5 MeV/m
Length	37.8 m	41.4 m	38.3 m
Beam power (exit)	17 kW	34 kW	50 kW

The Fermilab proton driver design will benefit from new ideas and concepts emerging from the ILC study, the Spallation Neutron Source construction, and the RIA and APT projects. It is inspired by the SNS, RIA, and JPARC linac designs up to 1.3 GeV, and uses the ILC cryomodules in the energy range 1.3–8 GeV. Charge exchange injection is used to accumulate the 8 GeV H^- beam in the main injector. The small emittances delivered by the SC linac proton driver will assure small losses in the following machine.

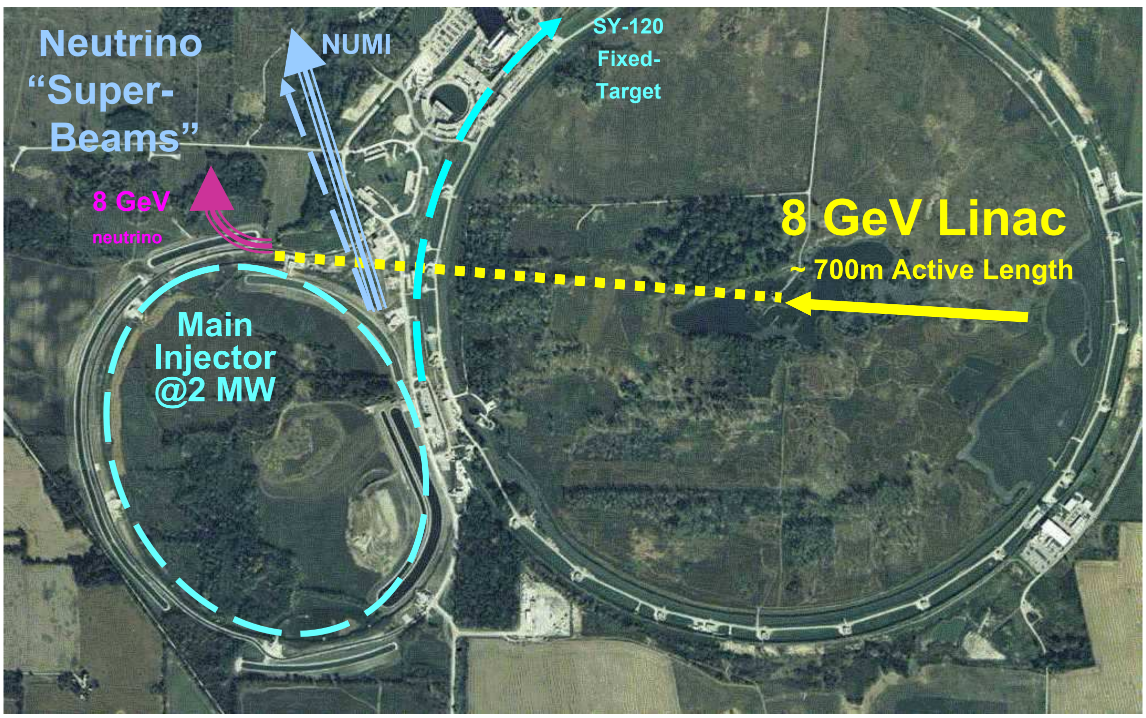

Fig. 9: The Fermilab proton complex with a 8 GeV SPL

'Superbeams' at Fermilab will be based on 2 MW beam power at 8 GeV with the linac alone, and up to 120 GeV when using the main injector.

The Fermilab linac design presents two phases (see Table 4):

– Phase A: 0.5 MW beam power (8.3 mA 3 ms 2.5 Hz 8 GeV = 0.5 MW) requiring 12 klystrons.

– Phase B: 2 MW beam power (25 mA 1 ms 10 Hz 8 GeV = 2.0 MW) requiring 33 klystrons.

Either phase is able to get 2 MW of beam power from the main injector (1.5 10^{14} 0.7 Hz 120 GeV = 2 MW).

Moreover, there is a very valuable synergy (Fig. 10) between the superconducting proton linac and the International Linear Collider programme at Fermilab. The technology is claimed to be the same in the energy range 1.5–8 GeV. Therefore for a small percentage of the total cost of the ILC, this machine would be an excellent demonstration of the ILC technology and would represent a very valuable basis for a reliable cost estimate. In addition, it would be a seed project for US industrialization of SCRF. Indeed, the building block of the 8 GeV linac is the TESLA RF station, made up of 36 SCRF cavities, 4 cryomodules, 1 klystron and 1 modulator, to reach ~1 GeV of beam energy.

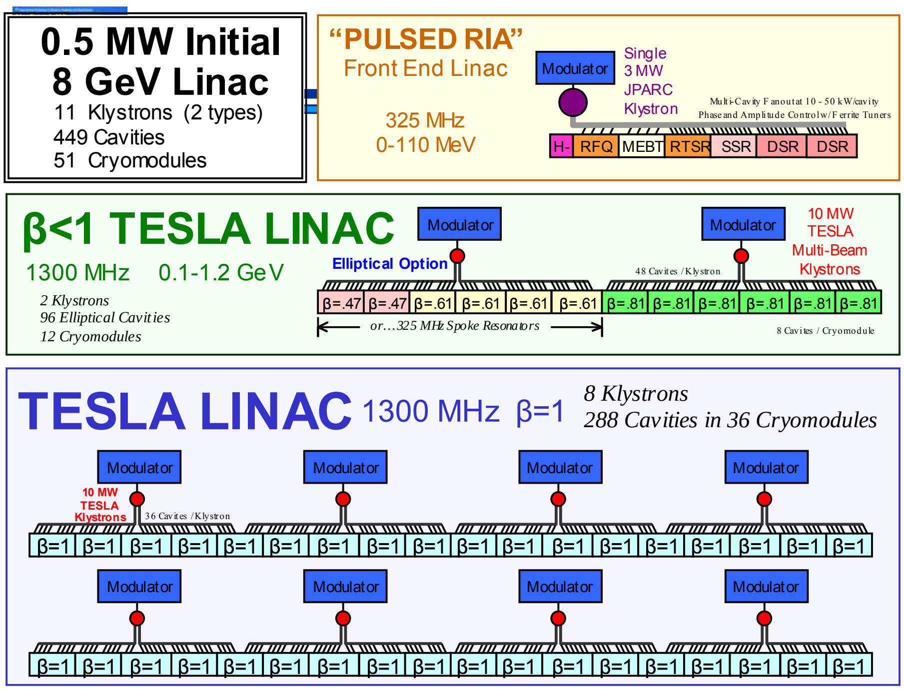

Fig. 10: Possible synergy at Fermilab between SPL and ILC

Following the selection of the cold SCRF option for the ILC, FNAL has chosen TESLA/XFEL compatible frequencies:

– 1300 MHz main linac (= ILC TESLA / XFEL)

– 325 MHz (=1300 MHz/4) front-end linac (= JPARC) (a gift !)

to benefit from the multiyear R&D on SRF cavities, RF couplers, cryomodules, klystrons etc.

Table 4: Characteristics of the 8 GeV FNAL superconducting linac

Main injector beam	(1.5 10^{14}, 1.5 s, 2 MW)
Pulse parameters	(8 mA 3 ms 2.5 Hz)
Ultimate upgrade	(25 mA 1 ms 10 Hz)
Operating frequency	(1300 MHz / 325 MHz)
Copper to SCRF transition	(15 MeV)
Spokes-to-elliptical transition	(110–400 MeV)

3 Proton driver activities in Japan [15]

In Japan, proton driver activities are related to the construction of the JPARC multipurpose facility (Figs. 11, 12, 13). The accelerator complex consists of a linac, a 3 GeV synchrotron, and a 50 GeV synchrotron. Four experimental areas are foreseen, focused, respectively, on nuclear transmutation, materials and life science, hadron beam physics, and neutrino generation.

They correspond to the three main goals of the JPARC complex. One is nuclear and particle physics using 50 GeV beams, that includes neutrino physics. Another is materials and life science using 3 GeV beams, and the other is R&D towards transmutation using 0.6 GeV linac beam. Phase I of the project, that excludes the nuclear transmutation facility and the superconducting part of the linac, is expected to be completed at the end of JFY2007.

Commissioning of the NC linac (Fig. 11) has already started at KEK Tsukuba where it has been designed and built. The measured transmission through the first DTL was 100%. The duty cycle is still lower than nominal, but there is no obstacle preventing it from reaching the design goal.

Fig. 11: The JPARC normal-conducting linac

Emittances from the linac almost meet the design goal. Other crucial components such as the RF chopper and S-DTL are fabricated and tested. Linac installation in the JAERI site has started.

With the nominal injection energy in the 3 GeV synchrotron, the 50 GeV synchrotron was expected to deliver 0.75 MW of beam power. With the reduced injection energy, the current in the 3 GeV synchrotron will be limited by space-charge effects and the expected beam power from the 50 GeV synchrotron will not exceed 0.4 MW. As long as the linac energy is not nominal, the only possibility is to arbitrate between the beam power available at 3 GeV and at 50 GeV. Plans based on increasing the number of pulses accumulated in the 50 GeV give the hope to approach the foreseen power from this machine, to the detriment of the power at 3 GeV.

A further increase of the beam power by a factor of two is planned to be achieved by increasing the repetition rate. Four major upgrades will be needed. First, an energy storage system has to be added. Secondly, an additional magnet power supply system has to be built. Thirdly, more RF cavities have to be installed. Fourthly, the water cooling system has to be upgraded.

To go beyond 1.5 MW and reach a few megawatts, more ambitious improvements are necessary and many studies remains to be made, although the basis of some upgrades are already under investigation. Barrier buckets are envisaged, for example, to reduce the space-charge tune shift at injection and possibly increase the number of pulses accumulated.

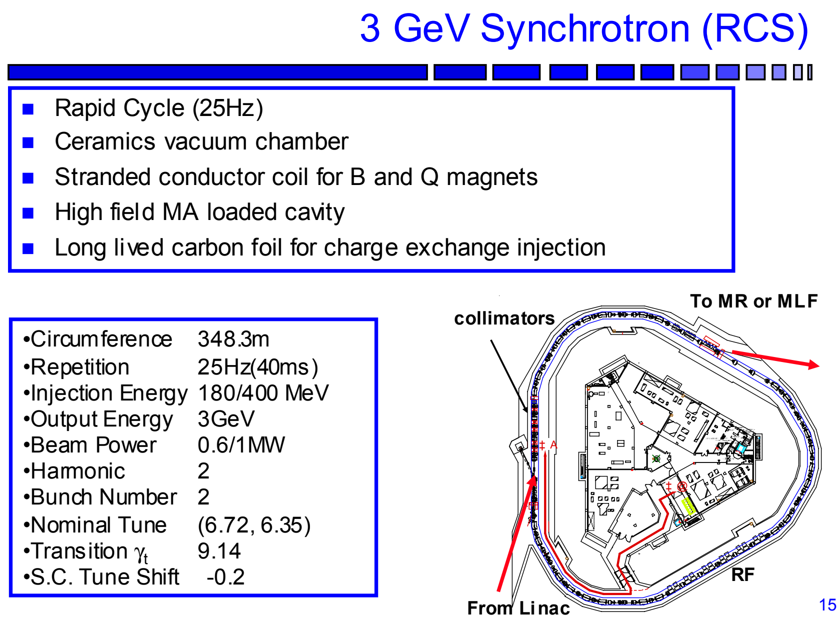

Fig. 12: Layout of the JPARC 3 GeV machine

Fig. 13: Magnet production for the 50 GeV synchrotron

4 Final remarks

Around the end of the year 2006, important study teams (ISS for neutrino factories with the support of BENE, PAF+POFPA for CERN and NUSAG for the USA) will have published their conclusions/recommendations/guidelines concerning high-intensity proton drivers and future neutrino facilities. Future decisions will undoubtedly be strongly influenced.

Regarding technology choice selection, a good summary was given by B. Weng during his concluding talk [16] on accelerators at the Physics with a Multi-MW Proton Source Workshop held at CERN in May 2004:

"The choice of an SPL for the CERN proton driver is a realistic and competitive option which has no show-stoppers in its current design. […]
Current conceived applications are too varied for an effective project. Intensive discussion among accelerator experts and physicists has to take place to identify realistic phase-I experiments to select proper accelerator configuration (SCL vs RCS), intensity, energy, pulse length, and target/horn design for optimal secondary beam spectrum. Then, other applications and further upgrades can be contemplated."

The next machine is the 3 GeV synchrotron. To reduce the eddy current effect in the magnets, aluminium stranded coil has been developed with radiation-hard insulation. Ceramic vacuum chambers with RF shield outside and TiN coating inside have been developed and tested. High-power testing of the RF cavity using magnetic alloy was successful. For the RF cavity, the direct water cooling method was adopted. The tunnel and buildings are ready for RCS installation. More than half of the magnets of the 50 GeV synchrotron have been measured. Bipolar kickers and septum for fast extraction are now under fabrication. In the initial phase, for cost saving reasons, the linac energy will be lower than nominal (200 MeV instead of 400 MeV).

Of course, the specificities of the host site of a future EU neutrino facility will strongly influence the choice between the various options.

References

[1] G. Rees, Nufact05, http://www.lnf.infn.it/conference/nufact05/talks2/WG3/Rees_WG3.ppt

[2] J.B. Dainton, Villars report, http://committees.web.cern.ch/Committees/SPSC/Villars-Report.pdf

[3] http://www.lnf.infn.it/conference/2005/nufact05/

[4] R. Garoby, Nufact05, http://www.lnf.infn.it/conference/nufact05/talks2/WG3/Garoby_WG3.ppt

[5] http://committees.web.cern.ch/Committees/SPSC/Villars-Report.pdf

[6] http://indico.cern.ch/conferenceDisplay.py?confId=a052

[7] http://paf.web.cern.ch/paf/

[8] Conceptual Design Report of the SPL, http://doc.cern.ch/yellowrep/2000/2000-012/p1.pdf

[9] http://science.istc.ru/ISTC/sc.nsf/html/projects.htm?open&id=2875

[10] http://science.istc.ru/ISTC/sc.nsf/html/projects.htm?open&id=2888

[11] http://science.istc.ru/ISTC/sc.nsf/html/projects.htm?open&id=2889

[12] G. Apollinari, Nufact05, http://www.lnf.infn.it/conference/nufact05/talks/Plenary/Apollinari_Plenary.ppt and http://protondriver.fnal.gov/

[13] http://www.aps.org/neutrino/

[14] http://www.fnal.gov/directorate/Longrange/Long_range_planning.html

[15] S. Machida, Nufact05, http://www.lnf.infn.it/conference/nufact05/talks/Plenary/Machida_Plenary.ppt

[16] http://physicsatmwatt.web.cern.ch/physicsatmwatt/Presentations/Weng_summary.ppt

APPENDIX: Excerpts from the PAF mandate

"In preparation for the strategic decisions foreseen to be taken in 2006 and 2010 concerning future facilities at CERN, […] an inter-departmental working group aiming at the definition of a baseline scenario of the possible development and upgrade of the present Proton Accelerator Complex is mandated below […]. The group reports to the DG; its findings will be discussed in the Executive Board.

The study is a natural extension of the analysis already done by the High Intensity Proton (HIP) Working Group which focused on intensity upgrade (CERN-AB-2004-022 OP/RF). Its scope is widened to cover other parameters such as beam energy and the needs of all possible users of CERN facilities. It is expected to make use of the EU supported initiatives, namely the Networks HHH and BENE, the Joint Research Activity HIPPI and the Design Studies EURISOL and DIRAC (FAIR project).

The working group will:

- Collect performance requests of the future users, taking into account the foreseen LHC upgrade, the possible Fixed Target Physics programme (including future options for neutrino physics) as recently discussed by the SPSC (Villars workshop) in the report CERN SPSC-2005-010 and the Nuclear Physics programme which will be discussed by the INTC (outcome of the future workshop in September 2005).

- Analyse the various development and upgrade options of the overall CERN proton complex including possible replacement of some of the present accelerators with Rapid Cycling Synchrotons (RCS) and/or Fixed Field Alternating Gradient (FFAG) accelerators.

- Identify technical bottlenecks and identify R&D that would be required to validate the various options if necessary.

- Identify synergies of R&D with non-CERN studies and projects.

- Report to the DG results from the above studies before the end of 2005. […]

- Define a preferred scenario together with a suggested implementation schedule, staged in time, and provide a preliminary estimate of the necessary resources (budget, man-power and expertise). A first presentation is expected by mid 2006 as an input for the critical decisions by the management in 2006 on a possible LINAC4. […]".

Multimegawatt pion production target and pion collector

1 Introduction

High-intensity neutrino beams [1,2] (superbeams, neutrino factories and muon colliders) require a high-power target as a pion source and an efficient pion collection system. Developments in high-power targets [3] are also needed in several different scientific and technological areas—linear collider positron sources [4,5], radioactive beam facilities [6,7], spallation neutron sources [8,9], accelerator production of tritium [10], and accelerator transmutation of radioactive waste [11–13]. Synergies already exist between some of these groups. However, pion collection is specific to neutrino beams.

Because the pions emerge from the target at a wide range of angles and momenta, it is necessary to collect and focus as many as possible into a forward direction to optimize the neutrino intensity. The collector could be either a strong magnetic solenoid or horn surrounding the target. The intimate relation of target and collector means that they must be designed as a unit.

2 Target design

The main problems of the target design are heat dissipation, radiation damage and, in addition, with pulsed beams, thermal stress, shock and fatigue. The high radiation can bring problems of heating, activation, and radiation damage to surrounding components.

The key issue is not total power dissipation but power density and, for pulsed beams, energy density per pulse. A high power dissipated in a large volume produces a small temperature rise and the heat is easily dissipated; similarly the radiation damage is low, although it can build up with time. The transmutation and tritium production facilities have the highest levels of beam powers—in the tens to hundreds of megawatts—but with the very large targets the energy density is comparatively low and hence the heating and radiation damage problems are eased.

In the current design the neutrino target will be bombarded by a 4 MW proton beam of 3–30 GeV, pulsed at 50 Hz with a pulse structure which will consist of one or more ~1 ns long micropulses within a ~1 μs macropulse. The heavy metal targets are 1–2 cm in diameter and 20–30 cm long. The length is dictated by the desire for an acceptable pion-beam longitudinal emittance and the diameter is restricted by self-absorption of the pions. The target will dissipate ~1 MW of the beam power, the remainder being dissipated in a beam dump. The energy density is 300–1000 J cm^{-3} per pulse, which is one of the highest of currently proposed targets for any type of machine.

To reduce the effective energy density, the target can be moved through the beam. Rotating solid targets are in use [14] and a contained flowing liquid metal target is being made at PSI [15]. The SNS [8] is also committed to a contained flowing mercury target. However, the SNS has a pulsed proton beam, unlike the cw PSI beam, which creates shock effects in the target. In particular, cavitation bubbles are formed and those near the surface erode the container wall. Currently, the expected lifetime is only a few weeks at 1 MW [16].

Another solution is to form a free metal jet [17] which will disintegrate after each beam pulse and then re-form between pulses. The jet has many advantages since heating, radiation damage and shock are not a problem. However, safety, containment, and thin beam windows could still be issues for concern.

To reduce the thermal shock in solids it is advantageous to have a small target so that the transit time for the shock is small compared with the pulse length. For pulses of 1 μs length this requires a size of a few millimetres. Using this principle, a target consisting of small beads has been suggested by Sievers [18].

There is some freedom to choose the pulse configuration of the proton driver. If the macropulse is split up into several micropulses separated by at least the shock transit time, then the energy density per pulse is effectively reduced by the number of micropulses in the macropulse. It appears feasible to have at least 10–20 micropulses thus reducing the energy density per pulse by an order of magnitude and reducing the effect of shock damage in the target accordingly [19].

2.1 The granular target

Peter Sievers [18] suggested a target consisting of small, solid, tantalum spheres (~2 mm diameter), cooled by flowing gas or liquid (see Fig. 1). This reduces the effect of thermal shock that is experienced by a target constructed from a single piece of solid material. To further reduce the average power density in the target it was proposed to sweep the beam across four targets on successive pulses and to collect the pions and recombine them into a single beam in a sophisticated arrangement of optics. An R&D programme to investigate heat evacuation and off-beam shock effects in the target was proposed in 2003, but work was stopped owing to lack of resources.

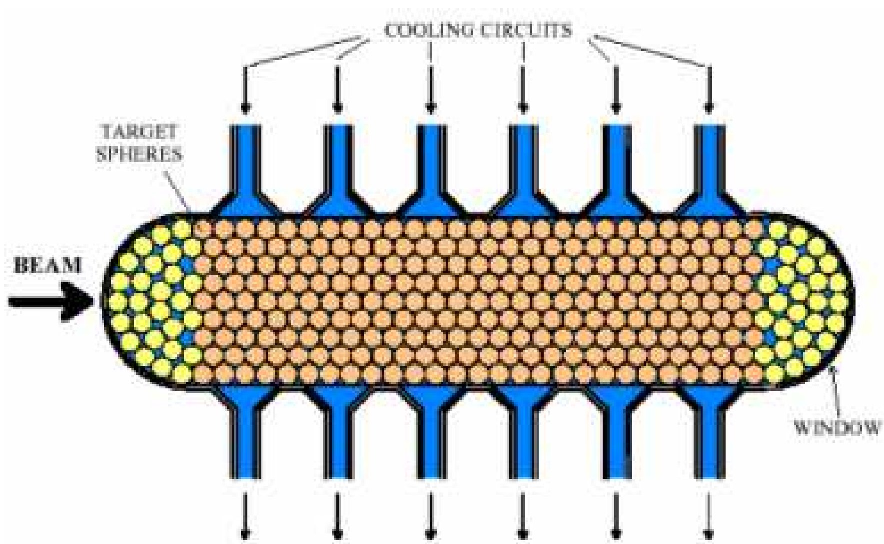

Fig. 1: Schematic section through the granular target

2.2 Solid-target studies at CERN

Jacques Lettry [11] and his colleagues are pursuing a detailed programme of tests of solid targets for radioactive beams and neutrino sources. Some of this extensive work is expected to be published soon. An investigation of shock in various solid materials including the CNGS [20] graphite target has been reported by Roman Wilfinger [21].

2.3 Solid-target studies in the USA

BNL [22] are currently investigating materials (various nickel iron alloys) that have low thermal expansion to circumvent the problem of thermal shock. It has been found that under irradiation the materials lose the low expansion properties, although they can be recovered by modest heating. The search for better (smart) materials is continuing.

2.4 Solid-target studies in the UK

The.proposed target [19] for the neutrino factory is a rotating tantalum toroid (see Fig. 2) operating at a temperature of ~2000 K to dissipate by thermal radiation 1 MW of power produced by the impact of a 4 MW proton beam. Alternatives to the toroid are being considered—such as firing individual target bars through the beam or passing a 'chain' of bars through the beam.

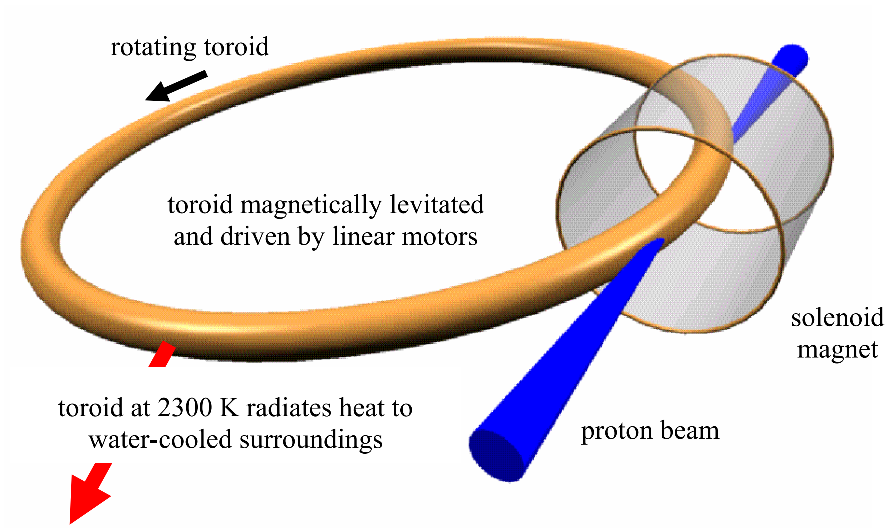

Fig. 2: Schematic diagram of the rotating solid tantalum toroid

The UK programme of target developments is centred on the study of thermal shock and the long-term fatigue effects. A high-current electric pulse will be passed through a thin tantalum wire to provide a thermal shock by ohmic heating. The radial acceleration of the surface of the wire will be measured by a VISAR [23] and the motion of the surface will be modelled using a commercial computer code, LS-DYNA [24]. In this way the constitutive equations of the tantalum at high temperatures under shock conditions will be realized and the full scale target can be modelled.

Finally, some in-beam testing is planned to confirm the VISAR measurements with the wire test and the resultant modelling. Tests at FNAL on the pbar target have already shown no disastrous effects at an energy density of 38 000 J cm^{-3} (two orders of magnitude higher than the neutrino factory) for 1100 pulses.

Tantalum has been chosen for the toroid because it is refractory and resistant to radiation damage [25]. However, the possibilities of carrying out studies of radiation damage at high temperature are currently being investigated.

2.5 Liquid-metal jet target studies – The MERIT experiment

Tests have been carried out at BNL [17,26,27] to test the effect of an intense beam pulse on the jet and have confirmed that the jet does disintegrate with droplet velocities of 10–20 m s^{-1} (see Figs. 3 and 4). The velocities increase with the energy deposited in the jet, but are not expected to cause damage to the surrounding walls. However, care will be needed to ensure that the fast droplets do not reach the beam windows, particularly the thin downstream pion window. Re-forming the jet between pulses was not a problem. Tests at Grenoble [17,27] showed that the jet was made more stable in an intense solenoidal magnetic field of 20 T.

Currently an experiment, MERIT [17], is being constructed (Figs. 5 and 6) to test the jet in both a magnetic field and with beam of the correct intensity (up to 28 10^{12} protons per pulse at 24 GeV) to fully simulate the neutrino factory conditions. This experiment is a collaboration between laboratories in the USA, Japan, and Europe. It will be installed in the nToF11 beam line at CERN for operation in 2007.

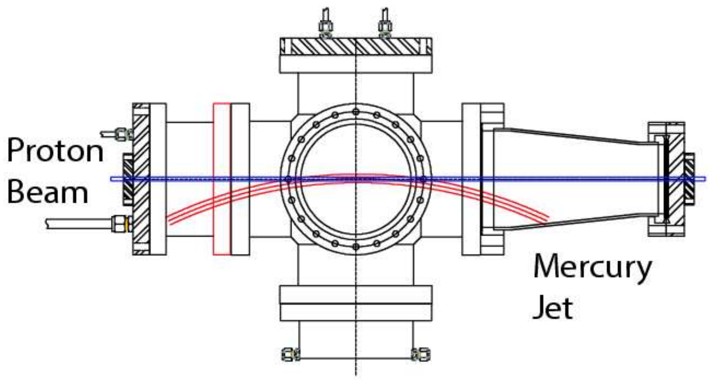

Fig. 3: BNL experiment. Schematic diagram of the mercury jet hit by a proton beam; no magnetic field.

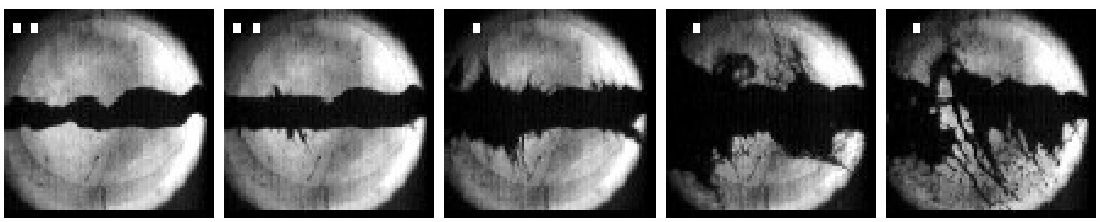

Fig. 4: Pictures of the mercury jet disintegrating when hit by the proton beam. No magnetic field. Exposures of 25 μs at t = 0, 0.75, 2, 7, 18 ms after a 1 cm diameter mercury jet was struck by a pulse of 2×10^{12} protons at 24 GeV.

Mercury has been chosen as the liquid for the jet although low-melting-point lead alloys are possible equally good alternatives. The jet is formed from a nozzle located at the entrance to the collector—in this case a pulsed magnetic solenoid.

The solenoid magnet is being fabricated from copper and cooled with liquid nitrogen to ~80 K to reduce the resistance and ohmic losses. The magnet is pulsed with a slow rise over ~10 s to reduce inductance effects and has a flat top of 1–2 s before slowly falling to zero. The cycle time between pulses is ~30 minutes to allow cooling to take place. The maximum field is calculated to be 15 T.

The jet will have a velocity of >10 m s^{-1} and be about 1 cm in diameter. Currently studies of the nozzle design are being undertaken at Princeton. The jet and proton beam are off the solenoid axis; the jet is at an angle of 100 mrad and the proton beam at 67 mrad. The proton beam size will be ≤1.5 mm r.m.s. The diagnostic of the beam-target interaction will be optical through four windows located along the length of the mercury jet recorded by high-speed cameras, while the secondary pion flux will be monitored by scintillator counters.

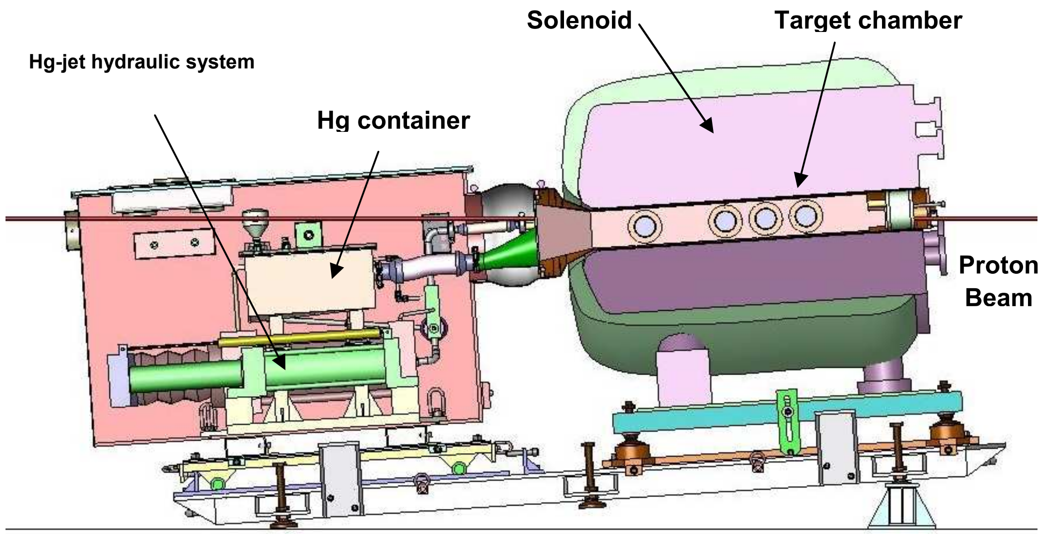

Fig. 5: Schematic view of the MERIT experiment

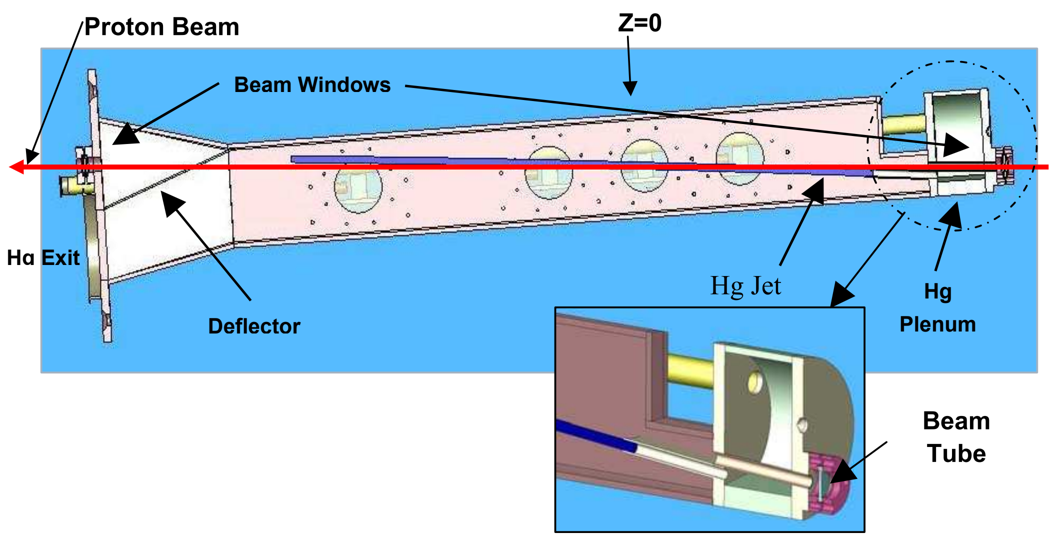

Fig. 6: Detail of the target volume showing the path of the Hg jet and of the beam. The four observation windows are also visible.

Only a few hundred pulses are required since, in principle, a single pulse will be able to show the success of the jet target concept. The goals of the experiment include studies of the jet entering the magnetic field, the jet dispersal by the beam in the magnetic field, the influence of the jet entry angle on jet performance at fields from 0 to 15 T, and the influence of the proton beam energy. Also, the CERN PS beam profile allows one to study the effect of varying the charge intensity from $5\ \ 10^{12}$ to $28\ \ 10^{12}$ protons per spill and to study the effects of the jet dispersal on the beam in long pulses. If the mercury has not dispersed sufficiently it could absorb pions. It is not possible directly to test the jet at 50 Hz operation, but it is possible at reduced beam energy (14 GeV) to extract two spills separated by

20 ms. This will be an important part of the test to confirm the correct re-establishment of the jet on successive beam pulses.

The MERIT experiment is an important proof-of-principle experiment which we hope will show that reliable long-life targets of almost unlimited power dissipation can be built. There is still an issue of safety with radioactive mercury; the use of a low-melting-point metal alloy could improve this situation.

3 Pion collection

Two options are discussed which relate to the neutrino facility: a superbeam would require a magnetic horn (see Fig. 7), sign-selecting the pions to be focused in the decay channel, whereas a neutrino factory would favour a solenoid magnet focusing both sign pions at the same time.

From an initial design made at CERN on a horn prototype system (horn + reflector) [28] foreseen for a neutron factory, an optimization and a redesign have been made in a superbeam context [29], driven by the physics case of a long-baseline experiment (130 km) between CERN and Fréjus (MEMPHYS detector location).

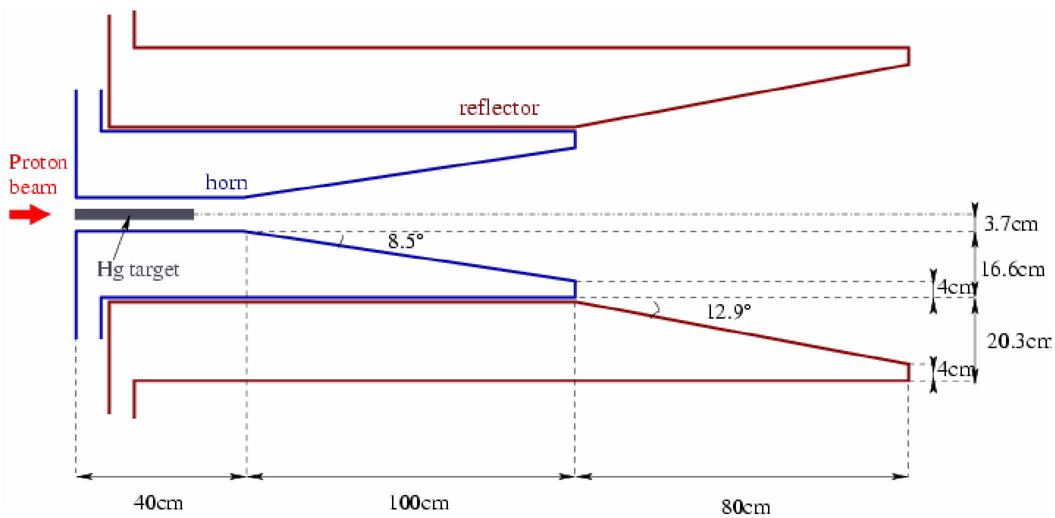

Fig. 7: Schematic section of the horn for pion collection

The proton energy appears to be best suited between 3.5 and 4.5 GeV proton kinetic energy and the current is then required to be 300 kA in the horn and 600 kA in the reflector. The horn must have a conductor thickness of only 3 mm to minimize the energy deposition by the secondary protons in the neck (<30 kW); a real challenge. Integration and testing with a target would need a dedicated R&D effort in an experimental area designed to face the various safety aspects (chemistry of heavy metals, high radiation levels, high voltage, high current, etc.), which would also include the design of a complete remote handling installation for the horn and target maintenance and exchange. The power supply design is an extrapolation of existing facilities and a first prototype version at only a fraction of the nominal current and repetition rate has been built. Hence it requires special attention and cost estimates on account of the high frequency envisaged, 50 Hz. A dedicated facility with prototypes of the different electrical components and a load (e.g. horn prototype) is needed to test existing components provided by manufacturers, and also to validate the mechanical design that has been chosen so far. This work should incorporate the latest knowledge acquired with the MiniBooNE and CNGS horns.

Generally, the solenoid collection is divided into two stages. The first one, where the field is constant, captures pions with a maximum transverse momentum, whereas a second part, where the field decreases to lower values, does the real focusing. Usually, more pions are captured for a stronger magnetic field for a given aperture. A compromise between field and aperture has to be made, since the cost of the superconducting device increases with the magnetic volume. The US Design Study II [2] indicates that a 20 T solenoidal magnet is feasible, with a reasonable lifetime. The solenoid has water-cooled copper coils in the centre, which also act as radiation shields to the superconducting coils on the outside. A detailed study of the behaviour of the superconducting part under a quench would be mandatory.

The pion yield by 3–20 GeV protons is, however, still poorly known: Geant4 and Mars simulations give significantly different results (up to 50%) in the best phase-space regions both for superbeams and neutrino factories. The HARP experiment is in the process of publishing its first results [30] and should help clarify this point soon.

4 Integration issues

There is an awareness that many of the problems with targets are common to several communities. These issues are being discussed at a number of gatherings, such as the High Power Target Workshops series [3,11]; this is helping to bring the various communities together.

Groups working on neutrino factories around the world are already collaborating closely. A good example of this is the MERIT mercury jet experiment [17]; a collaboration between laboratories in the USA, Japan, and Europe which reflects the worldwide effort to master the technological challenges towards a neutrino factory and a muon collider. Although MERIT will explicitly test the system in a strong solenoidal field, the results in zero magnetic field will be very important for jet applications in a horn collector.

The absence of suitable in-beam test facilities is a severe problem. There has been a recent proposal [11] from ORNL to try and set up an in-beam facility to allow a target to be tested at high power. Radiation damage to materials is another area requiring access to proton beams. Pulsed facilities are scarce but PSI [14] is providing a good, although limited, service using cw proton beams. To have an accurate estimate on the lifetime of the system, i.e., target and collector components, extensive mechanical tests with the pulsed power supply combined with the radiation field are mandatory.

Because of the absence of testing facilities and the dependence on other ongoing developments, the role of simulation is very important in this R&D. It can enable the testing of different design concepts, reduce the experimental working load—on account of easier access to specific data such as deformation, temperature, field, etc.,—and provide a more cost-effective engineering of the system. It is intended to develop the use of an already existing simulation tool with the modelling of cross-disciplinary studies: thermomechanical and electromagnetic computations in the dynamic and transient domains. Experience from other academic and industrial fields such as RF cavity (modelling, design, tuning) and induction heating will be integrated in order to minimize the time to reach a solution. A tuning of these simulations (fatigue, deformations, modal analyses, transient thermomechanical excitation of the structure, skin effect and Joule heating, power dissipation, heat exchange and cooling, radiation resistance, etc.) could be done using input provided by the previously described tests and facilities. This software development has to be done in parallel and with a strong interaction with all related hardware tasks.

These studies may also indicate the road to a more effective use of existing resources in terms of hardware in the different laboratories.

5 Recommendations

The most important recommendations are as follows:

- At the moment progress is seriously limited by resources, so more resources would be of great benefit.
- Nevertheless some progress is being made with targets, particularly mercury jets and studies at CERN, BNL and in the UK on solid materials. This should continue with more resources for both targets and collectors.
- The opportunity for more interactions with other communities needing high-power targets must be continued and expanded. This also applies to collectors.
- High-power target R&D should be continued.
- Collector R&D should be continued, including a dedicated facility for the horn power supply for high-frequency tests.
- A facility to study corrosion damage to the horn conductor material should be envisaged, since it seems to be the main cause of failure in the high-frequency, water-cooled horn.
- An in-beam test facility available to all should be pursued.
- The design of the target station, beam dump, remote handling, maintenance and replacement of components has hardly been addressed. This is an important area and will need considerable engineering and scientific resources.
- Related simulations have to be done in parallel.
- Address the safety issues and assimilate safety and maintenance considerations already in the early stages of the design. It takes a considerable time to obtain the necessary authorizations to operate these high-power target stations.

References

[1] R.B. Palmer, C. Johnson and E. Keil, *Nucl. Instrum. Meth. A* **451** (2000) 265.

[2] S. Ozaki *et al.*, *Feasibility Study II of a Muon-Based Neutrino Source*, BNL report No. BNL-52623, June 2001.

[3] Workshop on High Power Targetry for Future Accelerators, Ronconcoma, Long Island, New York, USA, 8–12 September 2003, http://www.cap.bnl.gov/mumu/conf/target-030908/.

[4] The International Linear Collider, see:
http://www-project.slac.stanford.edu/ilc/default.htm.

[5] Workshop on Positron Sources for the International Linear Collider, CCLRC Daresbury Laboratory, 11–13 April 2005; http://www.astec.ac.uk/id_mag/ID-Mag_Helical_ILC_Positron_Production_Workshop.htm.

[6] The RIA website, http://www.phy.anl.gov/ria/.

[7] The EURISOL website, http://www.eurisol-ds.lnl.infn.it/.

[8] The SNS website, http://www.sns.gov/.

[9] The ESS website, http://www.kfa-juelich.de/ess/#.

[10] http://apt.lanl.gov/system.html.

[11] Second High Power Targetry Workshop, Oak Ridge, TN, USA, 10–14 October 2005, http://www.cap.bnl.gov/mumu/conf/target-051010/.

[12] http://www.nea.fr/html/trw/.

[13] http://apt.lanl.gov/index.html.

[14] The PSI website, http://www.psi.ch/index_e.shtml.

[15] The MEGAPIE website, http://megapie.web.psi.ch/.

[16] J. Haines, Second High Power Targetry Workshop, Oak Ridge, TN, USA, 10–14 October 2005, http://www.cap.bnl.gov/mumu/conf/target-051010/.

[17] Studies of a target system for a 4-MW, 24-GeV proton beam, CERN-INTC-2004-016 INTC-P-186, 26 April 2004, http://www.hep.princeton.edu/~mcdonald/mumu/target/cern_proposal.pdf.

[18] P. Sievers, *Nucl. Instrum. Meth. A* **503** (2003) 344.

[19] J.R.J. Bennett *et al.,* NuFact05, LNF, Frascati (Rome), Italy, 21–26 June 2005, see website: http://www.lnf.infn.it/conference/2005/nufact05/.

[20] K. Elsener, CNGS - CERN neutrinos to Gran Sasso, CERN-SL-2000-018 EA, http://proj-cngs.web.cern.ch/proj-cngs/PDF_files/sl-2000-018.pdf.

[21] R. Wilfinger, ENG/BENE, Target Section Meeting, March 2005, http://bene.web.cern.ch/bene/.

[22] N. Simos, Second High Power Targetry Workshop, Oak Ridge, TN, USA, 10–14 October 2005, http://www.cap.bnl.gov/mumu/conf/target-051010/.

[23] L.M. Barker and R.E. Hollenbach, *J. Appl. Phys*. **43** (1972) 4669.

[24] Livermore Software Technology Corp. http://www.lstc.com/.

[25] J. Chen *et al., J. Nucl. Mater*. **298** (2001) 248.

[26] H.G. Kirk *et al.,* Target studies with BNL E951 at the AGS, Proc. 2001 Part. Accel. Conf., Chicago, IL, 2001 (IEEE, New York, 2002), p. 1535.

[27] J. Lettry *et al.,* Thermal shocks and magnetohydrodynamics in high power mercury targets*, J. Phys. G: Nucl. and Part. Phys.* **29** (2003) 1621.

[28] A. Ball *et al.,* CERN-NUFACT-Note-42.

[29] J.E. Campagne, CERN-NUFACT-Note-138.

[30] HARP Collaboration to appear in Nuclear Physics B.

The front-end of a Neutrino Factory

1 Overview

The particles produced by the bombardment of the target form the input to the muon front-end of the Neutrino Factory. The front-end is required to capture the pions produced in the target, to contain the muons produced by pion decay, to produce an appropriate energy and bunch structure in the beam, and to reduce the phase-space volume (cool) the muon beam so that it is well matched to the subsequent acceleration systems. Recent progress in the development of the various subsystems that make up the muon front-end is described in detail in Refs. [1,2] and is summarized below.

2 Pion capture and decay channel

Two schemes have been proposed by which the particles produced in the target may be captured. The first uses high-field solenoid magnets to capture both positive and negative particles at the same time [3–5]. The second calls for a magnetic horn to focus either positive or negative particles into the subsequent transport and decay sections [6]. The horn scheme has the advantage that the focusing element closest to the target itself is relatively simple. The advantage of the solenoid scheme is that an efficiency gain of a factor of two can be achieved if the downstream accelerator complex is designed to manipulate and store $^{+}$ and $^{-}$ simultaneously [5]. In each case, significant engineering work needs to be carried out to ensure that the target station can be operated safely.

A large-aperture (16–30 cm) focusing channel consisting of high-field (1.2–5 T) superconducting solenoids is used to transport the pions and to capture and transport the decay muons. The pion lifetime ($\tau \approx 2.6$ 10^{-8} s) yields $c\tau \approx 10$ m, therefore decay channels with lengths of up to 100 m have been considered.

3 Phase rotation and bunching

By the end of the decay channel a strong energy–time correlation has developed in the longitudinal phase space of the muon beam; energetic muons arrive at the end of the channel early, low-momentum muons arrive late. The system that receives the beam from the decay channel must accommodate this large longitudinal phase space. The Japanese scheme for a Neutrino Factory [7] calls for the beam emerging from the decay channel to be injected directly into a large-acceptance, fixed-field, alternating-gradient (FFAG) accelerator of the PRISM type [8]. The FFAG effects both the rotation of the longitudinal phase space and the acceleration of the muon beam from 0.3 GeV/*c* to 1 GeV/*c*.

While the CERN Neutrino Factory scheme maintains the SPL bunch structure and so requires no bunching section, each of the US schemes employs an RF system to bunch the beam. The most recent study, Study IIa, proposes the use of RF cavities with frequencies decreasing from 333 MHz to 234 MHz to bunch the beam.

The various European and US Neutrino Factory schemes all call for phase rotation to reduce the energy spread of the muon beam in preparation for the ionization cooling channel. The CERN scheme uses a series of 44 MHz or 88 MHz RF cavities. No buncher is required as the bunch structure of the proton driver (the SPL) is preserved through the capture channel. In Study IIa, a sequence of RF cavities the frequencies of which decrease from 234 MHz to 201 MHz is used to perform phase rotation. The phase space produced is shown in Fig. 1. A relatively long muon pulse is produced in 201 MHz bunches that are well matched to the subsequent cooling channel.

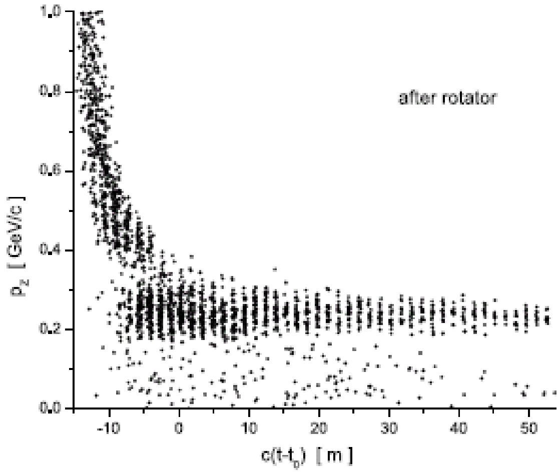

Fig. 1: The longitudinal phase space of the muon beam at the end of the phase-rotation section of Study IIa

4 Ionization cooling

The muon beam that emerges from the phase-rotation and bunching sections fills a large volume in transverse phase space. For example, in US Study II the transverse emittance at the exit of the decay channel is 12 mm [9]. The spread of the muons in the longitudinal phase space is also very large (~60 mm in Study II). Efficient, cost-effective acceleration of the muon beam requires that the phase space be modified. The phase-rotation and bunching systems that follow the decay channel are required to produce a beam with an energy spread of ~60 MeV which is appropriately bunched to match the subsequent cooling sections.

Each of the five Neutrino Factory conceptual design studies has considered the benefit of reducing the emittance of the muon beam (cooling) before injecting it into the acceleration and storage systems. There are two principal motivations for this: to increase the number of muons inside the acceptance of the downstream accelerators; and to keep the cost of the muon acceleration system to a minimum.

At the end of the decay channel, the muons have a momentum of roughly 200 MeV/*c*. The time-dilated lifetime of the muon is short (~4.7 s) making it essential that cooling and acceleration take place as rapidly as possible. Ionization cooling, a process in which the muon beam is caused to pass through an alternating series of liquid-hydrogen absorbers and accelerating RF-cavities, is the technique by which it is proposed to cool the muon beam prior to acceleration. Various ‘gain factors' have been defined to quantify the gain in performance due to the cooling channel (see Table 1). Systems that give gain factors of between 2 and 10 have been devised. Since a factor of Γ gain in stored muon-beam intensity implies a reduction, by a factor Γ, in the running time required to achieve a particular total neutrino flux, and a decrease in emittance of the muon beam entering the acceleration section is likely to lead to significantly lower costs for muon acceleration, it will be important to make a careful optimization, for performance and cost, of the cooling and acceleration systems. The engineering demonstration of the ionization-cooling technique will be carried out by the international Muon Ionization Cooling Experiment (MICE) Collaboration [9]. The MICE experiment, which has been approved, will take place at the Rutherford Appleton Laboratory (RAL), using muons produced by the ISIS 800 MeV proton synchrotron. The status of the experiment is reviewed later.

The US MuCool Collaboration [2] is carrying out an R&D programme by which each of the components of the cooling channel will be built and operated. The principal components of the cooling channel that have been built and tested over the past year are the liquid-hydrogen absorber and the 201 MHz cavity. During the past year, the Muon Test Area (MTA) at FNAL has become available. Component tests are currently under way in the MTA which will eventually be served by a high-intensity proton beam so that the operation of the cooling channel components can be proved using realistic particle fluxes.

Table 1: Survey of the gain afforded using ionization cooling in a number of conceptual design studies of the Neutrino Factory

Design	Number of cooling cells	Gain factor per cell (%)	Cooling factor	Comment
Study II [4]	26	6	7	Increase in phase-space density in acceptance of downstream accelerator.
Study IIa [5]	26	2	2	Increase in number of muons in acceptance of downstream accelerator.
CERN [6]	36	10	7	Increase in muon yield at 2 GeV over optimized Neutrino Factory without cooling.
NuFactJ [7]	–	–	1.5–2	Acceleration based on FFAGs. Performance improvement when absorber is included in FFAG ring giving 6D cooling effect.

4.1 The international Muon Ionization Cooling Experiment liquid-metal jet

The principal components of the MICE experiment are shown in Fig. 2 [9]. Two, functionally equivalent, spectrometers are placed upstream and downstream of a single lattice cell of the Study II cooling channel. In the Study II design approximately 10^{14} /s pass through the channel. The lateral dimensions of the beam are such that space-charge forces can be ignored making it possible to run MICE as a single particle experiment in which the Neutrino Factory bunch is reconstructed offline using an ensemble of particles recorded in the experiment. At the nominal input emittance of ε_{in} = 6 π mm a cooling effect ($\varepsilon_{in}/\varepsilon_{out}$ – 1, where ε_{out} is the output emittance) of ~10% is expected. The cooling effect will be measured with a precision of 1% (i.e., $\varepsilon_{in}/\varepsilon_{out}$ – 1 will be measured with an absolute precision of 0.1%).

The US MuCool Collaboration [2] is carrying out an R&D programme by which the MICE cooling channel consists of three absorber/focus-coil (AFC) modules and two accelerating-cavity/coupling-coil (RFCC) modules. The AFC modules each contain a 21 litre liquid-hydrogen absorber inside a pair of superconducting coils that bring the beam to a focus in the centre of the absorber. Liquid hydrogen is the most efficient ionization-cooling material because it has a large specific ionization and a comparatively large radiation length. Safe operation of the system in the presense of liquid hydrogen leads to significant engineering constraints. The AFC modules and the hydrogen system each have both active and passive safety systems. The hydrogen will be stored in the form of metal hydride when the absorber is emptied. A vigorous R&D programme is under way to demonstrate the safe operation of the hydrogen system. The superconducting coils and the liquid-hydrogen vessel itself are refrigerated using closed-cycle ‘cryo-coolers’ [10].

The RFCC module must restore the energy lost by the muons as they pass through the absorber. The coupling coil, a short, large-diameter solenoid, provides the magnetic field that transports the muons through the module. The acceleration is produced by four 201 MHz copper cavities which produce a gradient of 8 MV/m. To produce the required field gradient, the cavities must be electrically closed, yet, to preseve the cooling effect, the amount of material through which the beam passes must be minimized. Thin beryllium windows have been developed for this purpose through the MuCool programme [2]. The degree of emission from the cavity surfaces is significantly enhanced by the Lorentz force produced by an intense magnetic field [11]. While reducing the field emission in a Neutrino Factory cooling channel, in which the cavities must operate at 16 MV/m, is a challenging problem, it has been estimated that for operation in MICE, the emission can be kept within acceptable bounds.

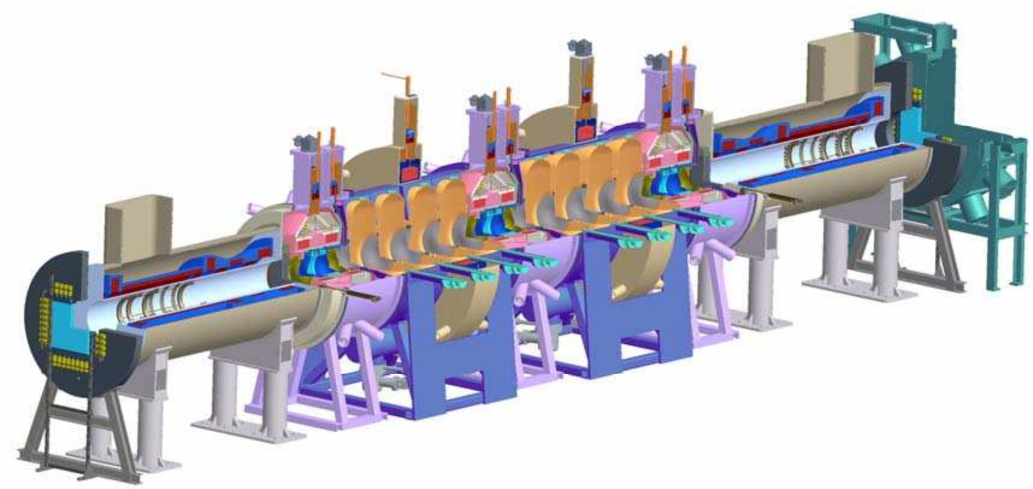

Fig. 2: Drawing of the MICE experiment [9]. The beam enters the experiment from the bottom left-hand corner. The beam first passes through one of the scintillator hodoscopes that form the time-of-flight system. After passing through the upstream spectrometer, the beam passes through three absorber/focus-coil modules and two cavity/coupling-coil modules before it passes through the downstream spectrometer and, a second time-of-flight hodoscope, the downstream Cherenkov counter and is stopped in the electromagnetic calorimeter. The beamline and upstream instrumentation is not shown.

The muon beam that enters the experiment may contain a small pion contamination. The instrumentation upstream of the cooling channel is therefore required to distinguish pions from muons and to measure the phase-space coordinates of the muons entering the channel. Downstream of the cooling channel, the instrumentation is required to identify electrons produced in the channel by muon decays and to measure the muon phase-space coordinates. The upstream particle identification will be performed using a scintillator-based time-of-flight (TOF) system and a threshold Cherenkov counter. The TOF system will also be used to trigger the experiment and to determine the phase of the RF fields in the cavities as the muon traverses the experiment. The upstream and downstream spectrometers are each composed of a 4 T superconducting solenoid instrumented with a scintillating-fibre tracking device. Downstream of the cooling channel a final TOF station, a Cherenkov counter, and a calorimeter are used to distinguish muons and electrons.

The MICE Collaboration will take enough data to make the uncertainty on the measured cooling effect systematics limited. It is therefore crucial that the systematic errors be understood in detail. To do this, the experiment will be built up in stages. A first measurement of cooling, using the two spectrometers and one AFC module, is scheduled for 2008. The first RFCC module and a second AFC module will then be installed and the full MICE cooling channel will be assembled in 2009.

The MICE experiment will be mounted on ISIS at the CCLRC Rutherford Appleton Laboratory. The preparation of the MICE Muon Beam on ISIS, the MICE Hall and the first phase of the MICE experiment is proceeding on schedule. The first data-taking period, in which the muon beam will be characterized, the instrumentation calibrated, and the relative systematics of the two spectrometers will be measured, will begin in April 2007.

References

[1] R.C. Fernow, Muon front-end for the Neutrino Factory, contributed paper to the 7th International Workshop on Neutrino Factories and Superbeams, NuFact05, Laboratori Nazionali di Frascati, Frascati (Rome), June 21–26, 2005.

[2] Y. Torun, Muon cooling: MuCool and MICE, contributed paper to the 7th International Workshop on Neutrino Factories and Superbeams, NuFact05, Laboratori Nazionali di Frascati, Frascati (Rome), June 21–26, 2005.

[3] D. Finley and N. Holtkamp, Eds., *Feasibility Study on a Neutrino Source Based on a Muon Storage Ring* (2000). See http://www.fnal.gov/projects/muon_collider/reports.html.

[4] S. Ozaki, R. Palmer, M. Zisman and J. Gallardo, Eds., *Feasibility Study-II of a Muon-Based Neutrino Source*, BNL-52623, June 2001.

[5] C. Albright *et al., Neutrino Factory and Beta Beam Experiments and Development*, BNL-72369-2004, FNAL-TM-2259, LBNL-55478. See http://www.cap.bnl.gov/mumu/study2a/ and http://www.cap.bnl.gov/mumu/studyii/FS2-report.html.

[6] A. Blondel, Ed., *ECFA/CERN Studies of a European Neutrino Factory Complex*, CERN-2004-022, http://preprints.cern.ch/cernrep/2004/2004-002/2004-002.html.

[7] NuFactJ Working Group, *A Feasibility Study of a Neutrino Factory in Japan*. See http://www-prism.kek.jp/nufactj/nufactj.pdf.

[8] The PRISM Working Group, *The PRISM Project - A Muon Source of the World-Highest Brightness by Phase Rotation*, submitted to J-PARC Letter of Intent L24, unpublished, http://www-ps.kek.jp/jhf-np/LOIlist/LOIlist.html.

[9] G. Gregoire *et al.,* The MICE Collaboration, MICE, an International Muon Ionisation Cooling Experiment: proposal to the Rutherford Appleton Laboratory, submitted to CCLRC and PPARC on the 10th January 2003: http://mice.iit.edu/cooldemo/micenotes/public/pdf/MICE0021/MICE0021.pdf.

[10] http://www.janis.com/p-a4k10.html.

[11] J. Norem, Breakdown in RF cavities, TPPT025, paper contributed to PAC05, Particle Accelerator Conference, Knoxville, TN, USA, 16–20 May 2005.

Muon acceleration and storage in a Neutrino Factory

Because of the manifest superiority of FFAGs over other techniques for muon acceleration in a Neutrino Factory and following decisions taken in December 2003, work in this area has focused on the FFAG method. This year has again seen an increase in the participation of the EU in FFAG research and design. The active fields within CARE/BENE are (i) design of an electron model of a non-scaling muon FFAG, (ii) design of an isochronous FFAG, (iii) developement of simulation and tracking tools, (iv) participation in the design of the US linear muon FFAGs, and (v) collaboration in Japanese scaling FFAG studies. In addition, the EU is proposing to construct the first non-scaling FFAGs ever built. This and the NuFact International Scoping Study will be the next challenging activities. All of this work is the subject of internal reports and of contributions in conferences and workshops.

1 The context [1–3]

Muon acceleration in the Neutrino Factory is taking advantage of modern accelerator technologies, which should permit the construction of a facility capable of bringing intense beams—in the 10^{21} muons/year range, to multi-GeV energies, 20–50 GeV—in the near future. Various muon acceleration methods have been investigated so far, and have yielded a number of different layouts, as described below. However, the accelerator community is now particularly concentrating on the method of FFAGs and is bringing new, modern ideas and concepts to the field, that are very promising both for muon acceleration and for proton driver applications.

The ‘why’ and ‘how’ of this strong increase in activity in the FFAG domain will be addressed in the following sections, along with the corresponding engagement within the BENE MuEnd Work Package, as planned from the very beginning, and the consequences for future plans.

2 Muon acceleration concepts

Recirculating Linac Accelerator based designs. Linac acceleration presents the essential property of allowing fast acceleration in a short distance, thanks to the use of high-gradient/high-frequency RF systems, compatible with the short lifetime of muons, thus ensuring a high transmission—typically, more than 80% at an average gradient of 5 MV/m. With regard to the large muon beam phase-space, superconducting linacs also offer a good geometrical acceptance, owing in particular to the large iris of the ~200 MHz RF cavities, and the possibility of accelerating trains of bunches, all of which are properties that translate into 6-D acceptance performance.

Two recirculating linac accelerator (RLA) schemes have been produced, namely:

– The US Study I, in 2000 [4], based on linac pre-acceleration followed by two RLAs that bring the muon beam up to 50 GeV; a follow-on, Study II, in 2001 [5] (Fig. 1), differed mostly, from the point of view of the acceleration, in having a lower muon energy (20 GeV), using a single RLA; and, in 2004, Study IIa [6], which benefits in particular from cost-effective approaches, allows both signs of muons, and sees the first introduction of FFAGs in a combined Linac/RLA/FFAG acceleration scheme.

– The EU study, a design produced in 2004, with 50 GeV top energy, based on the acceleration of muons by a two-stage RLA system [7], and operating in a bunch-to-bucket mode (Fig. 2).

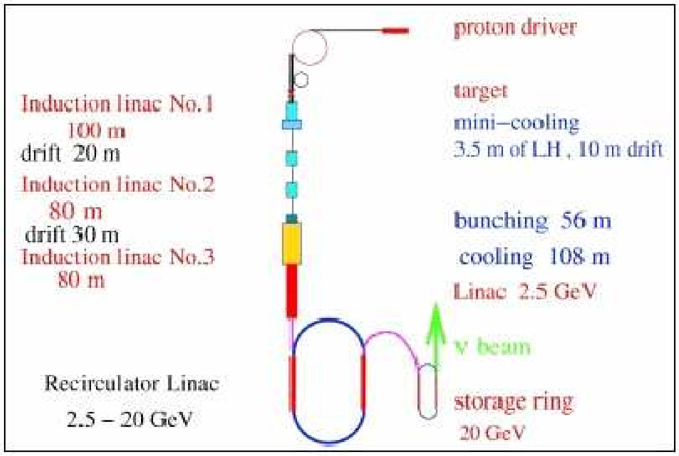

Fig. 1: US Study II layout. Muon beam structure: a train of six bunches spaced by 20 ms (hence target and accelerators rep. rate of 50 Hz), 3 ns bunch length at origin (target), rep. rate 2.5 Hz to be upgraded to 5 Hz. Muon bunches undergo 200 MHz 'micro-bunching' (about 60 sub-bunches) prior to launching in the acceleration chain. Muon decay rate: 1.2 10^{20}/year/MW/straight. Proton driver: an upgrade of BNL AGS, 26 GeV, repetition rate 2.5 Hz, 10^{14} ppp.

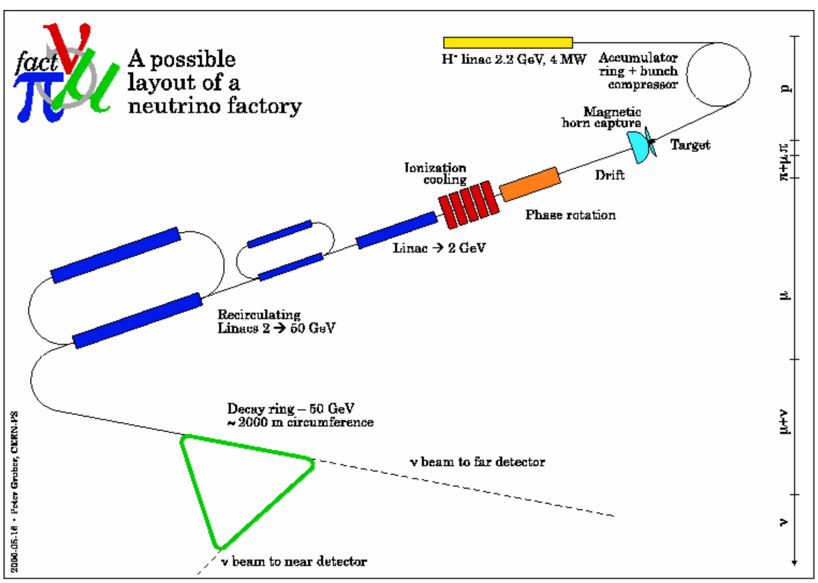

Fig. 2: The CERN NuFact layout. Muon beam structure: 3.2 μs long trains of 140, 23 ns spaced bunches (44 MHz structure), at a repetition rate of 50 Hz. 1 ns bunch length at origin (target). Bunch-to-bucket operation: next to capture, phase rotation and cooling, each muon bunch occupies a 220 MHz linac RF bucket. 50 GeV top energy reached in three stages: linac up to 3 GeV, followed by 3–11 and 11–50 RLAs. Muon rate: 10^{21}/year in the storage ring.

Amongst other conclusions, these design studies are said to have "demonstrated technical feasibility (provided the challenging component specifications are met), established a cost baseline and achieved the desired range of physics performance", and to have shown that "progress is still needed [...] towards optimising the design, developing and testing the required accelerator components, and significantly reducing the cost" [6]. The cost of the NuFact installation is very high with the muon accelerators representing about a third of it, and the possibility that "FFAG rings could be also considered" (page 6.2, in Ref. [5]), as a cheaper solution, has already arisen in the US Study IIa.

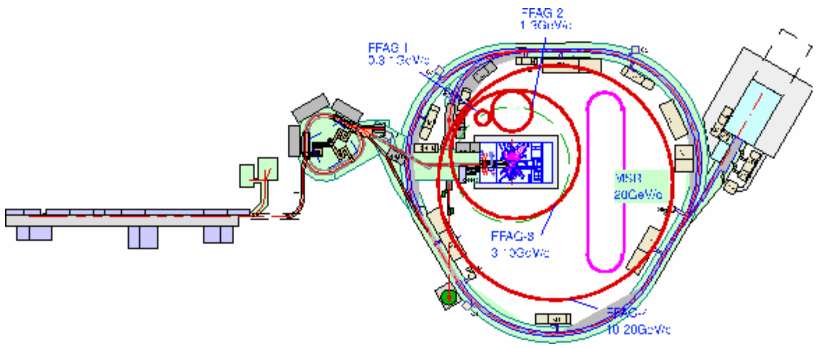

Fig. 3: Japanese NuFact layout. Proton driver: JPARC, 50 GeV; phase I at 0.75 MW: repetition rate 0.3 Hz, 3.3 10^{14} ppp, 8 bpp, upgradable to 4 MW. The first FFAG ring (0.2–1 GeV) assures muon bunch capture at the exit of the pion decay channel; 20 GeV is reached in three more stages (1–3, 3–10 and 10–20 GeV). Muon decay rate in the storage ring: 2 10^{20} /year/MW/straight.

Scaling FFAG and Japan R&D. Independently, in 2001 a NuFact based on the JPARC 50 GeV proton installation and on the capture and acceleration of the muons to 20 GeV by scaling FFAGs was proposed (Fig. 3) [8]. Acceleration in the high-energy regime uses high-gradient (up to 10 MV/m), low-frequency (5–25 MHz) RF, and is based either on a huge-bucket method, with injection at the bottom and rotation upward in the manner of the RF manipulation in the PRISM experiment (see below) or, alternatively, on the use of frequency modulation. The FFAG method yields large transverse acceptance (on the order of 3π cm), large longitudinal acceptance (1.5 eV.s) and reasonably fast acceleration (1 MV/m on average), resulting in about 50% muon survival.

Extensive R&D programmes have been pursued in Japan. They comprise, amongst other RF and component studies, the building of a proof-of-principle 500 keV proton machine (Appendix C, in Ref. [8]), followed by a larger 150 MeV accelerator [9], both based on a radial sector DFD triplet. These two machines proved in particular the feasibility of ultra-fast cycling, repetition rate in the kHz range, by means of high-gradient RF systems based on special magnetic alloy cores [10]. This is now followed by the prototype ADS/Reactor experiment facility under construction at the KURRI institute, Kyoto [11].

The first muon FFAG will be the PRISM project, a 2003–2007 programme [12]. The PRISM lattice is based on a DFD triplet similar to the KEK FFAGs design, and comprises 10 cells. This FFAG is intended for muon-bunch phase rotation aiming at momentum spread compression, from 68 MeV/*c* ±20% down to ±5% in six turns, for use in a muon-beam physics facility. The remarkable features of PRISM are its 2 MV/turn RF system, and its challenging injection and extraction systems, a benchmark towards the NuFact accelerators.

Non-scaling FFAGs. This represents the main field of activity within BENE/MuEnd. The concept was introduced in the US in the late 1990s [13] and uses a synchrotron type of cell, i.e., using linear optical elements, with fixed fields. Hence the orbit position moves in the course of acceleration, and the tunes change (in contrast to scaling FFAGs) because of the change in beam rigidity. Compared to RLAs, these 'linear, non-scaling FFAGs' allow more turns, and hence less RF, and in addition there are a smaller number of FFAG rings (2–3) than there are arcs in RLAs (2 × 4–5 passes).

Linear, non-scaling optics have a number of advantages: (i) large transverse acceptance due to the linear fields and large momentum acceptance due to the small dispersion function, up to the point where the necessity of cooling is now questionable; (ii) rapid acceleration (energy gain of 2 to 3 over about 10 turns), due to high-frequency/high-gradient RF and near-crest acceleration; (iii) reduced circumference (and muon decay loss) compared to scaling FFAGs; (iv) reasonable-sized magnets, due to the limited horizontal beam excursion. There are drawbacks to the method, however, such as strongly non-linear longitudinal motion, and resonance crossing during acceleration. This is addressed in the last section.

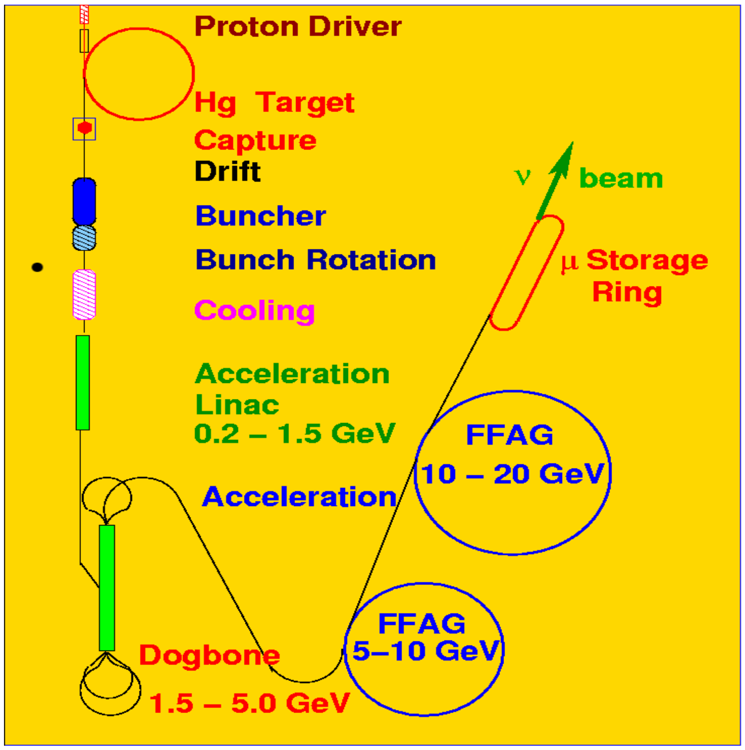

Fig. 4: US Study IIa. 1.5 GeV SC Linac, followed by a 3.5-pass 5 GeV dogbone SCRF RLA [14] and two FDF-lattice FFAGs, 5–10 and 10–20 GeV. Muon beam structure as in Study II (Fig. 1). Muon rate ~0.3/p_20 GeV, twice that of Study II.

Some preliminary conclusions have been drawn from the work undertaken so far: (i) linear FFAGs yield lower cost/GeV than RLAs above 5 GeV, and possibly also below, though this needs further investigation; (ii) a new muon acceleration scheme has emerged, US Study IIa [6] (Fig. 4), combining Linac, dogbone RLA [14], and non-scaling FDF-lattice FFAGs. The acceleration in these machines is based on 201 MHz SCRF and 3π cm/0.05 eV.s acceptance is reached (twice the transverse acceptance in Study II). Higher energy could be attained using additional FFAG rings.

Isochronous FFAG: Isochronism to high order allows on-crest acceleration, a cyclotron-like regime. This type of FFAG has been developed in the EU recently [15]. The current design is based on a five-magnet cell (Fig. 5) using three different types of combined multipole magnets. The cell acts as a DFD triplet at low energy and as an FDF triplet at high energy. This use of two families of cells allows the design of a ring with insertions. The horizontal tune varies (less than 0.15 per cell), whereas the vertical tune is about constant. An 8–20 GeV muon ring has been designed this way, accelerating in 16 turns using 201 MHz RF, with a circumference close to 1000 m. Alternative designs have been proposed as well [16].

The isochronous FFAG with insertions has a number of advantages, in particular optimum, on-crest acceleration, resistive beam loading, the flexibility of insertions (for injection, extraction and collimation), fewer RF systems by the use of four-cell cavities, and no crossing of integer or half-integer vertical betatron resonances during acceleration (in contrast with linear FFAGs). Dedicated tracking tool developments [17] have allowed numerical simulations of 6-D transmission in this FFAG [18].

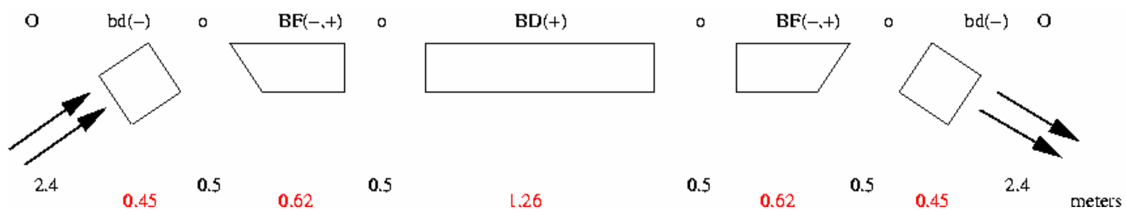

Fig. 5: Five-magnet cell of an isochronous FFAG

3 Electron model

A proof-of-principle of non-scaling FFAGs is needed, with the goal of demonstrating in particular the viability of the concepts of (i) rapid acceleration, in 5 to 10 turns, (ii) resonance crossing and the related constraints on field and alignment defects, (iii) large acceptance. These considerations have motivated the emergence of the EMMA electron model project [19], a 10 to 20 MeV ring, with a 42-cell FODO lattice, about 15 metres in circumference, using 1.3 GHz RF. It is hoped to build EMMA in the Daresbury Laboratory in the UK, once the necessary funding has been obtained. It is also planned to construct a proton non-scaling FFAG as a prototype for hadron therapy in Oxford. Experiments on fixed-field acceleration are also taking place at existing pulsed synchrotrons [20].

4 Muon decay rings

Muon decay rings are under study as part of the International Scoping Study (ISS) for a future Neutrino Factory. Racetrack and isosceles triangle shaped rings are both being considered for a muon energy of 20 GeV, but with an upgrade potential for 50 GeV. The designs are influenced by the stages ahead of the rings, the high-power proton driver, the pion production target, the generation of trains of 80, μ^+ and μ^- bunches, the ionization cooling channel and the stages for rapid muon acceleration. An additional influence is the distance requirements to the far-off neutrino detectors.

There are long ring straight sections where the stored muons decay into neutrinos, which pass on to one or two distant detectors. Racetrack rings have one such production region, aligned with one detector, while triangular rings use two shorter straights, aligned to two detectors. The μ^+ and μ^- bunch trains are injected in separate rings and, for the racetrack designs, the rings lie one above another, in a plane tilted downward to the horizontal. In the case of the isosceles triangle rings, detector distances required are 7500 km for one, and 2500 km to 3500 km for the other. With such distances, the smallest, triangle apex angle (and best production efficiency) is at approximately 48˚, for rings in side by side, vertical planes. On a gnomonic projection map, the detectors are then in opposite directions from the ring positions. Some modified directions, with some ring inclinations to the vertical plane, are expected for most pairs of detector sites.

Detailed designs are under way for a pair of racetrack rings and for a pair of isosceles triangle rings of apex angle 52.8˚. For the latter, the circumference is 1573.05 m and the production straights have eight, symmetrically spaced, superconducting solenoid magnets over a length of 378.0 m, for a neutrino efficiency of 2   24%. The third straight for the triangular rings houses the beam loss collimators, radio frequency containment systems and adjustable, tune control quadrupoles. An intense neutrino beam is directed at the accelerator site from this region, as the two rings are in a vertical, or near vertical, plane.

Bunch patterns have been identified for a 10 GeV, 50 Hz, 4 MW proton driver, the $\mu^{\pm}$ accelerators and the 50 Hz decay rings. In one scheme, five trains of 80 μ^{+} bunches are injected in one decay ring, and five trains of 80 μ^{-} in the other. Time gaps of more than 100 ns are created in between the μ^{+} and μ^{-} beams, to allow particle identification. Single, $\mu^{\pm}$ bunch trains are accelerated sequentially before being separately, box-car stacked over the decay rings. A key condition for the box-car stacking is that the proton driver, bunch separation frequency, at 10 GeV, be a sub-harmonic of 201.25 MHz, the fixed frequency used for muon acceleration. Injection of the separate bunch trains requires 16, fast kicker pulsers for each ring.

The racetrack rings are being studied at FNAL, USA, the isosceles triangle rings at RAL, UK, and detailed, muon tracking simulations are in progress at CNRS, Grenoble. In the future, optimum accelerator and detector sites will be identified and, it is only after this stage, that it will be possible to specify the final ring parameters.

5 Perspective

It is evident from what precedes that a large amount of work has already been undertaken in the quest for better performing and less expensive muon acceleration techniques, but that much is still required.

At the present stage of the research, it is clear that more collaborators are needed on the EU side, to match those in Japan and the US. Areas requiring particular attention are

1. Lattice design
   - A task force needs now be devoted to muon storage ring studies.
   - Optimization work is needed to improve the muon transmission in the accelerators.
   - EU participation in both EMMA and the proton FFAG is currently very limited.
   - There is limited activity in the design of the FFAGs for muon acceleration, with no contributions at all to the crucial question of linear FFAGs below 5 GeV.
   - Error studies are needed (field, alignment, tolerances).
2. Magnet
   - It is time now to launch magnet studies, 3D design, etc. Some work has already started, mainly at Fermilab and mostly focused on EMMA. Designs relating to the muon machines would allow progress with the lattice design studies as well.
3. Model
   - There are two proposals, e (10–20 MeV) (EMMA) or p (> about 100 MeV). EMMA would be a proof of linear FFAG acceleration of muons. The p model can be considered relevant to the proton driver case and would be the non-scaling equivalent of the machine our Japanese colleagues built in the late 1990s (POP) with a scaling lattice. This was a success and promoted significant progress in the field.

References

[1] F. Méot, The acceleration of muons in the neutrino factory, Proc. NuFact05 Workshop, Frascati (2005).

[2] H. Haseroth, The technical challenges of superbeams and Neutrino Factories, Proc. NuFact05.

[3] C. Ohmori, Achievements at NuFcat05, Proc. NuFact05.

[4] N. Holtkamp and D. Finley, Eds., Technical Report, Fermilab-Pub-00/108-E, Fermilab (2000).

[5] S. Ozaki, R. Palmer, M. Zisman, and J. Gallardo, Eds., Technical Report, BNL-52623 (2001).

[6] http://www.cap.bnl.gov/mumu/study2a/ REPORT/NF-BB-WG.pdf

[7] The study of a European neutrino factory complex, CERN/PS/2002-080 (PP).

[8] A Feasibility Study of a Neutrino Factory in Japan, NufactJ Working Group (2000).

[9] M. Aiba *et al.,* 150 MeV FFAG accelerator [...], EPAC-2002, Paris.

[10] C. Ohmori, High field-gradient cavities loaded with magnetic alloys, PAC99 Conf.

[11] M. Tanigaki *et al.,* Construction of FFAG Accelerators in KURRI [...], PAC05 Conf.

[12] Y. Kuriyama, Development status of PRISM-FFAG ring [...], Proc. NuFact05.

[13] F.E. Mills and C. Johnstone, 4th Int. Conf. on Physics at $\mu+\mu-$ colliders, San Francisco, UCLA (1999).

[14] A. Bogacz, Beam dynamics of low energy muon acceleration, Proc. NuFact05.

[15] G.H. Rees, FFAG studies for Neutrino Factory accelerators, Proc. NuFact05; F. Lemuet, F. Méot and G. Rees, Numerical 6-D acceleration in an isochronous FFAG ring, PAC05 Conf.

[16] H. Schonauer, An isochronous 10–20 GeV muon ring with constant tunes, operating above transition, Proc. NuFact05.

[17] F. Lemuet, F. Méot, Developments in the ray-tracing code Zgoubi for 6-D multiturn tracking in FFAG rings, *Nucl. Instrum. Methods A* **547** (2005) 638–651.

[18] F. Lemuet, 6D beam dynamics in an isochronous FFAG ring, Proc. NuFact05.

[19] E. Keil, for the EMMA Collaboration, Electron model: lattice and performance, Proc. NuFact05; R. Edgecock, for the EMMA Collaboration, Introduction to the non-scaling electron model FFAG EMMA, *ibid.;* G. Rees, Isochronous, FFAG rings with insertions for the rapid acceleration of muons or electrons, *ibid.*

[20] S. Machida, Experimental study of resonance crossing at HIMAC, Proc. NuFact05.

A slow muon facility at a Neutrino Factory

High-intensity, slow muon beams can be obtained at the very front end of a neutrino facility. They could be very useful in a wide variety of experiments which are usually divided into three categories: (1) precision measurements, (2) searches for rare processes, and (3) applications. A non-comprehensive list of some of these experiments subdivided in the three categories is shown in Table 1.

Table 1: Overview of experiments with slow muons

Category	Topic	Comment	Beam
Precision measurements	Muon lifetime	G_F determination	Pulsed
	Muon capture rates	Nuclear physics	Pulsed or DC
	Muonic X-ray	Nuclear physics	Pulsed or DC
	Muon $g-2$	SM allowed, new physics	Pulsed
Rare processes	Muon EDM	SM suppressed, new physics	Pulsed
	Charged-lepton mixing	SM forbidden, new physics	Pulsed or DC
Applications	Catalysed fusion	Aim break-even	Pulsed
	Materials science	SR	DC

A more comprehensive list with details of the beam characteristics needed can be found in Ref. [1].

From the point of view of particle physics, very important measurements are those of the muon anomalous magnetic dipole moment (MDM) $a = (g - 2)/2$, of the possible muon electric dipole moment (EDM) and of rare decays in which charged-lepton flavour is violated (CLFV). These measurements are often called 'the muon trio' because in SUSY models their respective amplitudes can be derived from the slepton mass matrix as in Fig. 1 where MDM and EDM are related to the real and imaginary part of the smuon diagonal element while CLFV is related to the off-diagonal elements.

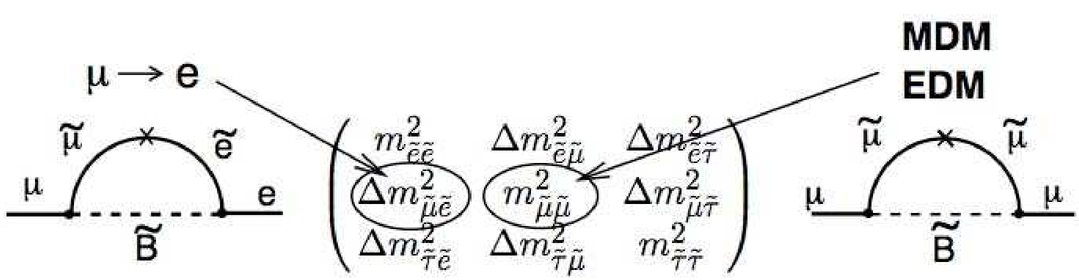

Fig. 1: Slepton mass matrix and its contributions to the three processes: MDM, EDM, CLFV

As is well known the present best experimental MDM measurement [2]:

$$a \quad = \frac{g-2}{2} = 1.1659208(6) \quad 10^{-10} \qquad\qquad (0.5\ \text{ppm})$$

deviates 2.6 or 0.9σ from the SM value depending on whether this is computed by using e^+e^- or τ data. This possible deviation can be explained by SUSY contributions with parameters that will be explored by the LHC experiments. It is possible to improve the experimental result down to 0.05 ppm [3] with higher muon beam intensities, though to fully realize the potential of the improved experimental measurement the hadronic contribution would need to be known with an equivalent uncertainty.

The current limit [4] on the muon EDM (~10^{-18} e-cm) could also be improved by several orders of magnitude, down to 10^{-24} e-cm, by using high-intensity muon beams in a storage ring with a suitable electric field [5]. EDMs of this order of magnitude are again predicted by several SUSY models.

Relevant non-diagonal terms of the slepton mass matrix (Fig. 1) are predicted in 'SUSY-GUT' models, where these terms arise from radiative corrections from the Planck scale to the weak scale and in 'SUSY-seesaw' models, where a suitable scheme of neutrino masses and chiralities is introduced consistently with the existing experimental data of neutrino oscillation experiments. These models predict CLFV with branching ratios from just below to a few orders of magnitude below the current experimental upper limits. CLFV due to neutrino mixing included in the SM frame would be completely unobservable (for instance a *BR* ≈ 10^{-54} is predicted for → eγ). The detection of → eγ events would thus be a clear, unambiguous sign of physics beyond the Standard Model, even including neutrino masses.

In → eγ searches, a beam of positive muons is stopped in a thin target and a search is made for a back-to-back positron–photon couple with the right momenta and timing. The main background in present experiments comes from the accidental coincidence of independent positrons and photons within the resolutions of the used detectors. The best available detectors for low-energy positrons and photons must therefore be employed. In the MEG experiment at PSI (see Fig. 2) a surface muon beam with an intensity greater than 10^7 /s will be stopped in a thin target. A magnetic spectrometer, composed of a superconducting magnet and drift chambers, will be used for the measurement of the positrons trajectories. Positron timing will be measured by an array of scintillators. Photons will be detected by an innovative electromagnetic calorimeter in which a total of about 800 photomultipliers will detect the light produced by photon-initiated showers in about 800 litres of liquid xenon. In a recent test at PSI the design energy resolution of 4.5% FWHM was obtained in a 100 l liquid xenon prototype for 55 MeV photons. The aim of this experiment is to reach a sensitivity down to *BR* of the order of 10^{-13}, with an improvement of two orders of magnitude with respect to the present experimental limit. The start of data taking is foreseen in 2006.

Another channel for CLFV investigation, which is not limited by accidental background and can therefore be used to improve the sensitivity to CLFV, is muon to electron (μe) conversion in nuclei. The ratio of the rate for this process with respect to μ→eγ has been calculated by several authors, for various nuclei, under assumptions on the relevant matrix elements which are valid in many SUSY models (see Fig. 3, from Ref. [6]).

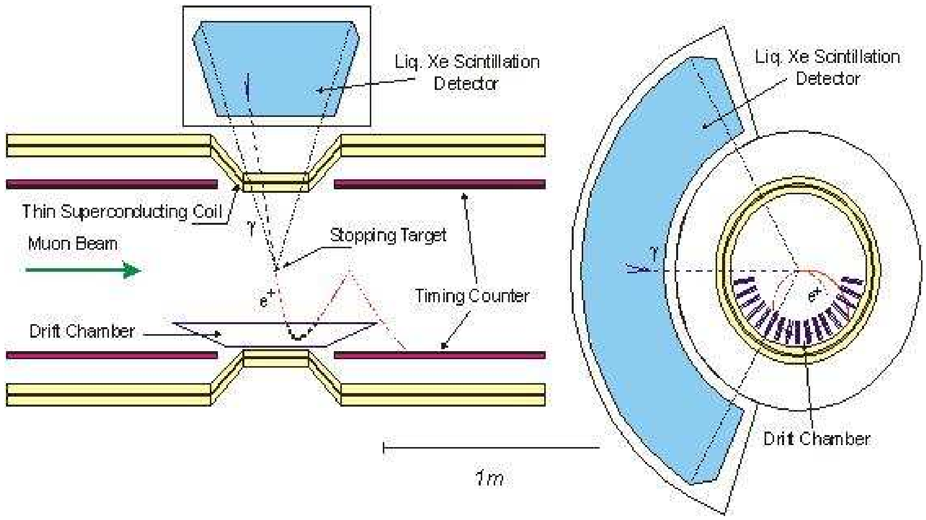

Fig. 2: A sketch of the MEG detector

Experimentally, negative muons are brought to a stop in a thin target and are subsequently captured around a nucleus. The energy of a possible converted electron would be equal to the rest muon mass minus the muon binding energy *EB*. Two main sources of background are i) beam-correlated background due mainly to radiative pion capture followed by $\gamma \to e^+e^-$ conversions, and ii) electrons from muon decay in orbit (DIO). The first source of background can be controlled by improving the muon beam quality, the second one is intrinsic; the DIO electron spectrum extends up to the energy region of electrons from μ*e* conversion but with a spectrum proportional to $(m\ -EB\text{-}E_e)^5$. An excellent electron momentum resolution is fundamental in order to keep this background under control.

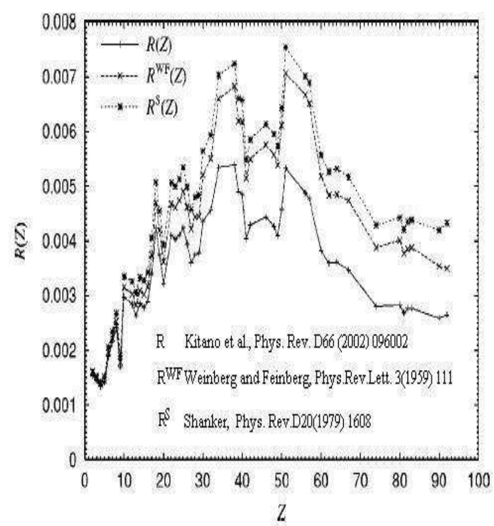

Fig. 3: Computed ratio of $BR(\mu e)/BR(\mu \to e\gamma)$

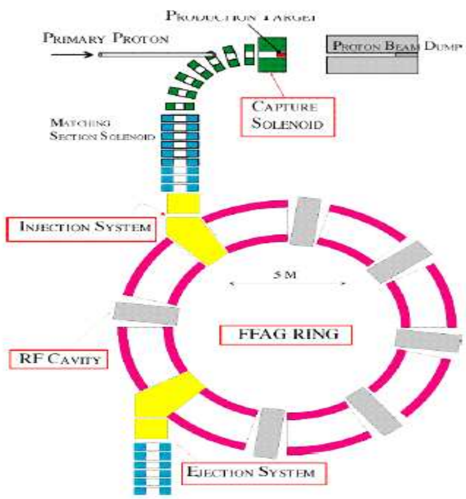

Fig. 4: Muon production in the PRISM/PRIME project at J-PARC

In the PRISM/PRIME (Fig. 4) project at J-PARC a pulsed proton beam is used to produce low-energy pions that are captured by placing the target inside a superconducting solenoid magnet. The pulsed structure of the beam helps in reducing the beam correlated background. The beam is then transported in a circular system of magnets and RF cavities (FFAG ring) which acts as a pion decay section (increasing beam cleaning) and reduces the muon energy spread. The features of this beam would be an extremely high intensity (10^{12} /s) of very clean muons of low momentum (≈70 MeV/*c*) with a narrow energy spread (few per cent FWHM). The last feature is essential to stop enough muons in thin targets. If the electron momentum resolution were kept below 350 keV/*c* (FWHM) the experiment will be sensitive to μe conversion down to $BR \leq 10^{-18}$.

If CLFV were discovered, the angular distribution of electrons from the CLFV decay of polarized muons could be used to discriminate among the different SUSY-GUT SU(5), SUSY-GUT SO(10), SUSY-seesaw models or others.

It is finally important to stress the complementarity between SUSY searches at the LHC and CLFV searches, as shown in Fig. 5, where the different sensitivity to possible neutralino masses for these two classes of experiments, for some parameters of the SUSY model investigated [7], is shown.

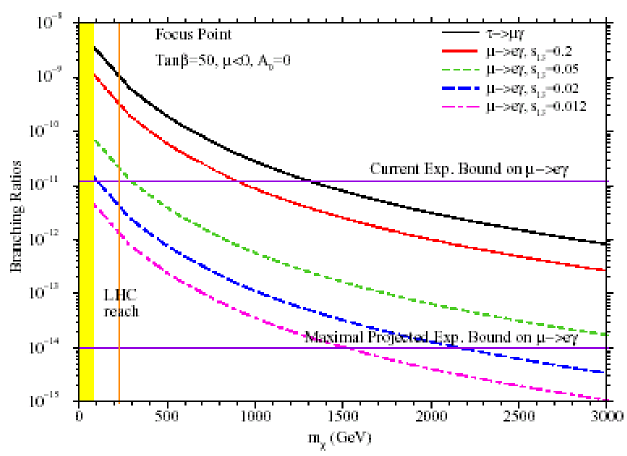

Fig. 5: Complementarity between SUSY search at the LHC and CLFV searches

References

[1] J. Aysto *et al*., Physics with low-energy muons at a Neutrino Factory complex, CERN-TH/2001-231, in ECFA/CERN Studies of a European Neutrino Factory Complex, A. Blondel *et al*., (Eds.), CERN-2004-002, ECFA-04-230, p. 259.

[2] H.N. Brown *et al., Phys. Rev. Lett*. **92** (2004) 161802.

[3] J-PARC Letter of Intent L17: An improved Muon (g–2) Experiment at J-PARC, contact person: B.L. Roberts.

[4] J. Bailey *et al., Nucl. Phys. B* **150** (1979) 1.

[5] F.J.M. Farley *et al., Phys. Rev. Lett*. **92** (2004) 052001.

[6] R. Kitano *et al., Phys. Rev. D* **66** (2002) 096002.

[7] A. Masiero *et al*., hep-ph/0401138.

Betabeams

1 Introduction

The betabeam concept for the generation of an electron (anti)neutrino beam was proposed [1] in 2002. A first study [2,3] of the possibility of using the existing CERN machines for the acceleration for radioactive ions to a relativistic gamma of roughly 100, for later storage in a new decay ring of approximately the size of the SPS, was made in 2002. The results from this very first short study were very encouraging, but as no resources could be allocated at CERN for this work, it was not continued. In 2004 it was decided to incorporate a design study for the betabeam within the EURISOL DS proposal. EURISOL [4] is a project name for a next-generation radioactive beam facility based on the ISOL method [5] for the production of intense radioactive beams for nuclear physics, astrophysics, and other applications. The proposal was accepted with the betabeam task as an integral part. The design study officially started on 1 February 2005 and will run for four years resulting in a conceptual design report for a betabeam facility as one potential user of EURISOL.

2 First study

The first study of the feasibility of using the existing CERN accelerator complex for a betabeam facility was made over a period of a few months with very limited manpower (Fig. 1). The main objectives were twofold: i) to identify a possible scenario for bunching, acceleration, and storage in a few very short bunches of a sufficient amount of radioactive ions for a betabeam and ii) to identify possible bottlenecks in the proposed scheme. A main objection raised early on concerned the possible activation of the accelerators. Consequently, some time was spent to simulate the activation problem in the decay ring and to calculate the average losses in the accelerator chain. The overall result was encouraging but unfortunately no further work was approved due to other commitments for the accelerator departments at CERN. The study proposed to use a thick ISOL target for production of ^{6}He and ^{18}Ne as both isotopes can be produced in large quantities and are easy to handle. Neither of the isotopes has any long-lived daughter products that could create a problem in the low-energy part of the facility. Several iterations were required for the ‘bunching’ but eventually a high-frequency (60 GHz) ECR source was identified as a possible highly efficient tool to create sufficiently short bunches after the target for multiturn injection into a synchrotron. For the first stage of acceleration, it was proposed to use the 100 Mev/u linac of the EURISOL facility. Further acceleration was to be done with a new rapid cycling synchrotron (RCS), the PS, and finally the SPS. A new injection and stacking method was proposed to keep the duty factor of the decay ring low. The method makes use of a dispersion orbit in the decay ring to avoid the injection elements interfering with the circulating beam bunch rotation to bring the fresh bunches to the central orbit; and asymmetric bunch merging to take the newly injected ions into the centre of the circulating bunch [6,7]. The maximum gamma of 150 that can be reached for fully stripped ^{6}He ions in the SPS was initially chosen for the coasting beam in the decay ring but later revised to lower values taking physics reach considerations into account. The main bottlenecks in the scenario chosen for the first study were shown to be the tune shift at PS and SPS injection, and the activation of the PS ring.

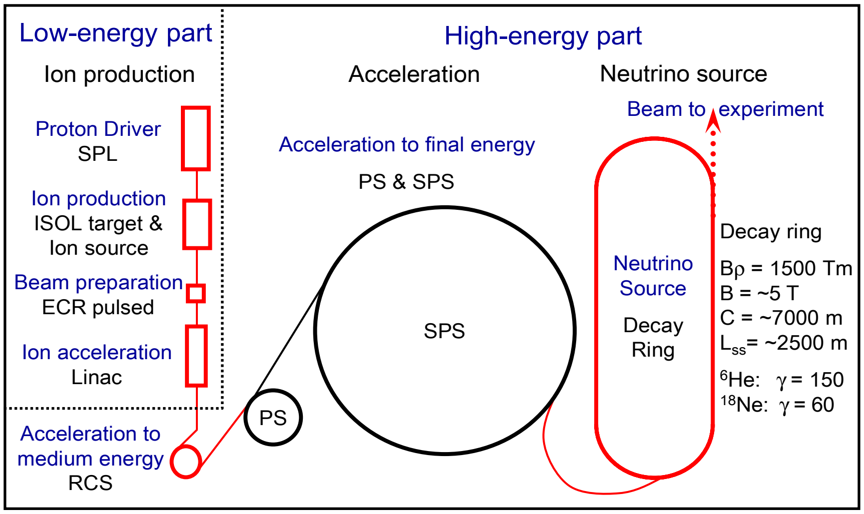

Fig. 1: CERN betabeam conceptual design

3 The betabeam task in EURISOL

The betabeam task within EURISOL has six participating institutes and is receiving close to 1 M€ over four years from the EU. Together with the contribution from the participating institutes, a total of almost 35 man-years is available for the study. The study officially started on 1 February 2005 and the short-term objective is to freeze a parameter list by the end of 2005. The deliverable of the study is a Conceptual Design Report (CDR) for a betabeam facility at CERN by the end of 2008.

3.1 Version 1

In the first study, no consideration was made of the charge state distribution after the ECR. While it seems feasible to extract most He ions in the fully stripped charge state 2^+, it is unlikely that more than a maximum of 30% of Ne ions can be extracted in one single charge state. Furthermore, the multiturn injection into the RCS is typically done with an efficiency of 50%. Revising the first study with these points taken into consideration, the annual rate of neutrinos from ^{18}Ne was found to be drastically reduced [8], while the annual rate of antineutrinos from ^{6}He was acceptable.

3.2 Version 2

The second version [9] was primarily motivated by the need to deal with space-charge issues in the PS and SPS. The first study had a duty factor of the neutrino beam of 2×10^{-3}; with a moderate increase the known space-charge-induced limitations of the PS and SPS were shown to be respected for an annual rate of 10^{18} (anti)neutrinos per year. However, the second version still fails to deliver this rate for neutrinos. In Table 1 the main differences between the different versions are listed together with the resulting annual rate. The increase of the number of bunches also resolves a problem with a RF incompatibility at transfer between the 40 MHz RF system and the 200 MHz RF system during acceleration.

Table 1: A comparison of three different scenarios for a CERN betabeam facility

		NuFact02	**Version 1**	**Version 2**
		2002	April 2005	Aug 2005
Target	Rate to ECR [s^{-1}]	2×10^{13} (0.8×10^{12})	2×10^{13} (0.8×10^{12})	2×10^{13} (0.8×10^{12})
ECS	Type	Compact	60 GHz pulsed	60 GHz pulsed
	T ejection [keV/u] efficiency	20 keV/amu	U = 50 kV	U = 50 kV
Post accel.		Cyclotrom	LINAC	LINAC
	T ejection [MeV/u]	50	100	100
RCS	Rep. rate [Hz]	16	16	10
	T ejection [MeV/u]	300	500 (1124)	500 (1124)
PS	Number of RCS bunches/cycle	16	16	20
	T ejection [GeV/u]	3.5 (7.8)	7.8 (14)	7.8 (14)
	Number of ejector bunches	8 (top merge)	8 (top merge)	20
SPS	*T* ejection [GeV/u]	139 (55)	92.5	92.5
	γ	150 (60)	100 (100)	100 (100)
Decay ring	Cycle time [s]	8	6 (3.6)	6 (3.6)
	I_{max}, stored [ions]	2.02×10^{14} (9.11×10^{12})	5.88×10^{13} (1.19×10^{12})	9.7×10^{13} (3.11×10^{12})
	Neutrino flux (ν/year)	Not given	1.76×10^{18} (0.02×10^{18})	2.9×10^{18} (0.046×10^{18})
	Duty factor	2×10^{-3}	2×10^{-3}	$4.5(3.9) \times 10^{-3}$

Values given for the two baseline isotopes as ^{6}He (^{18}Ne).

4 Technical challenges

The main challenge for the betabeam study is to reach the required annual rate for a physics reach that would make the betabeam an attractive option for neutrino physics in 10–15 years time. Detailed physics studies show that a betabeam facility must deliver at least 10^{18} (anti)neutrinos at the end of the straight section per year in the direction of a megaton detector to be of any interest in this time perspective. At a higher rate of some 10^{19} (anti)neutrinos per year the detector size could be greatly reduced and still leave the facility as a highly competitive alternative to even the neutrino factory.

The achievable production rate of the isotopes of interest for a betabeam facility was a major issue in the first study at CERN. The numbers presented in Ref. [2] were compiled from general parameters for beam current and targets taken from the EU-supported EURISOL RTD project [10]. The possibility of increasing these numbers has been discussed ever since then. Different options have been proposed, such as multiple targets of MgO in series for the production of ^{18}Ne. However, the production of the baseline isotopes will again be carefully investigated within the EURISOL DS [4] target tasks. Any improvements will translate linearly into an annual rate making it the most straightforward way to increase the flux of (antineutrinos). In Table 2 the required production rate for version 2 of the betabeam facility with an annual rate of 1.1×10^{18} antineutrinos and 2.9×10^{18} [11] neutrinos are given.

Tests with a 28 GHz ECR source at LPSC in Grenoble [12] have demonstrated that short pulses of noble gas in a high charge state can be extracted through the so-called pre-glow effect. Theoretical estimates show that the increased plasma density at 60 GHz could produce an intense pulsed beam of noble gases suitable for a multiturn injection into a synchrotron. Such a source, at a 10 Hz repetition rate, could feasibly generate 10–20-microsecond-long pulses of up to a few 10^{12} charges per pulse. A similar set-up in Louvain-La-Neuve operates with high efficiency for the production of a radioactive ion beam where the ions are produced on-line in a thick target [13]. The He ions would, in the proposed 60 GHz ECR source, be extracted almost exclusively in the highest charge state (2^+) but the Ne ions would be extracted as a spectrum of several charge states with a maximum of 30% in one single state.

Table 2: The assumed possible production [2] (for atoms at the entrance to the ECR) compared to a theoretically required production [9]

	Nominal production rate [ions a/s]	**Required production rate [ions a/s]**	**Missing factor**
^{6}He	2×10^{13}	2×10^{13}	1
^{18}Ne	8×10^{11}	1.9×10^{13}	24

A high-energy ion beam requires acceleration in large synchrotrons. Such synchrotrons are costly and, consequently, the re-use of existing accelerators at CERN, for example, is essential to keep the cost down. The PS and SPS at CERN were built for fixed-target physics with protons and have later been adapted to accelerate ions for the CERN heavy-ion physics programme. The aperture and space-charge limitations of these two accelerators have been carefully studied over many years of operation. This is a great help for the study as it sets strict limits for the number of charges per bunch that can be injected and accelerated, but it also shows that neither of the two machines is well adapted for very high intensity ion beams. In the first study a modifications of the RF system was proposed to reduce the tune shift at injection in the SPS.

The activation of magnets and tunnels is a major concern for all accelerators and in particular for the betabeam where the ions decay (and are lost) during acceleration. The lost ions will be distributed all along the circumference making it very difficult to construct efficient beam collimation and magnet protection systems. Following the first study, a first attempt was made [14] to estimate the decay losses. The losses in the PS for He are serious enough to make further hands-on maintenance of the machine difficult while the losses in the SPS are comparable to losses already experienced with operational beams. The losses in the decay ring were simulated and shown to be important but not a cause of major concern as the subsequent secondary production of radioactivity in the surrounding rock were shown to be well below national limits.

Synchrotrons are highly efficient considering the space and number of RF cavities compared with linacs, but with the inherent limitation of requiring a long repetition time between macropulses as the synchrotron, once 'filled', has to ramp the magnetic field to accelerate. This produces long gaps between injections, of ions from the source. For the betabeam baseline scenario, the repetition time between injections can be several seconds and, as the injection is only sustained for a second, a large fraction of the ions produced are already lost at the exit of the ion source.

A further challenge is caused by the rather low energies reachable with the SPS at CERN as this implies a low duty factor ($< 2 \times 10^{-3}$) of the neutrino beam to permit a clean discrimination between atmospheric background and signal in the detector. This requires that the ions be kept in a few short bunches in the decay ring. The proposed injection scheme in the baseline scenario results in an acceptable duty factor, but on account of longitudinal aperture limitations, it quickly saturates and prevents a further increase of the total number of stored ions. The long-term stability of the short high-intensity ion bunches in the decay ring due to intrabeam scattering is another point of concern which has to be addressed in the next stage of the study.

5 Optimization of the betabeam baseline

A powerful method to understand the functional dependence of the many parameters influencing the figure of merit for a certain facility is available with modern analytical calculation software. The method requires that a symbolic analytical description be produced of the full accelerator chain and such a description has been done for the proposed betabeam facility at CERN using Mathematica [15,8,9]. The results can be visualized as, for example, two-dimensional plots for the figure of merit as a function of the different machine parameters. However, it is important to note that while such plots will help to identify the right parameter space for a requested machine design, they do not themselves guarantee that a realizable technical solution can be found. The work presented here has been done respecting the constraint of using the existing CERN accelerators, PS and SPS. In addition, the current decay ring design [16] is used even though it has been assumed that the Lorentz gamma of the stored ions can be changed easily. For the stacking we have assumed that 15 ^{6}He bunches and 20 ^{18}Ne bunches can be merged in the decay ring without major losses. The situation is slightly better for ^{18}Ne, which, because of a more advantageous charge-to-mass ratio, will see an almost three times larger longitudinal acceptance of the decay ring. Theoretically this would permit up to 45 merges for ^{18}Ne, but known limits in low-level RF beam control precision restrict it to a maximum of 20 merges. All parameters for the EURISOL DS baseline of May 2005 are documented in the appendixes of Refs. [8,9].

5.1 Annual rate

The figure of merit for the betabeam is the rate (R) of (anti)neutrinos at the end of one of the straight sections over a given period and it can be expressed as,

$$R = \frac{I_{\text{in}} \; f}{T_{\text{rep}}} \left(1 - 2\frac{m_{\text{r}} \; J_{\text{rep}}}{\gamma_{\text{top}} t_{\text{half}}}\right) T_{\text{run}}$$

where the m_r is the number of merges that can be done in the decay ring without major losses from the merging process itself, T_{rep} is the repetition period for the fills in the decay ring, γ_{top} the gamma factor of the decay ring, t_{half} the halflife at rest for the ions, I_{in} the total number of ions injected into the decay ring for each fill, f the fraction of the decay ring length for the straight section generating the neutrino beam, and T_{run} the length in seconds of the run. The first term gives the rate per chosen period for the ideal decay ring in which an endless number of merges can be accepted, the second term gives the limit set by the restriction on the maximum number of merges that can be accepted due to longitudinal emittance limitations, and the third term is by convention chosen as the length of a 'Snowmass year' [17] which is used as an international standard to calculate the running time of high-energy physics experiments and it is 10^7 seconds long.

5.2 Gamma dependence of the CERN baseline

The gamma dependence of the rate is mainly due to the gamma dependence of the acceleration time in the SPS, the lifetime of the ions in the decay ring, and the available longitudinal acceptance in the decay ring. The acceleration time in the SPS has a minimum length depending on hardware limitations and also increases in steps of 1.2 seconds due to the basic timing period of the CERN accelerator complex. For a given radio-frequency (RF) voltage, the longitudinal acceptance will to first order scale as the square root of gamma. In Fig. 2 dependence of ^{6}He is shown. The maximum gamma that can be reached with the CERN SPS for ^{6}He is 150 and for ^{18}Ne 250.

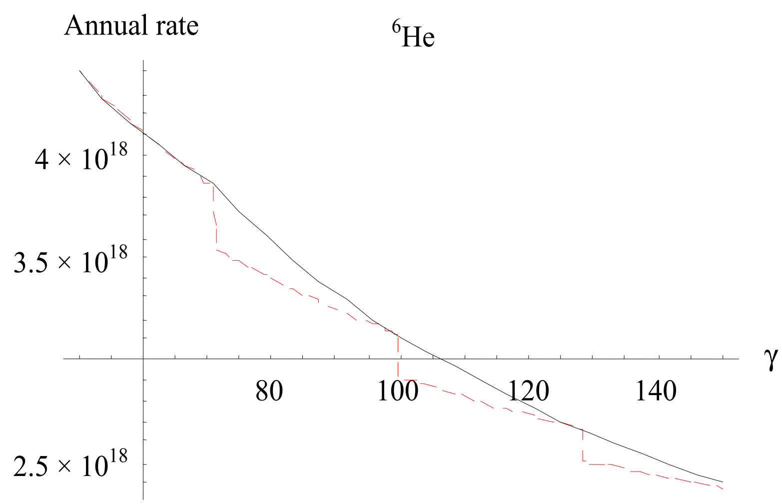

Fig. 2: The annual rate of antineutrinos from ^{6}He as a function of γ. The red dashed line shows the annual rate with the given source rate respecting a basic period of 1.2 seconds of the CERN accelerator complex. The solid line shows the same dependence but with a 'smooth' choice of acceleration time for the PS and SPS.

5.3 Duty factor dependence

The available longitudinal acceptance for stacking in the decay ring can be increased by increasing the number of bunches in the decay ring. This will increase the duty factor which is the total length in time of all bunches in the decay ring divided by the revolution time. The present limits of 15 merges for ^{6}He and 20 merges for ^{18}Ne will truncate the stacking well before the decay rate equals the stacking rate. In the formula for the annual rate (1) the second term is the result of this truncation. The duty cycle in the beta-beam baseline is 4.5×10^{-3} for 20 bunches ^{6}He and 3.9×10^{-3} for 20 bunches of ^{18}Ne at a gamma of 100. Figure 3 shows the annual rate for ^{18}Ne as a function of the number of bunches in the decay ring [8,9].

The constraint on the duty cycle is set by the atmospheric background and it becomes less severe at higher energies of the neutrinos. A betabeam facility operating at a higher gamma than the nominal value of 100 could accept a larger duty factor. Consequently, to fully understand the evolution of the annual rate as a function of gamma, the possibility to increase the duty factor must be fully explored.

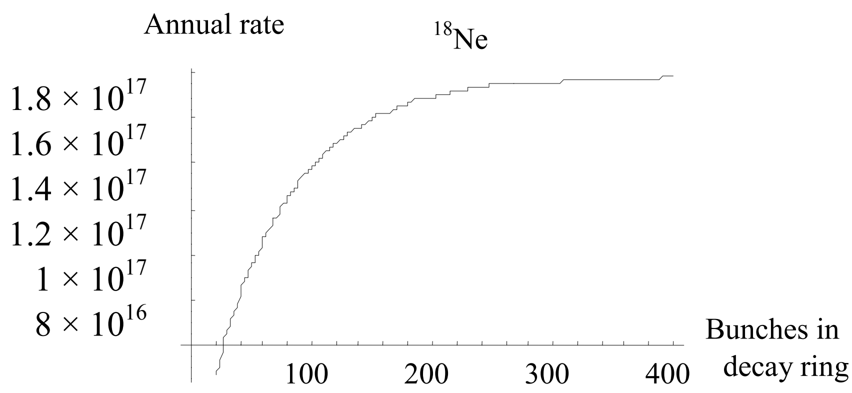

Fig. 3: The annual rate of antineutrinos from the decay of ^{18}Ne as a function of the number of bunches. The curve starts to the left with eight bunches at a duty factor of 2×10^{-3} and saturates when the decay rate equals the stacking rate.

5.4 Accumulation

In the betabeam baseline, the ions are produced for one second and thereafter accelerated during several seconds to a γ of 100. In theory, ions could be produced continuously as long as they can be stored while waiting for acceleration. The optimum storage time determined by the lifetime of the ion and the required acceleration time can be seen in the curve in Fig. 4. In these calculations the accumulation is done before the PS in a storage ring fitted with a cooling system, for an efficient storage through multiple injection cycles [18].

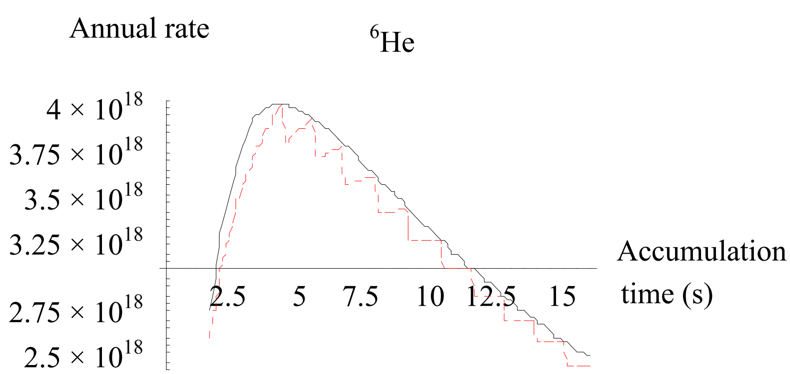

Fig. 4: The annual rate of antineutrinos from ^{6}He as a function of the accumulation time in a storage ring before the PS. The red dashed line shows the annual rate respecting the basic period of 1.2 seconds of the CERN accelerator complex. The solid line shows the same dependence but with a 'smooth' choice of acceleration time for the PS and SPS. All other parameters have been taken from the baseline design.

6 Conclusions

The conceptual design of the first study of the betabeam facility has been taken a step further with the start of the EURISOL design study's betabeam task. The first objective is to establish the annual rate of (anti)neutrinos from a given production rate [2] with the re-use of the PS and SPS for acceleration. The next step, which has already started, is to optimize the many machine parameters in the baseline to establish the maximum achievable rate. The work done so far shows that i) the increase of production rate translates linearly into an increase of the rate [19]; ii) an increase of the duty cycle permits more particles to be stored in the decay ring; and iii) accumulation can potentially be a powerful tool to make better use of the ions produced. The gamma dependence of the rate is often forgotten in physics reach calculations, but it should be noted that it is linked to longitudinal acceptance and duty factor and has to be calculated specifically for each choice of machine parameters.

A green-field study to establish the ultimate limit of the betabeam concept is beyond the scope of the ongoing design study. However, before a final decision on the construction of the next-generation neutrino source, such a study should be undertaken.

References

[1] P. Zucchelli, A novel concept for a neutrino factory: the beta-beam, *Phys. Lett. B* **532** (2002) 166–172.

[2] B. Autin, M. Benedikt, M. Grieser, S. Hancock, H. Haseroth, A. Jansson, U. Köster, M. Lindroos, S. Russenschuck and F. Wenander, The acceleration and storage of radioactive ions for a neutrino factory, CERN/PS 2002-078 (OP), Nufact Note 121, Proceedings of Nufact 02, London, 2002, *J. Phys. G: Nucl. Part. Phys*. **29** (2003) 1785–1795.

[3] M. Lindroos and T. Nilsson, The acceleration and storage of radioactive ions for a beta-beam facility, Proceedings of RNB6, Argonne, USA, 2003, *Nucl. Phys. A* **746** (2004) 316c–322c.

[4] http://eurisol.org.

[5] H.R. Ravn and B.W. Allardyce, On-line mass separators, in *Treatise on Heavy-Ion Science*, Ed. D. A. Bromley (Plenum Press, New York, 1989), ISBN 0-306-42949-7.

[6] M. Benedikt, S. Hancock and J.-L.Vallet, A proof of principle of asymmetric bunch pair merging, AB-note-2003-080 MD.

[7] M. Benedikt and S. Hancock, *Nucl. Instrum. Meth. A* **550** (2005) 1–5.

[8] M. Benedikt, S. Hancock and M. Lindroos, Parameter and intensity values, Version 1, April 2005, EURISOL DS/TASK12/TN-05-01.

[9] M. Benedikt, A. Fabich, S. Hancock and M. Lindroos, Parameter and intensity values, Version 2, July 2005, EURISOL DS/TASK12/TN-05-03.

[10] The EURISOL Report, Ed. J. Cornell (GANIL, Caen, 2003), European Commission contract No. HPRI-CT-1999-500001.

[11] J. Bouchez, M. Lindroos and M. Mezzetto, Beta-beams: Present design and expected performance, In the proceedings of Nufact 03, New York, 2003.

[12] P. Sortais, J.-L. Bouly, J.-C. Curdy, T. Lamy, P. Sole, T. Thuillier, J.-L. Vieux-Rochaz and D. Voulot, ECRIS development for stable and radioactive pulsed beams, *Rev. Sci. Instrum*. **75** (2004) 1610–1612.

[13] M. Gaelens, M. Cogneau, M. Loiselet and G. Ryckewaert, Post-acceleration of ^{7}Be at the Louvain-la-Neuve radioactive ion beam facility, *Nucl. Instrum. Meth. B* **204** (2003) 48–52.

[14] M. Magistris and M. Silari, Parameters of radiological interest for a beta-beam decay ring, TIS-2003-017-RP-TN.

[15] © Wolfram Research, Inc., http://www.wolfram.com.

[16] A. Chance and J. Payet, Storage ring for a beta-beam facility, Beta-beam task meeting, July 2005.

[17] http://snowmass2001.org/.

[18] T. Fritioff, M. Grieser, M. Lindroos and A. Trzcinska, *Nucl. Phys. A* **746** (2004) 384c–388c.

[19] M. Lindroos, The technical challenges of the beta-beam, in the Proceedings of Nufact05, Frascati (Rome), Italy, 2005, to be published in Nuclear Physics B.

Physics with a first very-low-energy betabeam

We describe the importance of having low-energy (10–100 MeV) neutrino beams produced through the decay of boosted radioactive ions ('betabeams'). We focus on the interest for neutrino–nucleus interaction studies and their impact for astrophysics, nuclear and particle physics. In particular, we discuss the relation to neutrinoless double-beta decay. Finally, we mention the current status regarding the feasibility of low-energy betabeams.

1 Introduction

Nuclei are a wonderful laboratory for searches on fundamental issues, such as knowledge about the neutrino mass scale, or the Majorana versus Dirac nature of neutrinos. Nuclei can also be a beautiful tool for the search for new physics. The original idea of 'betabeams', first proposed by Zucchelli [1], enter into this category. Betabeams use the beta-decay of boosted radioactive ions to produce well-known electron (anti)neutrino beams, while the conventional way exploits the decay of pions and muons. This simple but intriguing idea has opened new strategies, thanks to the future radioactive ion beams, at present under study, in various nuclear physics laboratories. In fact, the planned intensities of $10^{11\text{-}13}$ ions/s can actually render feasible neutrino accelerator experiments using ions.

In the original paper [1], a new facility is described, based on the betabeam method, the central motivation being the search for CP violation in the lepton sector—the Maki–Nakagawa–Sakata–Pontecorvo (MNSP) matrix, relating the neutrino flavour and mass basis, and might indeed be complex. With this aim the ions would be accelerated to 60–100 GeV/A (or $\gamma = 60$–100, where γ is the Lorentz factor), requiring accelerator infrastructure like the PS and SPS at CERN, as well as a large storage ring pointing to an (enlarged) Fréjus Underground Laboratory, where a big detector would be located.

The interest of this new concept for the production of low-energy neutrino beams was soon recognized [2]. Here the ions are boosted to a much lower γ, i.e., 5–15. High-energy scenarios have been proposed [3], requiring different (or revised) accelerator infrastructures to boost the ions at very high γ ($\gamma >> 100$). (Note that for this reason the original scenario [1] is sometimes referred to in the literature as 'standard', or misleadingly 'low-energy'.) Detailed work exists at present both on the feasibility [4] and on the physics potential of the standard [5] scenario, contributing to determining the conditions for the best CP violation sensitivity, in possible future searches. A feasibility study is now ongoing within the Eurisol Design Study [6]. Here we focus on the physics potential of low-energy betabeams.

2 Low-energy betabeam

2.1 Physics motivation

The idea of establishing a facility producing low-energy neutrino beams, based on betabeams, has been proposed in Ref. [2]. This opens new opportunities, compared to the original scenario. First one might use the ion decay at rest as an intense neutrino source in order to explore neutrino properties that are still poorly known, such as the neutrino magnetic moment [7]. In fact, direct measurements achieving improved limits are precious, since the observation of a large magnetic moment points to physics beyond the Standard Model.

The interest of low-energy betabeams in the tens of MeV, to perform neutrino–nucleus interaction studies, has been discussed in [2,8]. At present, there are a limited number of measurements available in this domain (essentially on three light nuclei), so that theoretical predictions are of absolute necessity. Getting accurate predictions can be a challenging task, as the discrepancies on the ^{12}C [9] and ^{208}Pb [10] cross-sections have demonstrated. Neutrino–nucleus applications are numerous and span from a better knowledge of neutrino detector response using nuclei, like supernova observatories or in oscillation experiments, to nuclear astrophysics, for the understanding of processes like the nucleosynthesis of heavy elements. (More information can be found, for example, in Refs. [11,12].)

In Ref. [2] we have pointed out that performing neutrino–nucleus interaction studies on various nuclei would improve our present knowledge of the ‘isospin’ and ‘spin–isospin’ nuclear response (the nuclear transitions involved in charged-current reactions are in fact due to the isospin, like, for example, $t_{\pm}$, and spin–isospin, like, for example, σt, operators). A well-known example is given by the super-allowed Fermi transitions (due to the isospin operator), which are essential for determining the unitarity of the Cabibbo–Kobayashi–Maskawa (CKM) matrix, the analogue of the MNSP matrix in the quark sector. Another (less known but still intriguing) example is furnished by the so-called Gamow–Teller transitions (these are due to the spin–isospin operator) in mirror nuclei, which can be used to observe second-class currents, if any. These terms transform in an opposite way under the *G*-parity transformation—the product of charge-conjugation and of a rotation in isospin space—as the usual vector and axial-vector terms [13], and are not present in the Standard Model. In Ref. [2] we have pointed out that spin–isospin and isospin states of higher multipolarity (than those just mentioned) contribute significantly to the neutrino–nucleus cross-sections, as the energy of the neutrino increases. Such contributions are larger when the nucleus is heavier. Since low-energy betabeams have the specificity that the average energy can be increased by increasing the Lorentz boost of the ions (more precisely $\langle E\nu \rangle \approx 2\gamma Q_{\beta}$), they appear as an appropriate tool for the study of these states. Apart from their intrinsic interest, neutrino–nucleus interaction measurements would put theoretical predictions for the extrapolation to exotic nuclei useful for astrophysical applications on really solid ground. They are also important for the open question of the nature of the neutrino.

One of the crucial issues in neutrino physics is to know if neutrinos are Dirac or Majorana particles. The answer to this question can be furnished, for example, by the observation of neutrinoless double-beta decay in nuclei, since this lepton-violating process can be due to the exchange of a Majorana neutrino. While the present limit is of about 0.2 eV [14], future experiments aim at the challenging 50 meV energy range. However, it has been debated at length that the theoretical situation, as far as the half-life predictions are concerned, should be clarified: different calculations present significant variations for the same candidate emitters. Reducing these differences certainly represents an important theoretical challenge for the future, and one might hope that dedicated experiments will help to make a step forward [15]. One way to constrain such calculations is by measuring related processes, such as beta decay [16], muon capture [17], charge-exchange reactions [18], and double-beta decay with the emission of two neutrinos [19] (the latter process is allowed within the Standard Model and does not tell us anything about the nature of the neutrino). Such a procedure has been used for a long time. However, each of these processes brings only part of the necessary information.

Recently we have been showing that there is a very close connection between neutrinoless double-beta decay and neutrino–nucleus interactions [20]. In fact, by rewriting the neutrino exchange potential in momentum space and by using a multiple decomposition, the two-body transition operators, involved in the former, can be rewritten as a product of one-body operators, which are essentially the same as the ones involved in neutrino–nucleus interactions. (Note, however, that there are some differences like short-range correlations which can play a role in the two-body process, but not in the one-body one.) Therefore besides the above-mentioned processes, an improved knowledge of the nuclear response through either low-energy betabeams or conventional sources (decay of muons at rest) could help to constrain the neutrinoless half-life predictions as well. Figures 1 and 2 show the contribution of different states for two impinging neutrino energies on ^{48}Ca taken just as an illustrative example.

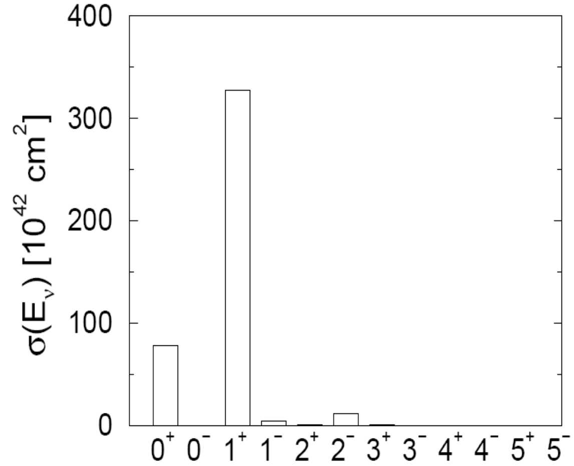

Fig. 1: Contribution of the states of different multipolarity to the total charged-current ν_e–^{48}Ca cross-section for neutrino energy $E_\nu = 30$ MeV. The histograms show the contribution of the Fermi ($J^\pi = 0^+$), the Gamow–Teller (1^+) and the spin–dipole (0^-,1^-,2^-) states and all higher multipoles up to 5 [20].

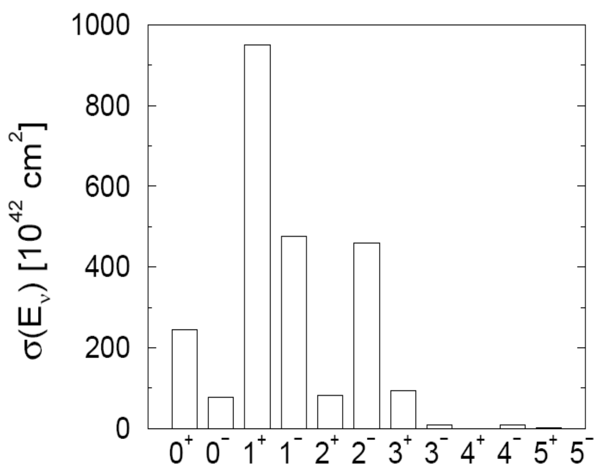

Fig. 2: One can see that the Gamow–Teller transition is giving the dominant contribution at low neutrino energies, while many other states become important when the neutrino impinging energy increases. These states are an essential part of the neutrinoless double-beta decay half-lives as well [2].

2.2 A small storage ring

The main aim of the work in Ref. [8] has been to calculate exactly: i) the neutrino–nucleus interactions rates expected at a low-energy betabeam facility, by using parameters from the first feasibility study [4]; ii) to study how these scale by changing the geometry of the storage ring. In particular, two sizes have been considered: a small one, i.e., 150 m straight sections and 450 m total length, like the one planned for the future GSI facility [21]; a large one, having 2.5 km straight sections and 7 km total length, such as the one considered in the original betabeam baseline scenario [1]. Table 1 shows the events for deuteron, oxygen, iron and lead, taken as typical examples, the detector being located at 10 m from the storage ring.

Table 1: Neutrino–nucleus interaction rates (events/year) at a low-energy betabeam facility [8]: rates on deuteron, oxygen, iron and lead are shown as examples. The rates are obtained with $\gamma = 14$ as boost of the parent ion. The neutrino–nucleus cross-sections are taken from the references cited. The detectors are located at 10 metres from the storage ring and have cylindrical shapes ($R = 1.5$ m and $h = 4.5$ m for deuteron, iron and lead, $R = 4.5$ m and $h = 15$ m for oxygen, where R is the radius and h is the depth of the detector). Their mass is indicated in the third column. Rates obtained for two different storage ring sizes are presented: the small ring has 150 m straight sections and 450 m total length, while the large ring has 2.5 km straight sections and 7 km total length. Here 1 year = 3.2×10^7 s.

Reaction	**Ref.**	**Mass (tons)**	**Small ring**	**Large ring**
$\nu + \mathrm{D}$	[11]	35	2363	180
$\overline{\nu} + \mathrm{D}$	[11]	35	25 779	1956
$\nu +^{16}\mathrm{O}$	[22]	952	6054	734
$\overline{\nu} +^{16}\mathrm{O}$	[22]	952	82 645	9453
$\nu +^{56}\mathrm{Fe}$	[23]	250	20 768	1611
$\nu +^{208}\mathrm{Pb}$	[24]	360	10 3707	7922

One can see that interesting interaction rates can be obtained on one hand, and that clearly a small devoted storage ring is more appropriate for such studies, on the other hand. The physical reason is simple. Since the emittance of the neutrino fluxes is inversely proportional to the γ of the ions, only the ions which decay close to the detector contribute significantly to the number of events, while those that decay far away see the detector under a too-small opening angle. The complementarity between a low-energy betabeam and conventional source is discussed in Ref. [25].

3 Conclusions

The use of the betabeam concept to produce neutrino beams in the tens of MeV energy range is very appealing. If both electron-neutrino and electron (anti)neutrino beams of sufficiently high intensities can be achieved, low-energy betabeams can offer a flexible tool, where the average neutrino energy can be varied by varying the γ of the ions. The studies realized so far indicate clearly that a small devoted storage ring is more appropriate to obtain such beams, in particular for performing neutrino–nucleus interaction studies, a promising axis of research. We have discussed in particular the interest of such measurements for a better knowledge of the nuclear response relevant for neutrinoless double-beta decay searches. The feasibility study of the small storage ring is now ongoing within the Eurisol Design Study. Several issues need to be addressed (e.g. stacking ion method, duty factor). The realization of low-energy betabeams would be a *proof of principle* that the betabeam concept works.

We thank A. Chance, M. Benedikt, M. Lindroos and J. Payet for useful discussions on the feasibility of low-energy betabeams. The author acknowledges the BENE (Beams for European Neutrino Experiments, CARE) funding.

References

[1] P. Zucchelli, *Phys. Lett. B* **532** (2002) 166.

[2] C. Volpe, *J. Phys. G* **30** (2004) L1 [hep-ph/0303222].

[3] J. Burguet-Castell *et al., Nucl. Phys. B* **695** (2004) 217 [hep-ph/0312068].

[4] B. Autin *et al., J. Phys. G* **29** (2003) 1785 [physics/0306106]. See also http://beta-beam.web.cern.ch/beta-beam/ and the contribution of M. Lindroos to this volume.

[5] M. Mezzetto, *J. Phys. G* **29** (2003) 1771 [hep-ex/0302007]; J. Bouchez, M. Lindroos, M. Mezzetto, AIP Conf. Proc. **721** (2004) 37 [hep-ex/0310059]; M. Mezzetto, *Nucl. Phys. Proc. Suppl.* **143** (2005) 309 [hep-ex/0410083] ; A. Donini *et al., Phys. Lett. B* **621** (2005) 276 [hep-ph/0411402]; C. Volpe, *Nucl. Phys. A* **752** (2005) 38 [hep-ph/0409357]; J. Burguet-Castell *et al., Nucl. Phys. B* **725** (2005) 306 [hep-ph/0503021]; J. Bernabeu, J. Burguet-Castell, C. Espinoza, M. Lindroos, hep-ph/0505054; P. Huber, M. Lindner, M. Rolinec, W. Winter, [hep-ph/0506237]; see also contributions of J. Burguet-Castell and M. Mezzetto to this volume.

[6] See http://www.ganil.fr/eurisol/.

[7] G.C. McLaughlin and C. Volpe, *Phys. Lett. B* **591** (2004) 229 [hep-ph/0312156].

[8] J. Serreau and C. Volpe, *Phys. Rev. C* **70** (2004) 055502 [hep-ph/0403293].

[9] E. Kolbe *et al., Phys. Rev. C* **52** (1995) 3437; S.K. Singh, N.C. Mukhopadyhay and E. Oset, *Phys. Rev. C* **57** (1998) 2687; E. Kolbe, K. Langanke and P. Vogel, *Nucl. Phys. A* **613** (1997) 382; A.C. Hayes and I.S. Towner, *Phys. Rev. C* **61** (2000) 044603; C. Volpe *et al., Phys. Rev. C* **62** (2000) 015501; N. Jachowicz *et al., Phys. Rev. C* **65** (2002) 025501; A. Brotugno and G. Co, nucl-th/0506028.

[10] G.M. Fuller, W.C. Haxton and G.C. McLaughlin, *Phys. Rev. D* **59** (1999) 085005; E. Kolbe and K. Langanke, *Phys. Rev. C* **63** (2001) 025802; C. Volpe *et al., Phys. Rev. C* **65** (2002) 044603; N. Jachowicz, K. Heyde and J. Ryckebush, *Phys. Rev. C* **66** (2002) 055501; M. Sajjad Athar et al., nucl-th/0506046.

[11] K. Kubodera and S. Nozawa, *Int. J. Mod. Phys. E* **3** (1994) 101.

[12] A.B. Balantekin, *Prog. Theor. Phys. Suppl.* **146** (2003) 227 [nucl-th/0201037]; A.B. Balantekin and G.M. Fuller, *J. Phys. G* **29** (2003) 2513 [astro-ph/0309519]; C. Volpe, *Nucl. Phys. B* **143** (2005) 43 [hep-ph/0409249]; E. Kolbe *et al., J. Phys. G* 29 (2003) 2569, and references therein.

[13] N.A. Smirnova and C. Volpe, *Nucl. Phys. A* **714** (2003) 441, and references therein.

[14] L. Baudis *et al., Phys. Rev. Lett.* **83** (1999) 41; H.V. Klapdor-Kleingrothaus *et al., Eur. Phys. J. A* **12** (2001) 147; C.E. Aalseth, *Phys. Rev. D* **65** (2002).

[15] K. Zuber et al., article in preparation.

[16] K. Muto, E. Bender and H.V. Klapdor, *Z. Phys. A* **334** (1989) 177 (1989); M. Aunola and J. Suhonen, *Nucl. Phys. A* **602** (1996) 133.

[17] M. Kortelainen and J. Suhonen, *Europhys. Lett.* **58** (2002) 666; M. Kortelainen and J. Suhonen, *Phys. Atom. Nucl.* **67** (2004) 1202.

[18] J. Bernabeu *et al.,* IPNO/TH-88-58, FTUV-88/20; H. Akimune *et al., Phys. Lett. B* **394** (1997) 23; S. Rakers *et al., Phys. Rev. C* **70** (2004) 054302; ibid **71**, (2005) 054313.

[19] V.A. Rodin, A. Faessler, F. Simkovic, P. Vogel, *Phys. Rev. C* **68** (2003) 044302.

[20] C. Volpe, *J. Phys. G* **31** (2005) 903 [hep-ph/0501233].

[21] See http://www.gsi.de/.

[22] E. Kolbe, K. Langanke, P. Vogel, *Phys. Rev. D* **66** (2002) 013007; W.C. Haxton, *Phys. Rev. D* **36** (1987) 2283.

[23] E. Kolbe and K. Langanke, *Phys. Rev. C* **63** (2001) 025802.

[24] J. Engel, G.C. McLaughlin, C. Volpe, *Phys. Rev. D* **67** (2003) 013005.

[25] G.C. McLaughlin, *Phys. Rev. C* **70** (2004) 045804 [nucl-th/0404002].

R&D on neutrino detectors: status and priorities

The challenge of very large detectors, assembling enough detector mass adequately instrumented for effective detection of neutrinos events, has accompanied neutrino physics since its early days. It has never been easy and today we have to deal with a much larger scale. Several detector options are being considered, in conjunction with different neutrino sources. The R&D in progress must be given all possible support.

1 Low-*Z* tracking calorimetry

Low-*Z* tracking calorimetry optimizes the detection of electrons in the final state by using a fine sampling in terms of radiation lengths, leading to the choice for a low-*Z* passive material. This is the technique used for the study of $\nu_\mu e$ scattering in the CHARM II experiment at CERN [1]. Here we discuss the status of the design of the NOνA experiment proposed for the detection of ν_μ–ν_e oscillations in the off-axis NuMI beam at Fermilab [2], with the observation of θ_{13} as its prime aim.

The NOνA detector foresees a mass one order of magnitude larger than MINOS [3] and at the same time, in relation to its aim, a finer sampling ($\Delta X_0 < 0.3$ to be compared to 1.5 with MINOS, which has iron as passive material). The principal technical issue is to improve the performance and substantially reduce the unitary cost of the trackers. The main technological innovation consists in the use of liquid scintillator read by Avalanche PhotoDiodes (APDs), instead of plastic scintillator read by multianode PMTs.

The detector is a 'Totally Active' Scintillator Detector (TASD), with a 30 kt mass, of which 24 kt are of liquid scintillator and the rest of PVC. In a TASD, the scintillator modules have cells along the beam 6.0 cm long and 3.9 cm wide. The TASD consists of a single block with overall dimensions 15.7 m × 15.7 m × 132 m. Lacking the particle board, the PVC must provide a self-supporting structure for a detector as high as a five-storey building. Since last year, progress has also been made in the mechanical design and in the assembling methods.

The electromagnetic energy resolution is $\Delta E/E \sim 10\%/\sqrt{E}$ (GeV), the almost continuous pulse-height information along the track helps in e/π_0 discrimination.

The use of APDs results in a considerably lower cost than with PMTs. APDs with 22 × 16 pixels are commercially produced in large quantities and already foreseen for the CMS experiment at the LHC. The high quantum efficiency, about 85%, allows one to have longer strips and fewer readout channels.

The NOνA design is in constant progress. If funding were to begin in late 2006, the NOνA detector could be ready in 2011. It is worth noting that the progress with the development of the trackers is potentially useful also for magnetized iron spectrometers for neutrino factories or colliders.

2 Magnetized iron spectrometers

This technique is conventional, but the mass to be considered is one order of magnitude larger than for present magnetized iron spectrometers, like MINOS.

Recent studies indicate that a magnetized iron toroidal spectrometer of the required mass is feasible [4]. On the one hand, the design of toroids with radius up to 10 m can be extrapolated from MINOS, with thicker plates for larger planes. On the other hand, the NOνA liquid scintillator technology with APD readout allows one to have transverse dimensions twice as large as in MINOS. Such a detector concept permits direct use of experience with MINOS.

The India Neutrino Observatory (INO) [5] foresees a dipole magnet equipped with RPCs, as in MONOLITH [6]. The INO basic motivation is the study of atmospheric neutrinos like with MONOLITH; a future use in a very long baseline experiment with a ν factory is also envisaged. The investigations started with MONOLITH on detector performance for design optimization have to be continued, so that it can be compared with other detectors.

A conceptual spectrometer based on a 40 kt iron solenoid magnetized at 1 T by a superconducting coil, with embedded solid scintillator rods as the active detectors, has been presented in Ref. [7]. Considerably more work is required to define its features and assess its practical feasibility.

In general, practical problems (mechanics, magnet design, etc.) must be thoroughly addressed. In addition, as already mentioned, more simulation work is required in order to understand and optimize the performance by a proper choice of the main detector parameters.

3 Water Cherenkov detectors

Water Cherenkov detectors can provide a very large target mass and, if the photosensors have a sufficient density, a sensitivity down to the low energies of solar neutrinos. Its capabilities concern ν astrophysics, ν oscillations and proton decay. Above a few GeV, DIS dominates over QE scattering and leads to frequent multiring events more complicated to reconstruct. A similar limitation in energy comes from difficulties in the e/π_0 discrimination at high energies. The technique is not suitable at the high energies of ν factories, where, in addition, a muon-charge measurement is needed. One should also note that the low neutrino cross-section at low energies reduces the advantage given by the very large mass which can be assembled.

The detectors currently under study represent the third generation of successful detectors, with in each stage an increase by one order of magnitude in mass. The performance of Super-KamiokaNDE has been widely simulated and observed, providing a basis for a mass extrapolation by one order of magnitude. The performance as well as the limitations are well known, also from K2K and related tests.

Two detector designs are being carried out, namely Hyper-KamiokaNDE [8] and UNO [9]. The design of a detector to be located at Fréjus has also been initiated.

Hyper-KamiokaNDE foresees two 500 kt modules placed sideways, each consisting of five 50 m long optical compartments. The cost is higher than for a single module, but maintenance with one module always alive and a staging in the detector construction become possible. The present design foresees about 200 000 20-inch PMTs, to be compared with 11 146 in Super-KamiokaNDE. The detector could be constructed in about 10 years, starting after a few years of T2K operation.

The UNO design provides a 650 kt mass subdivided into three optical compartments with different photosensor coverage. The central one has a 40% coverage as in Super-KamiokaNDE, allowing one to pursue solar ν studies. The side compartments have 10% coverage. The number of 20-inch PMTs is two times smaller than with 40% coverage for the full detector, but still amounts to 56 650. The question arises as to whether this subdivision, with its non-uniformity given by the lower coverage in 2/3 of the detector, is the optimal solution for reducing the global cost.

By giving appropriate aspect ratio and shape to the cavern, its realization does not seem a problem.

A large fraction of the total detector cost, reaching about half or more if PMTs are used, comes from the photosensors. The present cost of 100 000 to 200 000 20-inch PMTs is hard to cover. Moreover, their production would take about eight years, leading also to storage problems. The main issue is thus the development and acquisition of photosensors at acceptable cost and production rate, as well as an improvement in their performance. A better time resolution would improve neutrino vertexing and single-photon sensitivity would give better ring reconstruction. A strong collaboration with industry is essential, as for the development of 20-inch PMTs by Hamamatsu for KamiokaNDE and Super-KamiokaNDE.

The Hamamatsu 20-inch glass bulbs are manually blown by specially trained people. Automatic manufacturing does not seem a practical solution to reduce the cost and speed up the production rate, as the required quantity is still small compared to commercial PMTs. The question is whether a size smaller than 20 inches, with an appropriate coverage, is more practical and cost effective. With a smaller size, automatic bulb manufacturing is eased and the risk of implosion decreased, with a possible saving in the plastic protection needed to damp implosions. Collaborations for R&D on PMTs have been established with industries in Europe (Photonis) and the USA.

To explore alternatives to PMTs, studies on new photosensors have been launched. In addition to reducing cost, while improving production rate and performance, it is essential to achieve the long-term stability and reliability which is proven for PMTs.

Hybrid Photo-Detectors (HPDs) are being developed by Hamamatsu, in collaboration with ICRR of Tokyo University. The HPD glass envelope is internally coated with a photocathode and a light reflector. Electrons are accelerated by a very high voltage towards an Avalanche Diode (AD). The strong electron bombardment results in a high gain (about 4500 for 20 kV voltage) in this first stage of amplification. It gives a remarkable single-photon sensitivity and makes ineffective the AD thermally generated noise. The gain is lower than with PMTs, hence stable and highly reliable amplifiers are needed. The degradation in time resolution given by the transit time spread through the dynode chain is avoided, so that a 1 ns or so time resolution can be achieved, to be compared with the 2.3 ns of the 20-inch PMTs. The cost reduction with respect to PMTs essentially comes from the use of solid-state devices like the AD, avoiding the complicated PMT dynode structure.

The principle has been proved with a 5-inch HPD prototype. Successful results from tests of a 13-inch prototype operated with 12 kV are now available, showing a 3×10^4 gain, good single-photon sensitivity, 0.8 ns time resolution, and a satisfactory gain and timing uniformity over the photocathode area. The next step will be the operation at a voltage up to 20 kV, giving a higher gain and a wider effective area of the photocathode. The development of HPD has been initiated also in Europe, in collaboration with Photonis.

4 Liquid argon time projection chamber

The Liquid Argon Time Projection Chamber (LAr TPC) provides an excellent imaging device and a dense neutrino target. It is a true ‘electronic bubble chamber’ with a much larger mass (3 t for Gargamelle, up to 100 k now envisaged for LAr TPCs). The ‘state of the art’ is given by the 300 t T300 ICARUS [10] prototype module, tested at ground level in Pavia but not yet used in an experiment.

Two mass scales are foreseen for future experiments. For close ν detectors in superbeams, a mass of the order of 100 t is envisaged. Detectors with 50–100 kt mass are proposed for ν oscillation, ν astrophysics, and proton decay [11][12][13], implying a step in mass by more than two orders of magnitude with respect to the T300 ICARUS module.

Cryogenic insulation imposes a minimal surface/volume ratio. The modular ICARUS approach has thus to be abandoned for a single very large cryogenic module with about 1:1 aspect ratio.

To limit the number of readout channels, drift lengths have to be longer than the 1.5 m of the T300 module. The LAr TPC envisaged for the off-axis NuMI beam [11],[12] foresees 3 m drift lengths with readout, conceptually as in ICARUS. In another approach [13], the very strong attenuation over a much longer drift length (20 m) is compensated by the so-called 'Double Phase' amplification and readout [14], tested on the ICARUS 50 litre chamber [15]. In both cases, the signal attenuation imposes a liquid argon contamination by electronegative elements at the 0.1 ppb level.

In Ref. [13] a 100 kt detector consisting of a single module both for cryogenics and readout has been proposed. The 20 m drift in a field raised to 1 kV/cm results in a 10 ms drift time. With a 2 ms electron lifetime in liquid argon, the 6000 electrons/mm signal is attenuated by $e^{-t/\tau} \sim 1/150$ and becomes too low for a readout as in ICARUS. In the double-phase readout, electrons are extracted from the liquid by a grid and collected in the gas phase using gas chamber techniques. The $\sigma \sim 3$ mm spread from the diffusion in the 20 m drift gives an intrinsic limit to the readout granularity.

The design of the single large cryostat [13] can benefit from the techniques developed for transportation and storage of large quantities of liquefied natural gas, kept at boiling temperature by letting it evaporate. A large cryogenic plant is needed for the initial filling and for the continuous refilling to compensate the evaporation.

The R&D for the detector of Ref. [13] foresees drift under 3 atm pressure as at the tank bottom; charge extraction and amplification; imaging devices; cryogenics and cryostat design, in collaboration with industry; a column-like prototype with 5 m drift and double-phase readout, with a 20 m drift simulated by a reduced electromagnetic field and by a lower liquid argon purity; test of a prototype in a magnetic field (as for use in a ν factory); underground safety issues.

Tests on a 10 litre LAr TPC inserted in a 0.55 T magnetic field have been performed [16], together with a tentative layout for the implementation of a large superconducting solenoidal coil into the design of Ref. [13].

The experience accumulated in two decades with ICARUS is very important. However, a substantial R&D is required, to an extent that depends on the detector design and on the (underground) location. In the design of very large detectors, with or without magnetic field, one has to proceed from concepts or conceptual designs to a practical design.

5 The emulsion cloud chamber

The use of Emulsion Cloud Chambers (ECCs) has been proposed to detect 'silver events' from ν_e–ν_τ oscillations at a ν factory, in order to complement the ν_e–ν 'golden events' in resolving θ_{13}–δ ambiguities [17].

The ECC of the OPERA experiment [18] in the CNGS beam consists of a multiple sandwich of lead- and nuclear-emulsion sheets. The production and decay of τ leptons is expected to be observed with a very low background thanks to the emulsion submicron resolution. The 1.8 kt OPERA target is built up from about 200 000 lead-emulsion 'bricks'.

At the ν factory, a 4 kt mass is envisaged. By scanning only 'wrong-sign' muons like those coming from τ decays, the scanning load is expected to be comparable with that in OPERA. An increase in the speed of the automatic microscopes is foreseeable. The OPERA Collaboration is working to provide a milestone in the application of the ECC technique.

References

[1] D. Geiregat *et al., Nucl. Instrum. Meth., A* 325 (1993) 92.

[2] NOνA Collaboration, Proposal P929 (2004).

[3] MINOS Collaboration, Proposal P-875, Fermilab Report NuMI-L-63 (1995).

[4] J. Nelson, proceedings of Nufact 05, LNF (Italy), 21–26 June 2005.

[5] N.K. Mondal, proceedings of Nufact 05, LNF (Italy), 21–26 June 2005.

[6] P. Antonioli, for the MONOLITH Collaboration, *Nucl. Phys. (Proc. Suppl.)* **100** (2001) 142.

[7] A. Cervera *et al., Nucl. Instrum. Meth. A* **451** (2000) 123.

[8] K. Nakamura, *Int. J. Mod. Phys. A* **18** (2003) 4053, and references therein.

[9] UNO Proto Collaboration, SBHEP-01-03 (2000), Waseda Univ. (1992).

[10] ICARUS Collaboration, LNGS-P28/2001 and ICARUS-TM/2001-03, hep-ex/0103008.

[11] FLARE Collaboration, Letter of Intent hep-ex/0408121 (2004).

[12] D. Cline *et al., Nucl. Instrum. Meth. A* **503** (2003) 136.

[13] A. Rubbia, Proc. of the II Int. Workshop on Neutrinos, Venice (2003).

[14] B.A. Dolgoshein *et al., Fiz. El. Chast. Atom. Yad*. **4** (1973) 167.

[15] D. Cline *et al., Astropart. Phys.* **12** (2000) 373.

[16] A. Rubbia, proceedings of Nufact 05, LNF (Italy), 21–26 June 2005.

[17] A. Donini, D. Meloni and P. Migliozzi, hep-ph/0206034.

[18] OPERA Collaboration, CERN SPSC-2000-028, LNGS P25/2000.